Bioactive 4-methoxypyrrolic natural products from two South African marine invertebrates
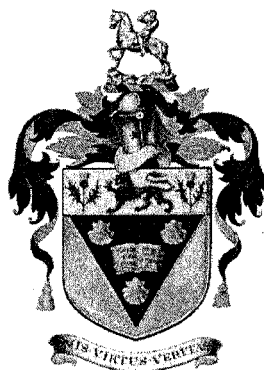
A thesis submitted in fulfillment of the requirements for the degree of

Master of Science

of

Rhodes University

by

Trevor Douglas Rapson

November 2004

Abstract

This thesis presents an investigation of the 4-methoxypyrrolic constituents of two South African marine invertebrates, the nudibranch *Tambja capensis* and the bryozoan *Bugula dentata*. Three known compounds tambjamine A (**7**), tambjamine E (**13**) and the tetrapyrrole (**15**) were isolated during this investigation. All three compounds were shown to be active against oesophageal cancer in accordance with the general anticancer and immunosuppressive properties observed for 4-methoxypyrrolic natural products. Tambjamine A (**7**), tambjamine E (**13**) and the tetrapyrrole (**15**), together with tambjamine K (**21**) and L (**22**) (previously isolated in our laboratory) were used as standards to quantitatively assess the presence of these tambjamines in *T. capensis* and *B. dentata* collected from three different sites along the South African coast. This study confirmed that *B. dentata* is the source of the 4-methoxypyrrolic natural products sequestered by *T. capensis* and eliminated the closely related bryozoan *B. neritina* as a source of these metabolites.

The paucity of tambjamine L (**21**) and K (**22**) obtained in previous investigations of the sequestered chemistry of *T. capensis* prompted an attempt at the development of synthetic methodology that could be used to synthesize tambjamines in sufficient yield for in depth bioactivity studies. In order to by pass the extensively reported problems associated with the synthesis of this group of compound 3-methoxy-2-formylpyrrole (**47**), readily accessible from 3-methoxypyridine N-oxide (**48**), was used as the starting material in a singlet oxygen induced 2,2' bipyrrole coupling reaction. Although **47** proved unreactive in this coupling reaction, when the N-Boc protected analogue of **47** was used, and the reaction worked up in the dark, the novel methyl 4-aza-5-oxo-6,6-di-(2-pyrrolyl)-2(*Z*)-hexenoate (**57**) was obtained in low yield.

The physical properties of tambjamine (E) (**13**) and the tetrapyrrole (**15**) were investigated to further the understanding of the proposed oxidative DNA cleavage mechanism and to determine the potential of the 4-methoxypyrrolic natural products as photodynamic therapy agents.

Table of Contents

List of figures

List of schemes

List of tables

List of abbreviations

AcOH	acetic acid
ATP	adenosine triphosphate
ATPase	adenosine triphosphatase
Boc$_2$O	di-*tert*-butyldicarbonate
br	broad
calcd	calculated
COSY	^{1}H – ^{1}H homonuclear correlation spectroscopy
d	doublet
DABCO	1,4-diazabicyclooctane
DMAP	4-dimethylaminopyridine
DMSO	dimethylsulfoxide
DPBF	1,3-diphenylisobenzofuran
EDTA	ethylenediaminetetraacetic acid
ESIMS	electrospray ionization mass spectrometry
EtCl$_2$	1,2-dichloroethane
EtOAc	ethyl acetate
EtOH	ethanol
GI$_{50}$	growth inhibition level
hr	hour/hours
HMBC	heteronuclear multiple bond correlation
HSQC	heteronuclear single quantum correlation
HPLC	high performance liquid chromatography
HRFABMS	high resolution fast atom bombardment mass spectrometry
IC$_{50}$	median inhibitory concentration
IR	infrared
LC$_{50}$	median lethal concentration
Lit.	literature
m	multiplet
MeCN	acetonitrile

Me$_2$CO	acetone
MeOH	methanol
min	minute/minutes
MJ	mega joules
mmHg	millimeters of mercury
mmol	millimoles
μmole	micromoles
m.pt	melting points
NBS	*N*-bromosuccinimide
NMR	nuclear magnetic resonance
ns	nano seconds
PDT	photodynamic therapy
ppm	parts per million
q	quartet
R	specified or unspecified alkyl group
ROS	reactive oxygen species
rt	room temperature
s	singlet
SCUBA	self-contained underwater breathing apparatus
t	triplet
TEAP	tetraethylammonium perchlorate
tert	tertiary
TFA	trifluoroacetic acid
THF	tetrahydrofuran
TLC	thin layer chromatography
p-TsOH	*para*-toluenesulfonic acid
UV	ultraviolet
Vis	visible
ZnPc	zinc phthalocyanine

Acknowledgements

There are many people who I would like to thank for their assistance during the course of my research.

Chapter One

Introduction

The 4-methoxypyrrolic natural products, include the tripyrrole prodigiosins, bipyrrole tambjamines and the tetrapyrrole, all sharing a common 4-methoxy-2,2'-bipyrrole system. As an introduction to this thesis an overview of the isolation of the naturally occurring 4-methoxypyrrolic natural products from microorganisms and marine invertebrates is provided. The international interest in the potential pharmaceutical applications of 4-methoxypyrrolic metabolites, led by Manderville's group at Wake Forest University in North-Carolina and Fürstner's group at the Max-Planck-Institute in Germany, have been recently reviewed.[1,2] Since the publication of these reviews, only one article of interest has appeared in the literature detailing the crystal structure of a prodigiosin-copper (II) complex.[3] Both reviews have therefore been extensively used to provide the necessary background to this thesis. Frustratingly, the numbering of 4-methoxypyrrolic natural products and synthetic analogues is not consistent in the literature. The first reported isolation of tambjamine natural products by Carté and Faulkner[4] number the bipyrrole natural products using the numbering scheme shown below in Figure 1.1. An alternative numbering scheme was used by Blackman and Li and is also provided in Figure 1.1. Later, Manderville and co-workers in their structure-activity studies alphabetically ordered (A-C) each pyrrole ring in their prodigiosin derivatives.[5] For the purposes of this thesis, the numbering scheme used by Carté and Faulkner coupled with Manderville's alphabetical ordering of the pyrrole rings will be used.

Carté and Faulkner[4]　　　　　　Blackman and Li[6]
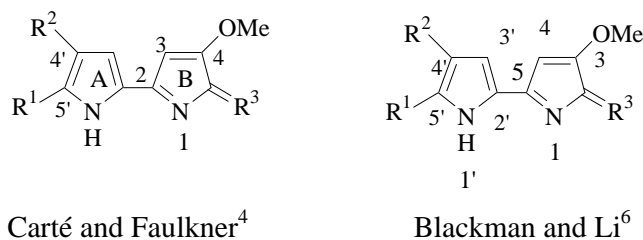
Figure 1.1: General structure of 4-methoxypyrrolic natural products and two different numbering schemes commonly used in the literature.

An attempt to synthesise a 4-methoxypyrrolic metabolite isolated from a South African opiothobranch mollusc necessitated a review of synthetic strategies directed towards the synthesis of this group of compounds and this is presented in Chapter 3.

1.1 Sources of 4-methoxypyrrolic natural products

1.1.1   Microorganisms

Figure 1.2: The red pigmented bacterium *Serratia marcescens* – a source of 4-methoxypyrrolic natural products.[2]

Bright red microorganisms such as *Serratia and Streptomyces* are occasional contaminants of bread and other foods. On reaching maturity, the colonies become fluid and resemble droplets of blood in the contaminated food leading to historical reports of "bleeding bread".[2] The red colour of these gram-negative bacterial colonies attracted natural product chemists interested in the chemical structure of the red pigment. The first isolation of a red alkaloid pigment from *Serratia marcescnes* was reported in 1929.[2] However, only in 1960 was the correct structure of the red pigment, prodigiosin (**1**), established through synthesis.[7] With advances in separation techniques and structure elucidation technology, prodigiosin has been shown to be several closely related analogues possessing the same pyrrolylpyrromethene core but differing in alkyl substitution at C-2 and C-3.[8-12] Today the prodigiosins, the general name given to this group of closely related metabolites, are divided into the linear and macrocyclic forms which both share a common 4-methoxy-2,2'-bipyrrole system with variation limited to the C-pyrrole ring.[1] The linear prodigiosins include prodigiosin (**1**) with a methyl and pentyl alkyl substituents at C-2 and C-3 respectively and undecylprodigiosin (**2**),[13] with an undecyl substituent at C-2.

1 $R^1 = C_5H_{11}$

    $R^2 = CH_3$

2 $R^1 = H$

    $R^2 = C_{11}H_{25}$
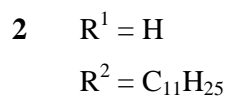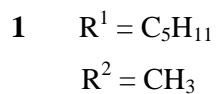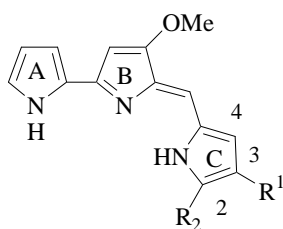
Examples of the macrocyclic prodigiosins include metacycloprodigiosin (**3**),[14] streptorubin B(**4**),[15] cycloprodigiosin (**5**)[16] and nonylprodigiosin (**6**).[17] Nonylprodigiosin differs from the other macrocyclic prodigiosins as the alkyl substituent is attached to both the A and C rings, locking the conformation of the prodigiosin molecular framework. All of the reported isolations of prodigiosin thus far have been from terrestrial microorganisms.[2]
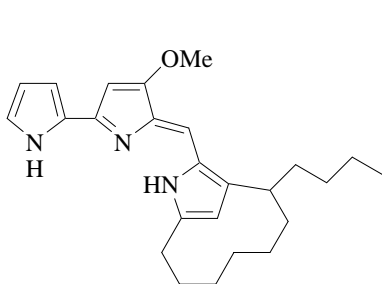
3
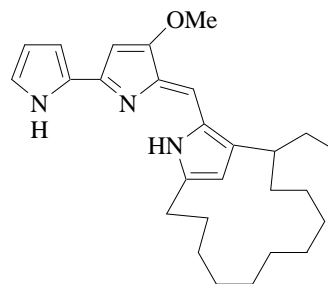
4
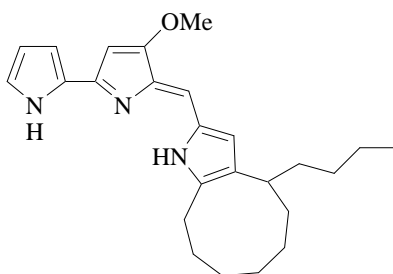
5
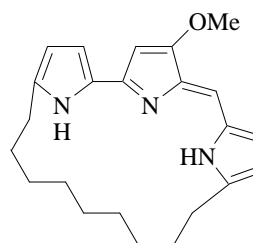
6

1.1.2 Marine organisms

Figure 1.3: *Tambja eliora*, a nudibranch that sequesters 4-methoxypyrrolic natural products from its bryozoan diet.[18]

The first isolation of tambjamine natural products from the nudibranchs *Tambja abdere*, *Tambja eliora* and *Roboastra tigris,* collected on the west coast of North America, was reported by Carté and Faulkner in 1983. Tambjamines A-D (**7-10**) were isolated from all of the nudibranchs together with the respective bipyrrole aldehydes (**11**,**12**), which were shown to be isolation artefacts rather than natural products.[4] Highly coloured secondary metabolites of unknown structure had been previously implicated in the chemical defence mechanism of the bryozoan *Sessibugula translucens.*[19] Since both *T. abdere* and *T. eliora* were observed feeding on this bryozoan, it was thought that the bryozoans sequestered the natural products to form their own chemical defence. Accordingly, in an elegant study by Faulkner and Carté, tambjamines were found to be present in the mucus secreted by *T. abdera* when attacked by *R. trigis* and present in low concentrations in the slime trail produced by the *Tambja* nudibranchs. Antimicrobial activity of the tambjamines against *Eschericia coli*, *Staphlococcus aureu*, *Bacillus subtilis* and *Vibrio anguillarum*

was also demonstrated.[4]   In 1991 the isolation of tambjamines A and C was reported from the marine ascidian *Atapozoa* sp. along with two new tambjamines E (**13**) and F (**14**) and the tetrapyrrole natural product (**15**)[20] which had previously been isolated from *S. marcescens*,[21] an unidentified Australian ascidian[22] and the bryozoan *Bugula dentata* collected in Japan.[23]
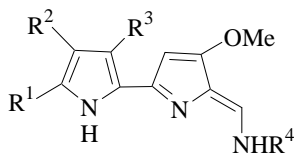
	R^1	R^2	R^3	R^4	Tambjamine
7	H	H	H	H	A
8	Br	H	H	H	B
9	H	H	H	$CH_2CH(CH_3)_2$	C
10	H	H	Br	$CH_2CH(CH_3)_2$	D
13	H	H	H	CH_2CH_3	E
14	H	H	H	CH_2CH_2Ph	F
16	Br	H	H	CH_2CH_3	G
17	Br	H	H	$CH_2CH_2CH_3$	H
18	Br	H	H	$CH_2CH(CH_3)_2$	I
19	Br	H	H	$CH_3CH(CH_3)CH_2CH_3$	J

11 $R^1 = R^2 = H$

12 $R^1 = Br, R^2 = H$
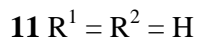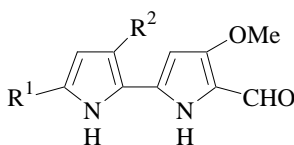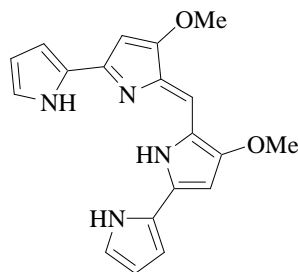
15

Interest in the tambjamines prompted Paul *et al.*[24] to investigate the role of the tambjamine and tetrapyrrole natural products in the chemical defence of the marine invertebrates producing these metabolites to protect themselves from predation. In their study of the ascidian *Atapozoa* sp. and its nudibranch predators in the tropical Indo-Pacific they found that both the ascidian and nudibranch predators contained tambjamine natural products. Only tambjamine A (**7**) and the tetrapyrrole natural product (**15**), however, were found in the nudibranchs, suggesting that the nudibranchs selectively sequestered the metabolites from their ascidian prey. Although the concentrations of the individual 4-methoxypyrrolic natural products was found to vary greatly between different collections, generally the nudibranchs showed a higher concentration of 4-methoxypyrrolic metabolites that would be expected if the nudibranchs were sequesting the 4-methoxypyrrolic metabolites from their diet. In an assay to determine the feeding deterrent potential of the 4-methoxypyrrolic natural products, it was found that a mixture of tambjamine natural products was an effective feeding deterrent against a variety of carnivorous fish found on the reefs from which the collections. The tambjamine natural products were found to not all be equally deterrent. When tested alone, **7** and **13** were not deterrent, whilst **9** and **15** showed increased individual and increasing deterrent activity.[24] In 1994, a further four new tambjamine natural products, tambjamines G-J (**16-19**), were isolated from the Australian bryozoan *B. dentata* together with the known tambjamines E (**13**) and tetrapyrrole (**15**).[6] More recently, **17** has been isolated from the nudibranchs *Nembrotha kubaryana* collected in Hawaii.[25]

The biosynthetic origin of 4-methoxypyrrolic natural products in marine organisms has not been rigorously established, however, the occurrence of these metabolites in such phylogenetically distinct organisms such as marine organisms[4,23] and terrestrial

bacterial sources[21] would seem to suggest a symbiotic, microbial source for 4-methoxypyrrolic natural products.[26]

1.2 Bioactivity of 4-methoxypyrolic natural products

The first attempts to isolate the red pigment from *Serratia* strains were aimed at utilising prodigiosin as a commercial dye. Unfortunately, the pure form of prodigiosin turned out to be too sensitive to light and was therefore unsuitable for commercial exploitation.[2] Since then, the 4-methoxypyrrolic natural products have attracted increasing attention because of their antibacterial, anticancer and immunosuppressive properties.[1,2]

1.2.1 Antibacterial, antifungal and antiprotozoa activity

4-methoxypyrrolic natural products appear to show broad spectrum activity against bacteria, protozoa and pathogenic fungi, however their high systemic toxicity has prevented further development of these compounds as antibiotics.[27,28] Of particular interest is the effect of 4-methoxypyrrolic metabolites on the life cycle of the plasmodium *Plasmodium falciparum*, the causative agent of malaria. Metacycloprodigiosin (**3**) at doses below the acute cytotoxicity threshold exhibited an IC_{50} of 5×10^{-3} µg/mL.[29] Attempts to improve their application profile through investigations into structure-activity relationships have shown that the therapeutic window of the prodigiosin analogues is too narrow for development as antimalarials and possible antibiotics.[27,29,30] A pharmaceutical with a large therapeutic window is one in which the efficacy of the pharmaceutical exceeds unwanted side effects.

1.2.2 Anticancer activity

The second pharmaceutical area in which the 4-methoxypyrrolic natural products have attracted attention is for their anticancer properties. The prodigiosins have been shown to cause cell death through apoptosis (programmed cell death).[31-35] They also exhibit activity against melanoma[36] and liver cancer cell lines.[31] Of particular interest is the development of pharmaceuticals for the treatment of hepatocellular carcinoma (liver cancer)[31] for which there is currently no treatment available.[37] In order to advance in the development of 4-methoxypyrolic natural products as anticancer drugs,

a full understanding of their mechanism of action is required.[1] Two modes of action have been proposed *viz* oxidative DNA cleavage and disruption of the H$^+$-ATPase.[1,2]

The acidic environment within cell organelles, including the synaptic vesicles, chromaffin granules, secretary granules, lysosomes and *trans*-Golgi networks, are maintained by vacuolar-type H$^+$-ATPases which are located on the membranes of these organelles.[38] The H$^+$-ATPases pump protons into and out of the organelles, using energy from ATP hydrolysis, to maintain the acidic environment important for various cellular functions including cell growth and death.[39-42] In support of this hypothesis, ATPase enzymes have been found on the membranes of cells such as osteoclasts, macrophages, activated neutrophils, renal epithelial cells and certain tumour cells which also require an acidic cytosolic pH.[38]

Metabolite **2** has been shown to raise the lysosomal pH and suppress glycoprotein processing through its ability to inhibit H$^+$-ATPase without showing apparent protonophoric activity.[43] Unlike other known Vacuolar-ATPase inhibitors, the prodigiosins do not bind directly to the proteolipids of V-ATPases and have no direct inhibitory effect on ATP hydrolysis,[44,45] making them the fourth general class of compounds capable of altering vacuolar pH after weak bases, acidic ionophores and V-ATPase inhibitors.[44] The proposed mechanism of inhibition by prodigiosins involves the initial protonation of prodigiosin with a chlorine counter ion to form a lipophilic ion pair that facilitates H$^+$-coupled transmembrane transport of chloride ions.[44]

There is also growing evidence of a relationship between the cytotoxicity of prodigiosins and their DNA-damaging capacity. Manderville proposed that the bipyrrole nucleus of **13** could bind to DNA with intercalation through hydrogen bonding from the methoxy and the ring nitrogens facilitating the DNA binding.[46] Polypyrroles are easily oxidised suggesting that the nuclease activity of the 4-methoxypyrrolic natural products could be enhanced in the presence of a redox-active metal such as zinc or copper.[46] Accordingly, Manderville and co-workers have shown that **1**, **13** and **15** were able to bind DNA, with a preference for adenine and thymine bases, and cleave supercoiled DNA in the presence of only copper (II) and not other metals such as zinc, iron or nickel. Interestingly, bipyrrole **13** caused single strand

DNA cleavage whilst **1** and **15** caused the more lethal double strand DNA cleavage.[1,46-49]

The mechanism by which the DNA cleavage occurs is similar to that of bilirubin (**20**). In both cases, the reduction of Cu (II) to Cu (I) results in the initial formation of the π-radical cation of the electron-rich pyrrolylpyrromethene chromophore. This chromophore generates reactive oxygen species which cause DNA damage.[46,49]
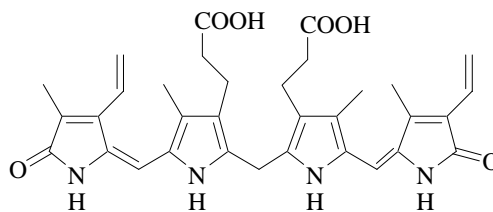
20

1.2.3 Immunosuppressive activity

One of the most interesting properties of the prodigiosins is their immunosuppressive activity at sub-cytotoxic doses. Although the therapeutic window of the prodigiosins is too small for direct clinical application, they may provide leads for novel immunosuppressive drugs.[2] The prodigiosins appear to operate through a mechanism different to that of currently used immunosuppressors such as cyclosporin or FK 506 which act as calcineurine inhibitors,[2] thereby preventing the proliferation of the immune system T cells in the early G_1 stages of their life cycle.[50,51] Conversely, prodigiosins have been shown to selectively inhibit phosphorylation and activation of the cytoplasmic Janus tyrosine kinase (JAK-3) by interfering with interleukin (IL-2) signal transduction.[44,45] Interestingly, when synthetic analogues of prodigiosin are administered in combination with cyclosporin A, they appear to have a synergistic effect and dramatically increase the mean survival time of heart-transplanted rats.[50,51]

1.3 Structure-activity studies

Work carried out at the National Cancer Institute (NCI) to determine the cytotoxic properties of prodigiosins (**1**), steptorubin B (**4**) and tambjamine I (**18**) using the COMPARE algorithm, a program which compares the patterns of activity of newly discovered cytotoxic compounds with known anti-cancer agents, revealed some interesting results. Although none of the prodigiosins tested compared favourably at

the growth inhibition (GI_{50}) level, some similarities were observed at the cytocidal (LC_{50}) level between **1**, **4**, **18** and pyrimidine analogues, which act as antimetabolites interfering with enzymatic reactions in nucleic acid synthesis,[52] and topoisomerase inhibitors. Topoisomerases control the topological state of DNA by preventing the DNA strands from becoming tangled up during replication, transcription and recombination. There are two forms of topoisomerases, Type I and Type II. Type I enzymes break only one strand of DNA whilst type II break both strands to release tension in the strands during the replication process. The inhibition of topoisomerase is thought to occur through an initial intercalation with DNA which prevents the topoisomerase from performing its function.[53,54] Similarities were also noted with 3,6-diaziridinyl-2,5-bis(carboethoxyamino)-1,4-benzo-quinone (AZQ) which crosses the blood-brain barrier and causes alkylation of DNA. From the trends observed using COMPARE analysis it was concluded that the 4-methoxypyrrolic natural products act as DNA-intercalative agents which form the largest class of clinically used anticancer pharmaceuticals.[55]

D'Alessio and co-workers carried out synthetic modifications of prodigiosin in order to develop compounds with a superior immunosuppressive activity/cytotoxicity ratio and therefore increase the therapeutic window of the prodigiosin type compounds. A range of analogues were synthesised to first investigating the importance of the A-pyrrole ring, secondly the alkoxy substituent (R^1) and thirdly substitution in the C-ring (R^2 and R^3). From their studies they showed that a nitrogen-containing heterocyclic A-ring and extensive conjugation of the π electron system is required for immunosuppressive activity. Furthermore, the addition of electron donating substituents on the A-ring enhanced potency whilst electron withdrawing groups decreased potency.[56]
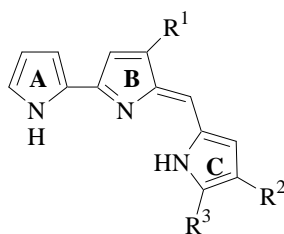
All the naturally occurring 4-methoxypyrrolic metabolites contain a methoxy substituent at R^1 and removal of this substituent leads to a drastic decrease in

immunosuppressive activity while increasing the size of the alkoxy substituent (e.g. OCH_2Ph) leads to a reduction in cytotoxicity whilst still maintaining the desired immunosuppressive activity.[28,56] Lengthening of the alkyl chain substituent in the C-ring (R^2 and R^3) also reduced cytotoxicity. Interestingly a complete loss of immunosuppressive and cytotoxic activity was observed when the C-ring substituents contained a carboxyl group.[56] Using this information, D'Alessio and co-workers synthesised the prodigiosin derivative PNU-156804 (**20a**) which has a therapeutic index almost ten fold that of the natural product, undecylprodigiosin (**2**).[56]
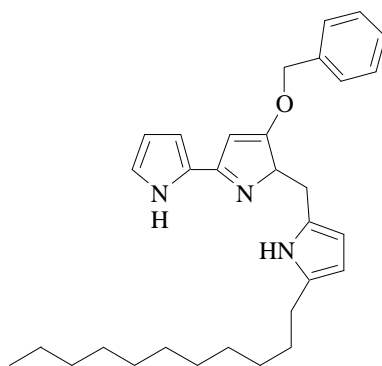
20a

Chapter Two

Investigation of the natural product chemistry of two South African marine invertebrates, *Tambja capensis* and *Bugula dentata*

2.1 Introduction

As part of an ongoing investigation of marine natural products sequestered by Southern African marine molluscs,[57-61] this chapter presents a study of the 4-methoxypyrrolic natural products isolated from extracts of the nudibranch *Tambja capensis* and the bryozoan *Bugula dentata*, and also includes a quantitative examination of the occurrence of these metabolites in a variety of nudibranch and byrozoan samples collected along the South African coast. Our interest in the natural product chemistry of *T. capensis* followed from the isolation of two novel tambjamines, tambjamine K (debromo tambjamine H) (**21**) and an inseparable mixture of tambjamines G (**16**) and a new isomer tambjamine L (**22**).[62] The paucity of tambjamine L (less than 1 mg), isolated from *T. capensis*, however hampered complete structural elucidation of this compound. The original aim of the natural product investigation was to isolate more tambjamine L to resolve the structural anomalies.
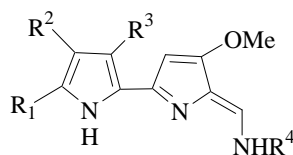
	R^1	R^2	R^3	R^4	Tambjamine
7	H	H	H	H	A
13	H	H	H	CH_2CH_3	E
17	Br	H	H	$CH_2CH_2CH_3$	H
21	H	H	H	$CH_2CH_2CH_3$	K
16	Br	H	H	CH_2CH_3	G
22	H	Br	H	CH_2CH_3	L
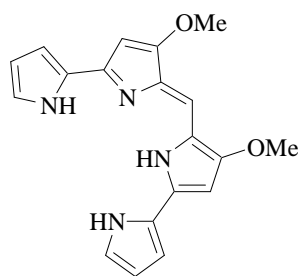
15

Two separate natural product isolations were carried out on firstly the nudibranch, *T. capensis* from which tambjamine natural products had been previously isolated and secondly, the bryozoan, *B. dentata* which as mentioned in Chapter 1 and was thought to be the source of the metabolites sequestered by *T. capensis*.

Tambja capensis appears to be endemic to the colder temperate waters of the Cape Province of South Africa and has been collected from Cape Town to as far east as Port Elizabeth and East London. This species is a common nudibranch in shallow subtidal waters and easily distinguished by its dark blue colour with green lines along the periphery of its dorsal surface. *T. capensis* is reported to feed on bryozoans such as *B. dentata* and *Bugula neritina*[18] supporting our supposition that *B. dentata* was the source of the sequestered chemistry of *T. capensis*.

Figure 2.1 *Tambja capensis*, a common nudibranch found along the temperate southeast coast of South Africa.[18]

B. dentata is a common dark blue-green bryozoan, abundant in the Indo-Pacific region, from the west coast of Australia to Queensland and the east coast of Southern Africa. The species is typically found in coastal waters on sheltered rocky reefs and usually a size of around 8 cm.[63]

Figure 2.2 *Bugula dentata* upon which *T. capensis* has been observed grazing and is putatively the source of 4-methoxypyrrolic natural products isolated from *T. capensis*.

The ongoing collection of marine invertebrates along the Southern African coast by the marine natural products research group at Rhodes University provided a unique opportunity to quantitatively study the diversity of 4-methoxypyrrolic metabolites in specimens of *T. capensis* collected from three different localities along the South African coast (Figure 2.3). In addition, the abundance of *B. dentata* in Algoa Bay enabled us to examine more closely the ecological relationship between this bryozoan and *T. capensis*.
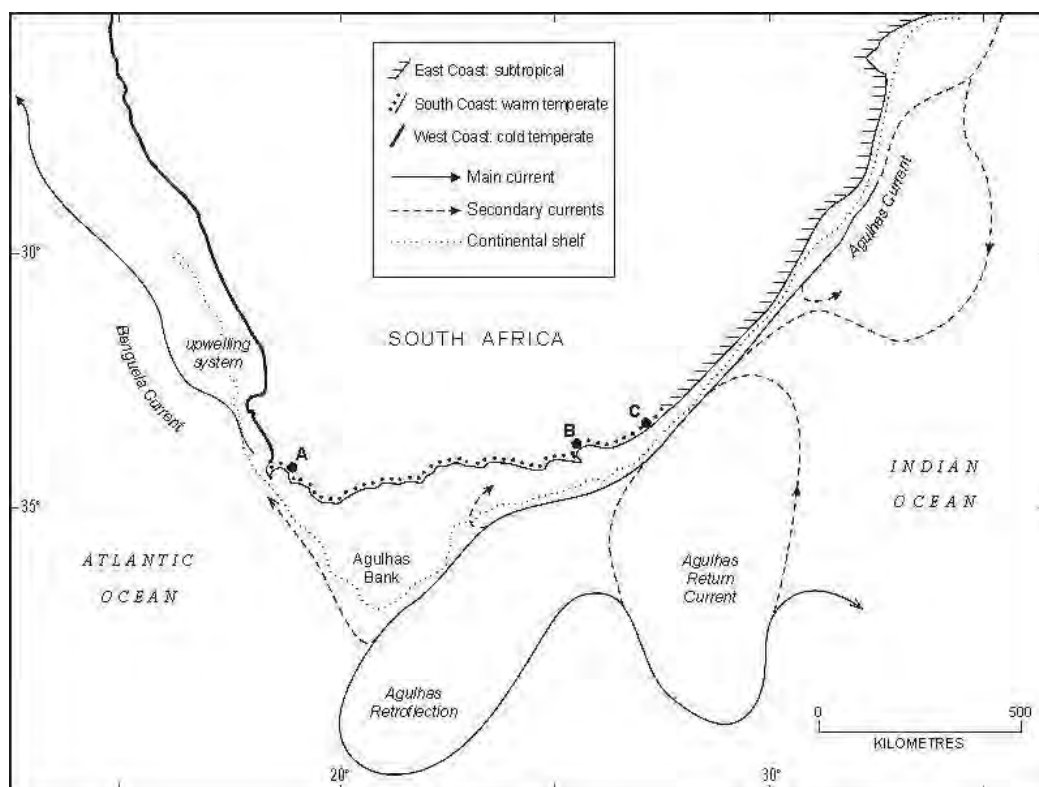
.Figure 2.3 Map of Southern Africa indicating the main collection sites for *T. capensis*, *B. dentata* and *B. neritina* (A = False Bay, B = Algoa Bay, C = East London).

.

2.2 Isolation of 4-methoxypyrrolic natural products from *T. capensis*

A total of 39 specimens of *T. capensis* were collected using SCUBA from depths between 3 and 10 m off Simonstown, False Bay, South Africa in August 1999. The specimens were steeped in acetone and the extracts were concentrated and partitioned between dichloromethane and water. The dichloromethane extract was dried and concentrated to yield a dark oil (427 mg) that was subjected to reversed phase vacuum liquid chromatography on a Waters C-18 solid-phase extraction cartridge employing a 0.1 M ammonium acetate buffered water/methanol solvent gradient. ^{1}H NMR spectroscopy showed that the dark blue fraction (276 mg) eluting with 1:1 methanol/water contained resonances indicative of 4-methoxypyrrolic alkaloids, and was purified further through semi-preparative C-18 reversed phase HPLC (both gradient and isocratic elution) to give the known tambjamines A (**7**) (11 mg), and E (**13**) (10 mg), and the tetrapyrrole natural product (**15**) (3 mg). All the isolated

tambjamines were isolated as their acetate salts, **13** and **15** were converted into their free base form through treatment with aqueous ammonia for later physical studies. Subsequent analysis of the ^{13}C data indicated the loss of the acetate resonance and supported the presence of the free bases. The ^{13}C and ^{1}H NMR data of **13** and **15** were consistent with those acquired previously by Gray and confirmed by comparison with literature values.[4,23,62] The structure elucidation of tambjamine A (**7**) using HRFABMS and standard 2D-NMR spectroscopic techniques is presented in the following section.

2.21 Structural elucidation of tambjamine A (7)

The molecular formula of **7**, $C_{10}H_{11}N_3O$, was obtained from HRFABMS analysis (M^+ = 189.0901, $C_{10}H_{11}N_3O$ requires 189.0902) implying seven degrees of unsaturation. Analysis of the IR spectrum gave an indication as to the functional groups present including stretching frequencies at 1675 cm^{-1} and 1605 cm^{-1} which were assigned to C=N and C=C respectively and two N-H absorbances at 3635 and 3480 cm^{-1}. All the carbon and proton resonances were observed in the ^{13}C and ^{1}H NMR spectra respectively.

A gradient HSQC experiment was used to establish the ^{1}H-^{13}C connectivity, from which seven protonated ^{13}C resonances were identified (including the acetate counter ion), accounting for seven of the nine ^{1}H resonances, suggesting the presence of two exchangeable ^{1}H resonances, which was consistent with the N-H absorbances observed in the IR spectrum. Five non-protonated carbons were observed in the ^{13}C spectrum and these were assigned as a carbonyl (δ_C 169.6) and aromatic ring (δ_C 165.2, 144.8, 122.7 and 112.8) carbons respectively as shown in Table 2.1. From the COSY spectrum of **7** (Figure 2.4), a contiguous ^{3}J coupling sequence between the three olefinic methines (δ_H 7.09, δ_C 124.7, H-3'; δ_H 6.28, δ_C 110.6, H-4'; δ_H 6.75, δ_C 114.1, H-5') and allowed establishment of the partial structure A.
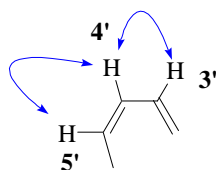
Partial Structure A

Figure 2.4: COSY correlations used in the establishment of partial structure A.
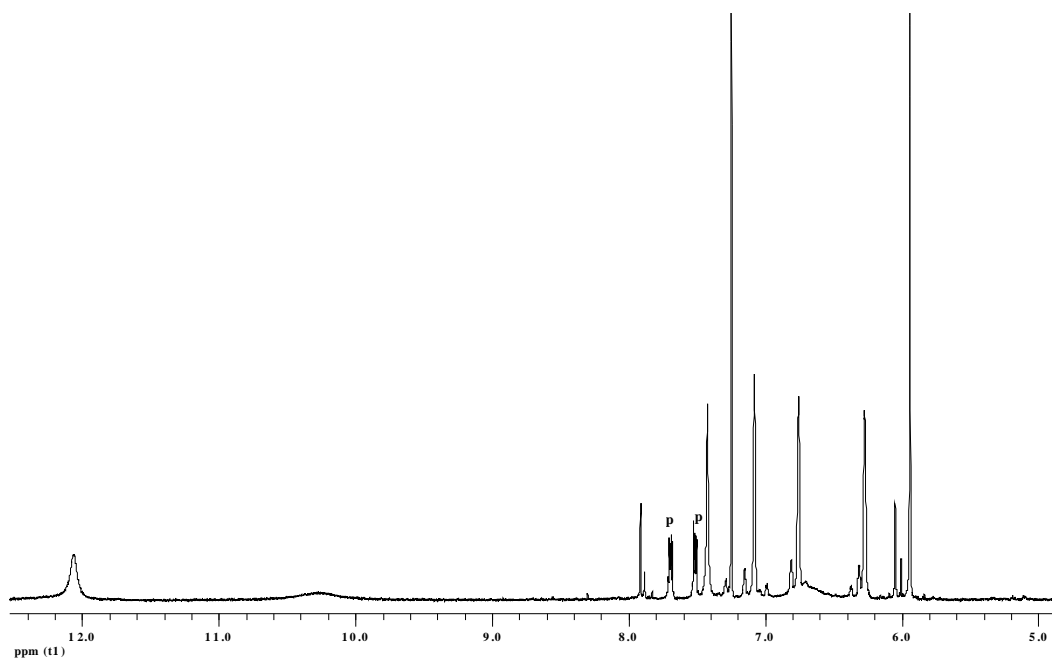
Figure 2.5 Expanded (δ 5.0-12.5 ppm) section of the ¹H NMR spectrum (400 MHz, CDCl₃) of **7** (p = phthalate ester plasticiser contaminant).
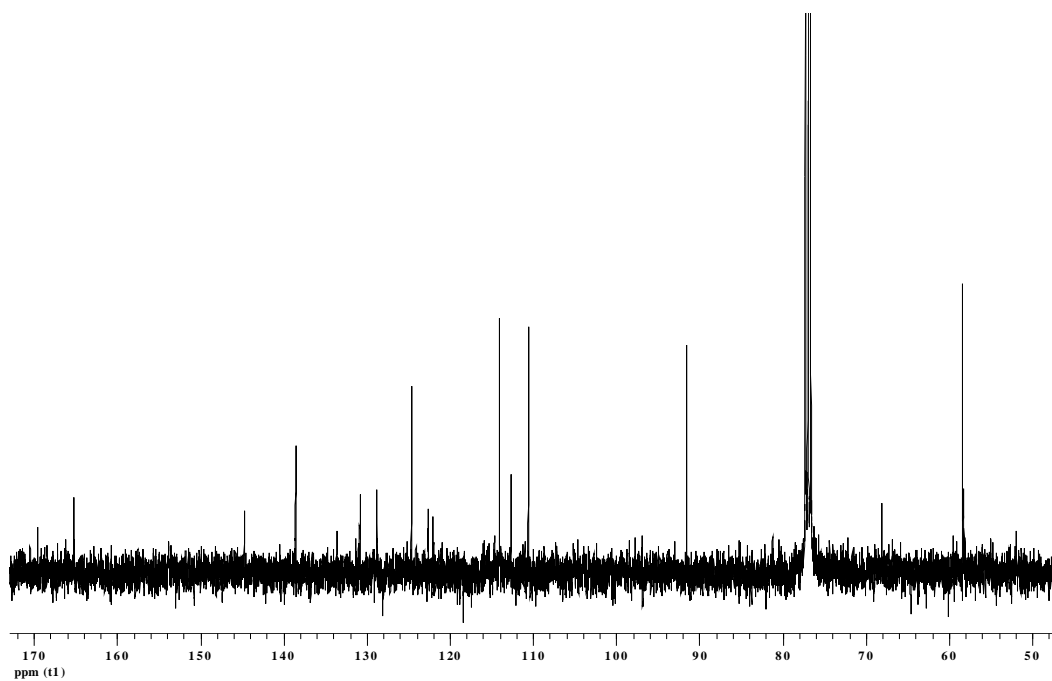
Figure 2.6 Expanded (δ 50–170 ppm) ¹³C NMR spectrum (100 MHz, CDCl₃) of **7**.
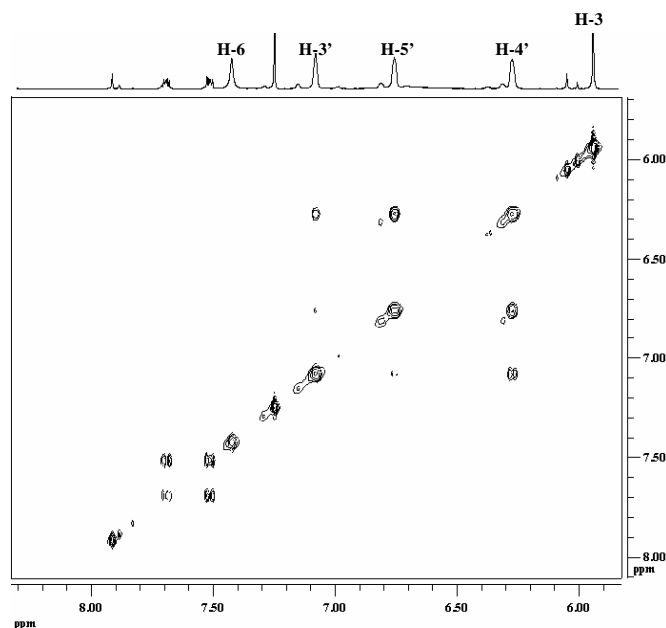
Figure 2.7 An expanded ($F_1 = F_2 = \delta$ 5-8 ppm) COSY NMR spectrum (400 MHz, CDCl$_3$) of **7**.

Partial structure A was confirmed by long range proton-carbon correlations observed in the HMBC spectrum of **7**. Correlations between the olefinic methine resonances (δ_H 6.75, δ_C 114.1, H-5') and (δ_H 7.09, δ_C 124.7, H-3') with the aromatic quaternary carbon (δ_C 122.7) suggested a connection between C-3' and C-2'. No correlations in the COSY or HMBC spectra were observed with the exchangeable protons. The chemical shifts of the protons at H-3', H-4' and H-5' suggested that these protons were part of a pyrrole ring, (partial structure B) in accordance with the A ring of tambjamine A.
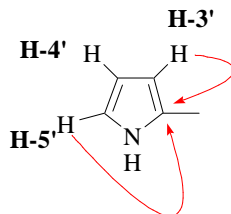
Partial structure B

Figure 2.8: Important HMBC correlations used in determining partial structure B.

Additional correlations in the HMBC spectra were observed between the methoxy protons (δ_H 3.89, δ_C 58.3) and the quaternary carbon (δ_C 165.2, C-4) indicating that the methoxy moiety is attached at this position. Further long range correlations were observed from the methine proton H-3 (δ_H 5.94, δ_C 91.6) to the quaternary carbons C-2 (δ_C 144.8) C-5 (δ_C 112.8) and C-2' (δ_C 122.7). A correlation was observed from the methine H-6 (δ_H 7.43, δ_C 138.6) with quaternary carbon (δ_C 112.8) suggesting that the enamine motif is substituted onto this carbon, requiring the carbons C-2 and C-2' to form the 2-2' bipyrrole bond allowing the structure shown in Figure 2.7 to be determined.
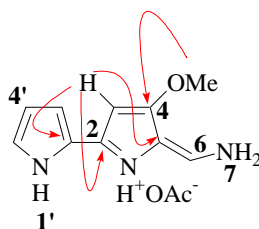
Figure 2.9 Important HMBC correlations used to confirm the structure of ring B in **7.**

Position	δ_C ppm	δ_H ppm	COSY coupling to	HMBC coupling to	Literature data δ_H^4
1	-	-	-	-	-
2	144.8	-	-	-	-
3	91.6	5.94 (s)	-	C-2, C-2', C-5	5.95
4	165.2	-	-	-	-
5	112.8	-	-	-	-
1'	-	10.31	-	-	9.20
2'	122.7	-	-	-	
3'	124.7	7.09, (dd), 3.7, 2.7	H-4', H-5'[*]	C-2', C-5'	7.09
4'	110.6	6.28 (m)	H-5'	C-2', C-3'	6.30
5'	114.1	6.75 (m)	H-4'	C-2', C-3'	6.78
OMe	58.3	3.89 (s)		C-4	3.92
6	138.6	7.43 (s)	-	C-5	7.49
7	-	12.06	-	-	11.30

Table 2.1 The [1]H (400 MHz), ^{13}C (100 MHz) and 2D NMR data obtained for **7** (CDCl$_3$).[*]

[*] see Figure 2.9 for numbering system

2.3 Isolation of 4-methoxypyrrolic metabolites from *B. dentata*

To explore the possible original source of 4-methoxypyrrolic natural products sequestered by *T. capensis*, we investigated extracts of *B. dentata* on which *T. capensis* had been observed grazing in Algoa Bay. *B. dentata* (wet mass –1500 g, dry mass- 217 g) was collected from Algoa Bay using SCUBA in the summer of 2003. The bryozoan was steeped in methanol (2 L) overnight in the dark at –20°C and then filtered to yield the first extract (96.4 g) The animal material was again steeped in methanol overnight and filtered in the same manner to give the second extract (14.8 g). Keeping the first and second extracts separate, the individual extracts were loaded onto an HP-20 column (500 mL, 45 x 5 cm) conditioned with acetone (1.5 L) and methanol (1.5 L).

The HP-20 column packing[64] comprises small cross-lined polystyrene beads and is particularly useful for fractionating aqueous marine extracts which require both the removal of sodium chloride and the concentration on the bead of organic metabolites present in the extract. Once absorbed, these organic metabolites can be sequentially stripped from the HP-20 beads by eluting the column with aqueous acetone eluents of increasing acetone concentration. The advantages of the chromatography technique, commonly known as cyclic loading, are not only that large masses of extract can be successfully processed but also that the beads can be re-used for several consecutive chromatographic runs.

Given the column size, only 15 g of extract in methanol (2 L) were loaded at a time. The eluent (2 L) was then diluted with ammonium acetate buffer (0.1 M, 2 L) and passed through the column. The eluent was again diluted with ammonium acetate buffer (0.1 M, 4 L) and passed through the column. The column was then stripped with 20%, 40%, 60% and 80% acetone/0.1 M ammonium acetate buffer (1.5 L) and 100% acetone. To remove excess water from the eluents making concentration less problematic, in a process termed back-loading, the four eluents were then diluted with 0.1M ammonium acetate buffer (1.5 L) and loaded onto a second HP 20 column (15 cm x 4 cm, 100 mL) and then stripped with methanol (200 mL) and acetone (200 mL).
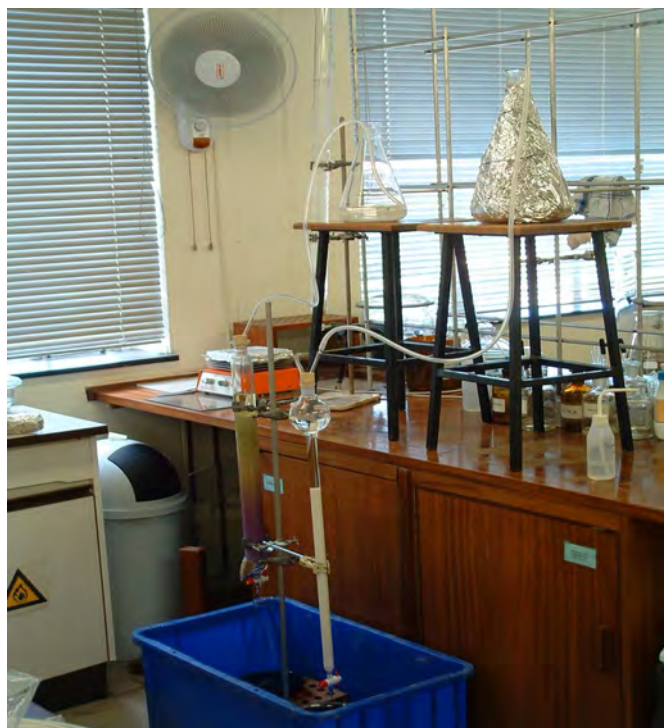
Figure 2.10 The set-up used for HP-20 cyclic loading of *B. dentata* extracts.

The ^{1}H NMR spectra of various fractions (40%, 60% and 80% acetone/ 0.1 M ammonium acetate buffer) showed resonances in the 6-8 ppm region, indicative of tambjamine natural products. From the masses of the samples obtained, only the 60% and 80% acetone/ammonium acetate buffer fractions were chosen to be purified further using semi-preparative C-18 reversed phase HPLC (both gradient and isocratic elution) to give the tetrapyrrole natural product (**15,** 130 mg). Unfortunately, attempts to isolate tambjamine natural products from the 60% acetone/ammonium acetate buffer fractions were unsuccessful, as the fractions were insoluble in methanol, water, or any combination of the two, making this fraction unsuitable for further reversed phase HPLC. In addition, substantial streaking was observed during thin layer chromatography of this fraction on silica plates making the fraction unsuitable for normal phase HPLC. Despite its insolubility in water and methanol, the fraction was soluble in chloroform and the ^{1}H NMR spectrum, acquired in $CDCl_3$, showed a resonance (δ 9.5 ppm) indicative of an aldehyde proton suggesting that the tambjamine natural products had hydrolysed to give aldehydes, a phenomenon previously reported by Carté and Faulkner.[4]

The tambjamine natural products appear to be very susceptible to hydrolysis, for this reason the later reports in the literature of tambjamine natural product isolation use a 0.1 M ammonium acetate buffer for all chromatographic separations. Under these conditions the natural product is isolated as an acetate salt, which appears to be vital for stabilising the enamine motif. In our workup procedure of the bryozoan, ammonium acetate was only added to the water used in the loading and stripping procedure but not to either the methanol or acetone. This means that the fraction of interest, the 60% acetone elution, the ammonium acetate concentration was reduced in the eluting solvent from the required 0.1M to 0.04 M. Furthermore in the back-loading procedure, no ammonium acetate was added to the acetone or methanol used to strip the column, meaning that the tambjamine natural products were probably not present as their acetate salts and for this reason they were more susceptible to hydrolysis. The tetrapyrrole natural product (**15**), which does not have an enamine motif, appeared to be more resistant to hydrolysis allowing it to be isolated in large quantities.

Using HP-20 to fractionate marine extracts as previously mentioned has the advantage that it allows large quantities of extracts to be worked up in a very convenient and time conserving manner. The process of cyclic loading, however, leads to a very large increase in aqueous volume, which could make it unsuitable for compounds such as tambjamines which are very prone to hydrolysis.

2.4 Quantitative analysis of tambjamine and tetrapyrrole metabolites in *T. capensis, B. dentata and B. neritina*

4-Methoxypyrrolic natural products are implicated in the chemical defence of marine invertebrates.[4,20,65] Both tambjamines and tetrapyrrole have been isolated from the nudibranch *T. capensis* and the bryozoan *B. dentata.* This section presents a quantitative study of tambjamines **7**, **13**, **21**, **22** and **15** in specimens of *T. capensis, B. dentata* and *B. neritina* collected from three sites off the South African coast (Figure 2.3). During the SCUBA collections of the marine invertebrates, *T. capensis* was observed grazing on both *B. dentata* and the related species *B. neritina*. *B. dentata* is dark blue-green in colour while the latter species is a dark maroon colour. Although the colour of *B. dentata* would suggest that the green tambjamines and the dark blue tetrapyrrole are sequestered from this species, we deemed it necessary to eliminate *B.*

neritina as a possible source of either the tambjamines or the tetrapyrrole natural product. The details of the organisms collected and the size and locality of the collection are presented in Table 2.2.

Sample Name	Species	Collection Site	Date	Sample Details
TamEL	*T. capensis*	Harbour, East London	1999	10 individuals
TamFB	*T. capensis*	Simonstown, False Bay	2000	15 individuals
TamAB(1)	*T. capensis*	Harbour, Algoa Bay	2001	29 individuals
TamAB (2)	*T. capensis*	White Sands, Algoa Bay	2001	2 individuals
BryAB	*B. dentata*	White Sands, Algoa Bay	2003	Wet mass = 29.5 g
NerAB (1)	*B. neritina*	White Sands, Algoa Bay	2001	Wet mass = 391.2 g
NerAB (2)	*B. neritina*	White Sands, Algoa Bay	2001	Wet mass = 267.8 g

Table 2.2 Nudibranch and bryozoan sample size and collection details.

In order to determine the concentration of the tambjamine and tetrapyrrole content of the *B. dentata, B. neritina* and *T. capensis* specimens, all the samples were steeped in acetone overnight followed by concentration and partioning between dichloromethane and water. The dichloromethane partition was concentrated under reduced pressure and injected onto an analytical reversed phase C-18 HPLC column with a suitable gradient to allow optimum separation of the natural products. The concentration in each of the dichloromethane partitions was calculated by comparing the area under the peaks absorbing at 405 nm and 590 nm against standard curves carefully constructed using standards of the tambjamines **7**, **13**, **21**, **22** and tetrapyrrole natural product (**15**). The wavelengths of 405 nm and 590 nm were chosen to monitor the concentration, as these wavelengths are the λ_{max} of the bipyrrole tambjamine and tetrapyrrole (**15**) natural products respectively. This study makes the assumption that the area of the peaks measured represents only a single compound, and ideally to eliminate this uncertainty a variety of reversed phase columns should be used to give different retention times of the natural products. Unfortunately, time constraints and the unavailability of suitable alternative HPLC columns prevented us confirming the reproducibility of these results under different chromatographic conditions. An

example of a typical chromatograph obtained in the analysis is shown below in Figure 2.11.
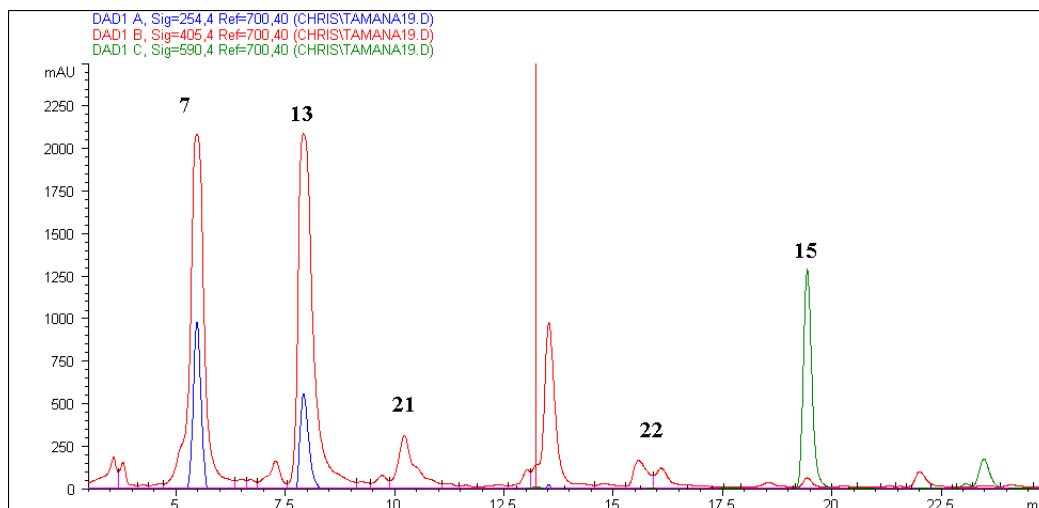
Figure 2.11 Chromatograph obtained for sample TamAB showing the presence of the respective tambjamine natural products.

Table 2.3 clearly indicates that all the samples of *T. capensis* and the *B. dentata* collected from Algoa Bay contained **15** while there appeared to be variation in the tambjamines present in *T. capensis* specimens collected from different localities. All four tambjamines were present in *B. dentata* extracts and neither **15** nor the tambjamines were found in *B. neritina*, thus eliminating the latter species as the source of the sequestered chemistry in *T. capensis*.

Two studies have been carried out investigating the concentration of the 4-methoxypyrrolic natural products in marine invertebrates. Carté and Faulkner collected samples of *T. abdere*, *T. eliora*, and *R. tigris* from the Gulf of California and an unidentified bryozoan from Mexico. They were able to isolate tambjamines A-D (**7–10**) and found that the *Tambja* species showed little variation in the chemical constituents. They reported that the concentration of the tambjamine natural products was lower in that of *R. tigris* and the unidentified bryozoan when compared to that of the nudibranchs.[4]

Sample Name	Extract mass (mg)	Total tambjamine yield (%) (% extract)	Tambjamine A (**7**) (% extract)	Tambjamine E (**13**) (% extract)	Tambjamine K (**21**) (% extract)	Tambjamine L (**22**) (% extract)	Tetrapyrrole (**15**) (% extract)
TamEL	136.9	20.6	0.6	19.2	-	-	0.9
TamFB	219.3	29.8	2.5	6.0	-	14.6	6.8
TamAB(1)	427.1	19.3	9.4	3.6	0.2	0.6	5.6
TamAB(2)	21.6	15.5	7.5	3.0	1.5	3.0	0.5
BryAB	141	15.0	1.8	1.5	1.0	1.2	9.5
NerAB(1)	192.9	-	-	-	-	-	-
NerAB(2)	648.1	-	-	-	-	-	-

Table 2: Tambjamine and tetrapyrrole natural product concentrations in *T. capensis, B. neritina and B. dentata* samples.

Later Paul *et al.* investigated the concentration of tambjamines and the tetrapyrrole natural product from the tropical ascidian *Atapozoa* sp. and its nudibranch predator *Nembrotha* spp. from various locations in the Philippine islands. Interestingly, tambjamine C (**9**) and tambjamine F (**14**) were shown to be present in the highest concentrations and as we have also observed, found the concentrations of the tambjamines varied between collections from different habitats.[24] Interestingly, we found tambjamine A (**7**) and E (**13**) in the highest concentrations, which contradicts the findings of Carté and Faulkner, and Paul *et al.*[4,24]

Paul *et al.* indicated differing deterrent potential of the tambjamines and proposed that a mixture of the natural products was superior to the pure natural product in its deterrent activity.[24] Unfortunately, individual animals were not analysed in our study and we therefore are unable to comment on the selectivity, if any, of individual specimens of *T. capensis* during the sequestration of tambjamines **7**, **13**, **21**, **22** and **15** from *B. dentata*. As would be expected from their sequestering ability, the nudibranchs appear to concentrate the natural products, generally showing higher concentrations than the bryozoan *B. dentata*.

2.5 Conclusion

Attempts to isolate the novel natural products, **21** and **22** from either *T. capensis* or *B. dentata* proved unsuccessful, however the known **7**, **13** and **15** natural products were isolated. Using the 4-methoxypyrrolic natural products isolated in our laboratory allowed a tentative quantitative analysis of the tambjamine and tetrapyrrole metabolites present in the nudibranch *T. capensis* and the bryozoan *B. dentata* which allowed as to demonstrate that *T. capensis* appears to concentrate the metabolites and could sequester the natural products from it bryozoan food source.

In order to complete the structural elucidation of tambjamine L, a synthetic methodology was investigated to enable the synthesis of tambjamine natural products and is described in Chapter 3. The physical properties of the isolated natural products, **13** and **15**, were studied to establish further the mechanism of oxidative DNA cleavage proposed by Manderville and co-workers and to determine the potential of the 4-methoxypyrrolic natural products as photodynamic therapy agents and is presented in Chapter 4.

Chapter Three

Attempted synthesis of 4-methoxyyrrolic natural products

3.1 Introduction

4-methoxy-2,2'bipyrrole carboxaldehyde (**11**), also referred to as the bipyrrole aldehyde in this chapter, is a key precursor in the synthesis of tambjamines (e.g. **7**), the tetrapyrrole natural product (**15**) and prodigiosins (e.g. **1**). Unfortunately, the synthesis of **11** is problematic. Difficulties associated with the synthesis of this compound include firstly the introduction of the methoxy substituent at the C-3 position, secondly the interconversion of the C-2 substituent (usually an ester) to an aldehyde and thirdly the coupling of the A and B rings.[1,2]

Although a number of semi-syntheses of the tambjamines[4,66] and tetrapyrrole[21] natural products have been reported, a total synthesis of both the tambjamine and tetrapyrrole natural products remains elusive. Conversely, total synthesis of prodigiosin and its analogues have regularly appeared in literature and are reviewed here.

3.2 Synthetic approaches to prodigiosin

The synthetic approaches to prodigiosin follow two distinct paths; a biomimetic approach in which **11**, the biosynthetic intermediate, is the initial goal and the more recent cross-coupling approach in which **11** is not a target.[2] Retrosynthetic analyses of these two approaches are presented in Schemes 3.1 and 3.2.
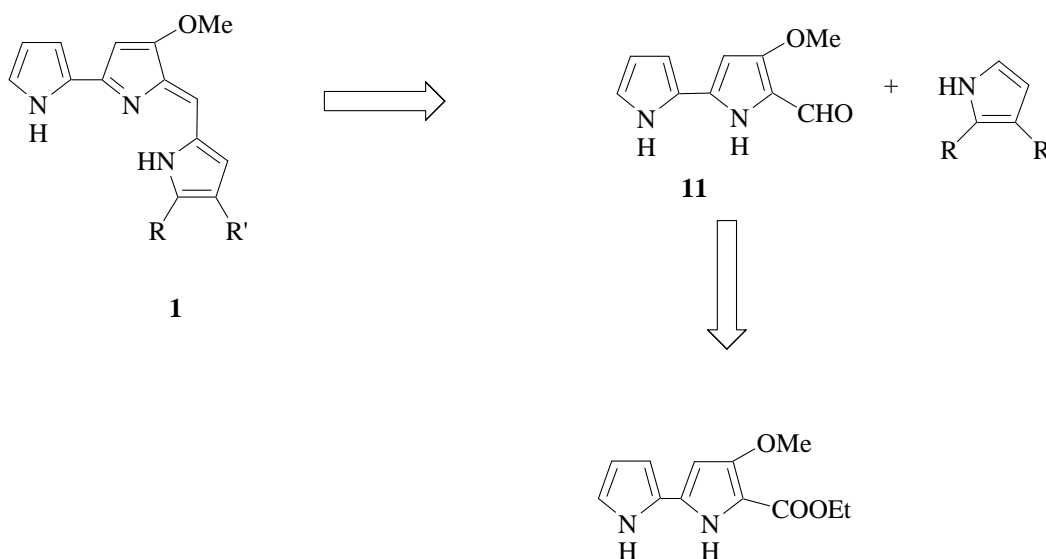
R, R' = alkyl substituents

Scheme 3.1 Retosynthesis of prodigiosin (**1**): a biomimetic approach.
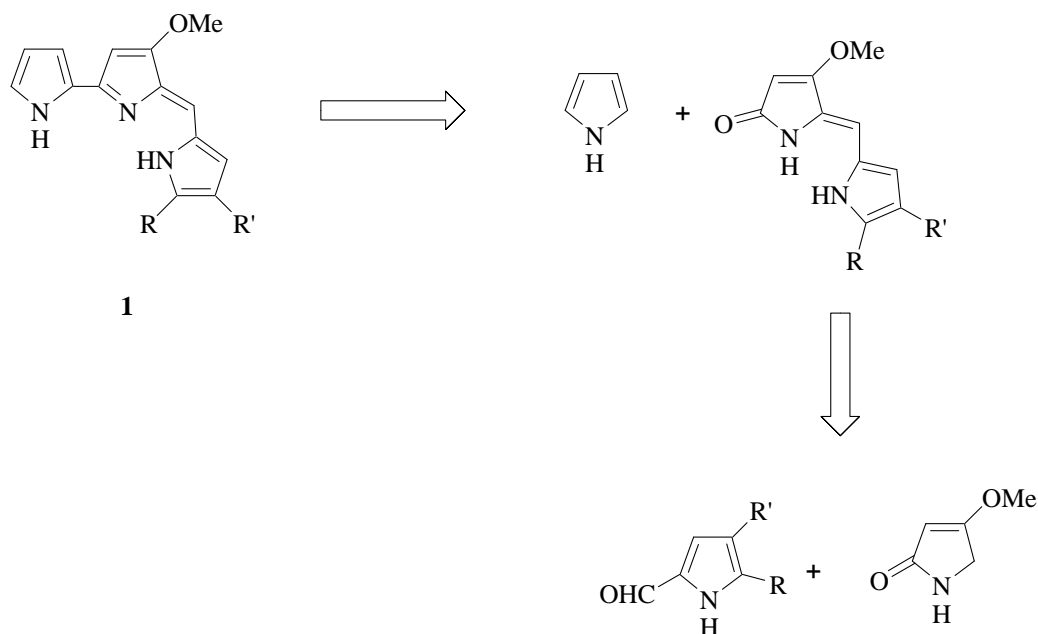
R, R' = alkyl substituents

Scheme 3.2 Retrosynthesis of prodigiosin (**1**): the cross-coupling approach.

3.2.1 Synthesis of prodigiosin using biomimetic condensation reactions

Rapoport and Holden reported the first total synthesis of prodigiosin (**1**) in 1962 (Scheme 3.3). In their ground breaking synthesis which confirmed the structure of prodigiosin (**1**), they targeted 4-methoxy-2,2'-bipyrrole carboxyaldehyde (**11**) as a key intermediate. The intermediate was prepared firstly by the condensation of diethyl ethoxymethylenemalonate (**23**) with the sodium salt of diethyl N-ethoxycarbonyl glycinatinate (**24**) to produce diethyl 3-hydroxypyrrole-2,4-dicarboxylate (**25**) in low yield. This transformation was proposed to proceed through an initial Michael addition followed by the loss of ethoxide and ring closure. Methylation of **25** with diazomethane, followed by selective removal of the ester substituent at C-4 through hydrolysis and subsequent decarboxylation yielded 3-methoxy-2-ethoxycarbonylpyrrole (**26**). This selective hydrolysis was not commented on by the authors, however Boger later proposed that the selectivity observed could be accounted for by the greater electronic and steric accessibility of the C-4 substituent.[27] The low yielding coupling of the A and B rings was achieved *via* reaction of **26** with pyrroline, subsequent dehydrogenation of the coupled

product yielded ethyl-3-methoxy-2,2'-bipyrrole-5-carboxylate (**27**). The conversion of **27** to the corresponding aldehyde **11** could only be achieved using the low yielding (32%) McFayden-Stevens reduction which involved the treatment of **27** with anhydrous hydrazine followed by *p*-toluenesulfonyl chloride.[67] The final step in the synthesis of the prodigiosin natural product was the acid-catalysed condensation of **11** with 2-methyl-3-amylpyrrole (**28**).[7]
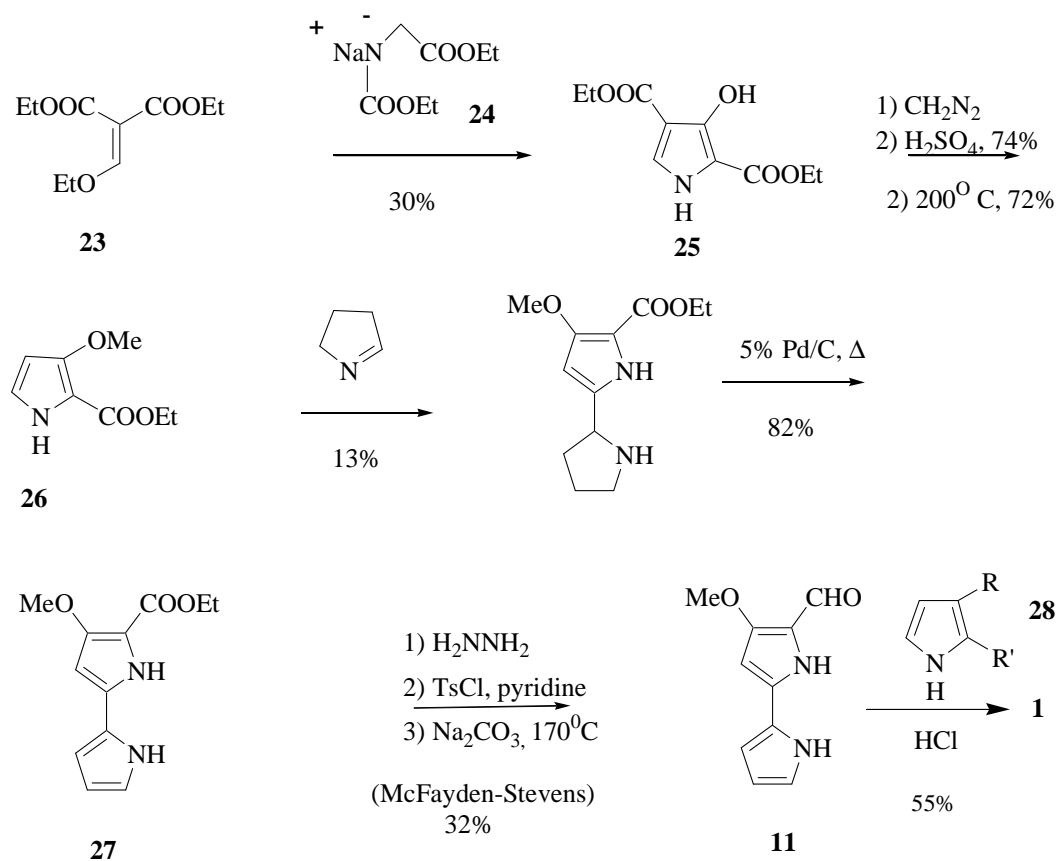
R, R' = alkyl substituent

Scheme 3.3 The total synthesis of prodigiosin (**1**) by Rapoport and Holdern.[7]

Despite the major breakthrough that this synthesis represented, the difficulties that have continued to plague the synthesis of the 4-methoxypyrrolic natural products were the low yielding ring coupling and McFayden-Stevens reduction steps. After this initial synthesis there were no more syntheses reported in literature until the late 1980s, when Brown *et al.* were able to synthesise N-substituted prodigiosin derivatives.[68] These derivatives

however lacked the methoxy substituent which has been shown to be essential for the bioactivity of prodigiosin type compounds.[28]

In the late 1980s Boger and co-workers and Wasserman *et al.* detailed two different approaches to the synthesis of the 4-methoxy-2,2'-bipyrrole carboxyaldehyde (**11**). Boger and co-workers' approach (Scheme 3.4) utilised the inverse-electron demands of the Diels-Alder reaction to form the Diels Alder cycloadduct (**29**) from reaction of 1,2,4,5-tetrazine-3,6-dicarboxylate (**30**) with 1,1-dimethoxyethylene (**31**).[27,28,30]
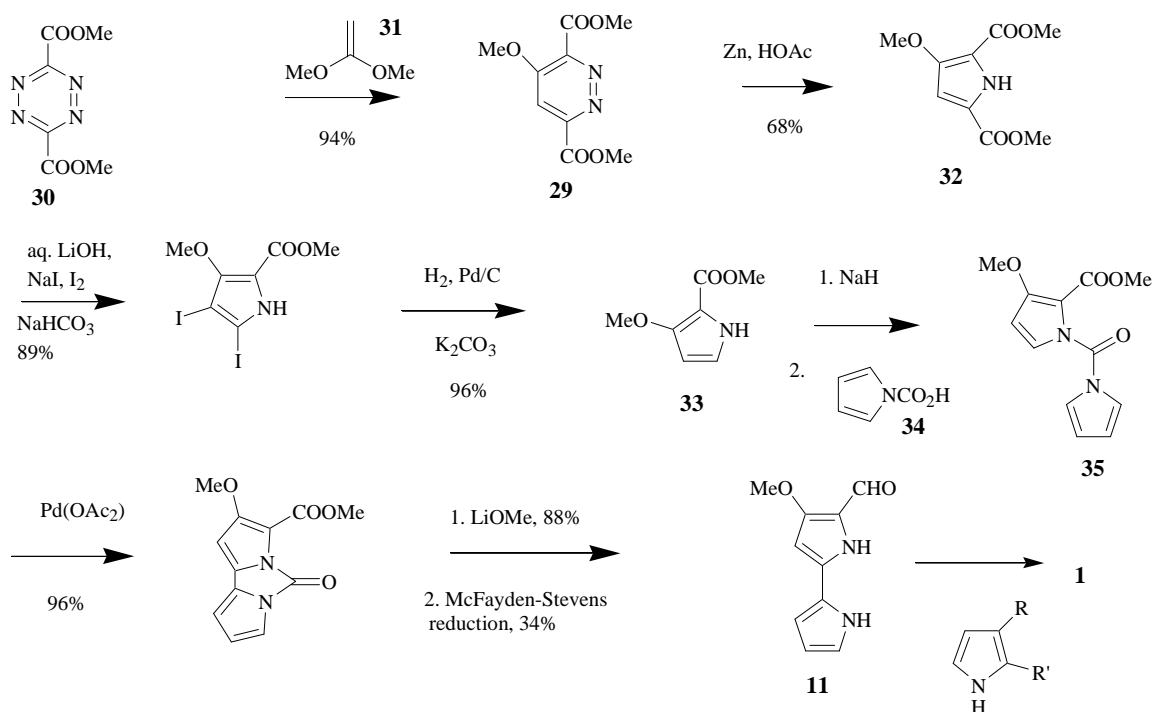
R and R' = alkyl substituent

Scheme 3.4 Boger and Patel's synthesis of prodigiosin.[28]

Zinc catalysed ring contraction gave dimethyl-3-methoxypyrrole-2,5-dicarboxylate (**32**). One of the ester groups was removed through selective hydrolysis with aqueous lithium hydroxide. Iodinative decarboxylation followed by hydrogenolysis yielded 3-methoxy-2-(methoxycarbonyl)pyrrole (**33**). An intramolecular palladium(II)-promoted 2,2'-bipyrrole coupling was employed to join the A and B rings. Coupling was achieved through initial reaction of the sodium salt of **33** with pyrrole-1-carboxylic acid (**34**) to

give **35**. Triphenylphosphine-tetrachloride and polymer supported palladium(II)acetate quantitatively promoted the required 2,2' coupling in **35**. Lithium methoxide was used to effect decarboxylation, while the low yielding McFayden-Stevens reduction was employed to convert the methyl ester into the aldehyde (**11**).[27,28,30]

Wasserman and co-workers developed two separate approaches to the synthesis of the bipyrrole aldehyde (**11**). The first of these approaches, shown in Scheme 3.5, involved the synthesis of the key intermediate (**36**) *via* treatment of the toluenesulfonyl pyrrole-2-carboxyaldehyde derivative (**37**) with the dianion of ethyl acetoacetate followed by dehydration with gaseous hydrochloric acid in chloroform. The activated methylene in the side chain was then oxidised with N,N-dimethyl-*p*-nitrosoaniline in ethanolic sodium hydroxide. Ring closure was achieved in low yield with 3,4-dimethoxybenzylamine in acetic acid. The bimethoxybenzyl group was removed using Evan's procedure which involved oxidation with sulphuric acid. The ether ester bipyrrole (**27**) was generated following detosylation using ethanolic sodium hydroxide. The ring closing step, which indirectly gave rise to the coupling of the A and B rings, was again a low yielding reaction while the reduction of the ester moiety to the aldehyde to give **11** again required the unsatisfactory low yielding McFayden-Stevens reduction.[67, 69]

Wasserman and co-worker's second approach involved using singlet oxygen ($^1O_2$) to oxidise *tert*-butyl 3-methoxypyrrole-2-carboxylate (**38**) (Scheme 3.6). The proposed intermediate (**39**) was more susceptible to electrophilic attack by pyrrole to give the coupling of the A and B rings in moderate yields.[70-72] The synthesis of **38** was achieved through the reaction of ammonia with a vinyl tricarbonyl ester to give **40** which was simply converted to **41** with dehydrating reagents such as silica gel.[69,70] This simple two-step procedure represented a vast improvement on previously used methods of synthesising the B-ring of **11**. Methylation was quantitatively achieved with sodium hydride and dimethyl sulphate. Interestingly, the formation of the C-3 methyl ether gave higher yields when the butyl ester was used when compared to other esters.[70]
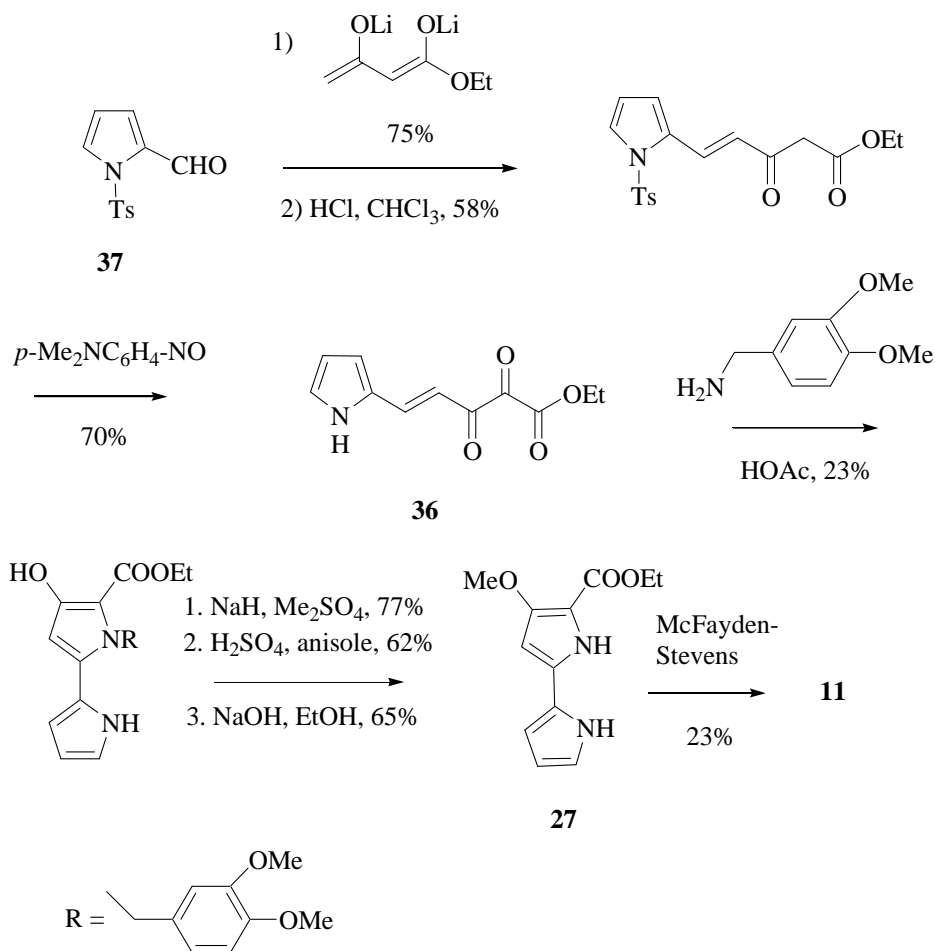
Scheme 3.5 Wasserman and co-workers vicinal tricarbonyl route to bipyrrole aldehyde (**11**).[69]
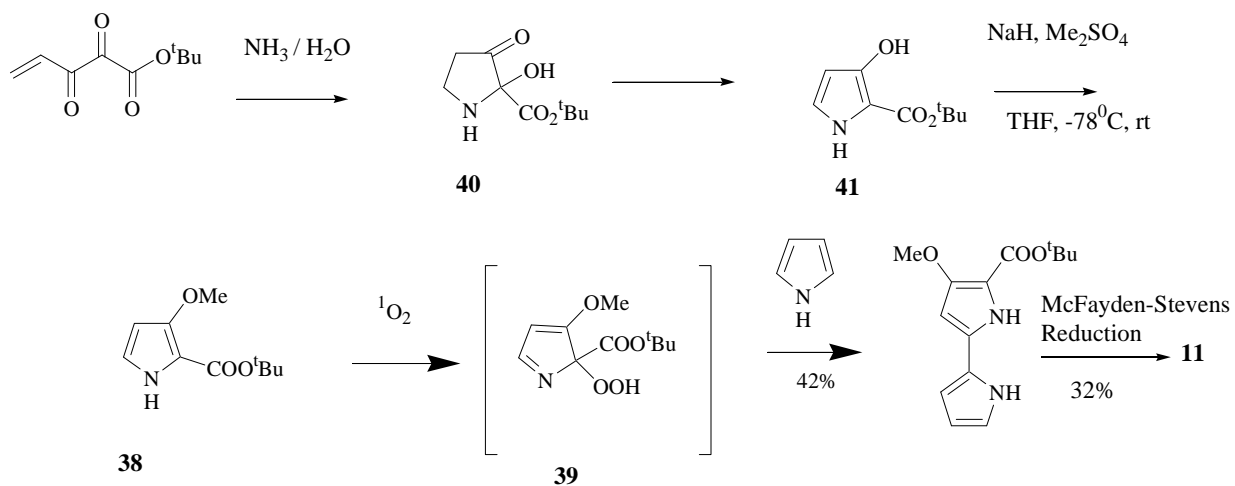
Scheme 3.6 Wasserman and co-workers singlet oxygen oxidation approach to bipyrrole aldehyde (**11**).[72]

Although Wasserman and Boger provided alternative routes for the synthesis of the bipyrrole aldehyde (**11**), the approaches still relied on the poor yielding McFayden-Stevens reduction as the final step.[67] Despite the problems in both Wasserman's and Boger's approaches, they were used in the synthesis of a variety of synthetic analogues of prodigiosin[28,69,72] for example streptorubin B (**4**).[9] The synthesis of these prodigiosin analogues allowed an investigation of the structure-activity relationships and hence the structural requirements for the bioactivity of this group of compounds.

3.2.2 Syntheses of prodigiosin *via* cross-coupling reactions

The synthesis of prodigiosin by cross-coupling reactions was pioneered by D'Alessio and co-workers in an attempt to optimise the immunosuppressive properties of prodigiosin (Scheme 3.7). The approach was developed to avoid the poor yielding McFayden-Stevens reduction and allow a combinatorial synthetic approach, more applicable for the synthesis of a large number of analogues. Rather than incorporating **11**, they targeted the enelactam **42** as their precursor of prodigiosin. Suzuki coupling reactions were employed to couple the A and B rings. This four step synthesis could easily be scaled up allowing them to produce a large number of derivatives relatively easily.[73]

Compound **43**, obtained via Vilsmeier formylation of 2-undecylpyrrole, was condensed with the commercially available pyrrolinone (**44**) to produce predominantly the Z-enelactam. (**42**) The triflate group required for the Suzuki coupling was introduced with triflic anhydride and Suzuki cross-coupling was performed using the N-Boc pyrrole-2-boronic acid (**45**). Various cross-coupling methodologies were attempted and interestingly Stille conditions were found to be unsuitable. The basic conditions of the reaction allowed Boc-deprotection to take place in the same step.[73] D'Alessio and co-workers' route was successful and allowed the synthesis of many different prodigiosin analogues including PNU-156804 (**20**), which has shown superior immunosuppressive properties and low cytotoxicity compared to the naturally occurring prodigiosins.[56,73,74]

Fürstner and co-workers used a similar cross-coupling approach to synthesise the macrocyclic nonylprodigiosin. The flexibility of the method allowed the generation of

many synthetic analogues incorporating aromatic rings other than pyrrole into their backbone.[2,75,76]
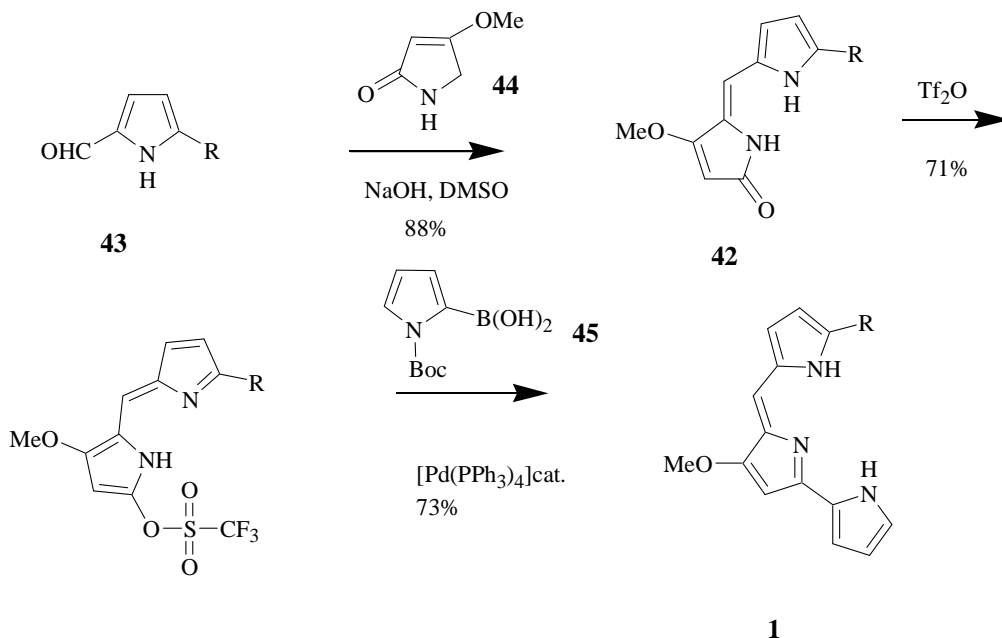
R = alkyl substituent

Scheme 3.7 D'Alessio and co-workers cross-coupling approach to the synthesis of prodigiosin.[73]

3.3 Semi-syntheses of tambjamine and the tetrapyrrole natural products

3.3.1 Semi-synthesis of the tetrapyrrole natural product (15)

Only one synthesis of the tetrapyrrole natural product has been reported in the literature. Wasserman *et al.* synthesised the tetrapyrrole (**15**) via condensation of 4-methoxy-2,2'-bipyrrole (**46**), prepared by the soda-lime distillation of prodigiosin, with 4-methoxy-2,2'-bipyrrole aldehyde (**11**) in ethanolic hydrochloric acid (Scheme 3.8).[21]
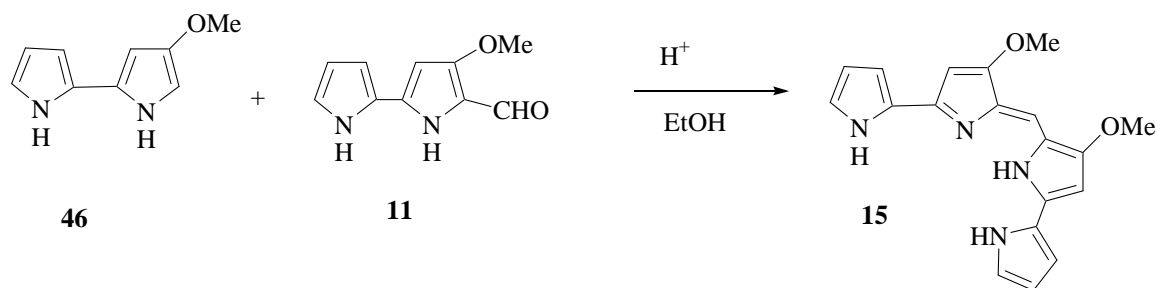
Scheme 3.8 Wasserman and co-workers semi-synthesis of tetrapyrrole natural product (**15**).

3.3.2 Semi-synthesis of tambjamine natural products

During their isolation of tambjamine natural products from nudibranchs, Carté and Faulkner also obtained the bipyrrole aldehyde (**11**), which they proposed was not a natural product but rather an artifact formed from the hydrolysis of the corresponding naturally occurring enamines i.e. tambjamines during the isolation. They were able to convert the bipyrrole aldehyde (**11**) into the respective tambjamines through treatment of **11** with the relevant amine using chloroform as the solvent in the presence of molecular sieves.[4] Using the bipyrrole aldehyde (**11**) as a template, Davis *et al.* were able to generate a tambjamine natural product combinatorial library by designing a semi-synthesis which avoided silica-based chromatography and used a simple liquid-liquid purification. Acid conditions were used, under which the enamine salt was preferentially soluble in dichloromethane, whilst the ammonium acetate was more soluble in water, allowing for a simple separation of these two salts as shown in Scheme 3.9.[66]
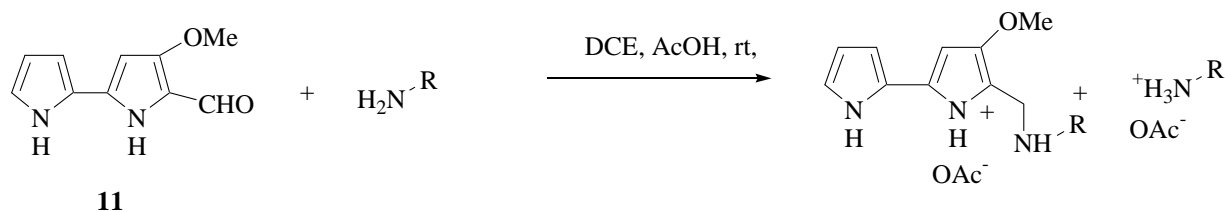
R = alkyl

Scheme 3.9 Davies *et al.* synthesis of a tambjamine combinatorial library.

3.4 An approach to the synthesis of tambjamine L (22)

Our interest in the synthesis of tambjamine natural products isolated from *T. capensis* arose from the paucity of the natural product, **22**, which hampered complete structural elucidation and investigations of biological activity of this compound. The bipyrrole aldehyde (**11**) was chosen as our initial target, as conversion to the enamine natural products had been shown to be a facile, high yielding procedure from **11**.[66] Wasserman's approach using singlet oxygen oxidation to drive the bipyrrole coupling[72] attracted us because of the expertise at Rhodes University in the development of dyes for photodynamic therapy, which in the presence of red laser light are able to generate singlet oxygen as a cytotoxic species.

Bellamy *et al.* reported the synthesis of 3-methoxy-2-formylpyrroles (**47**) from substituted pyridine N-oxide (**48**) with irradiation in the presence of copper sulfate.[77] This reaction was attractive to us as it produced in one step the B-pyrrole ring of **11** with the methoxy moiety in the correct position and the aldehyde functionality, rather than the ester moiety thereby potentially avoiding the poor yielding McFayden-Stevens reduction at a later stage in the synthesis.[67] Furthermore, 3-methoxypyrridine-N-oxide (**48**) is a cheap, commercially available starting material. Our proposed method of synthesising **22** is shown in Scheme 3.10.

The synthesis of 3-bromopyrrole (**49**) is not straightforward and therefore tambjamine K (**21**), in which the A ring is an unsubstituted pyrrole, was chosen as the initial synthetic target to develop the synthetic methodology.
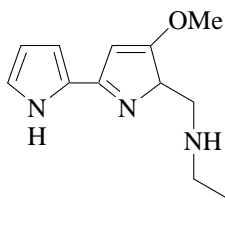
21
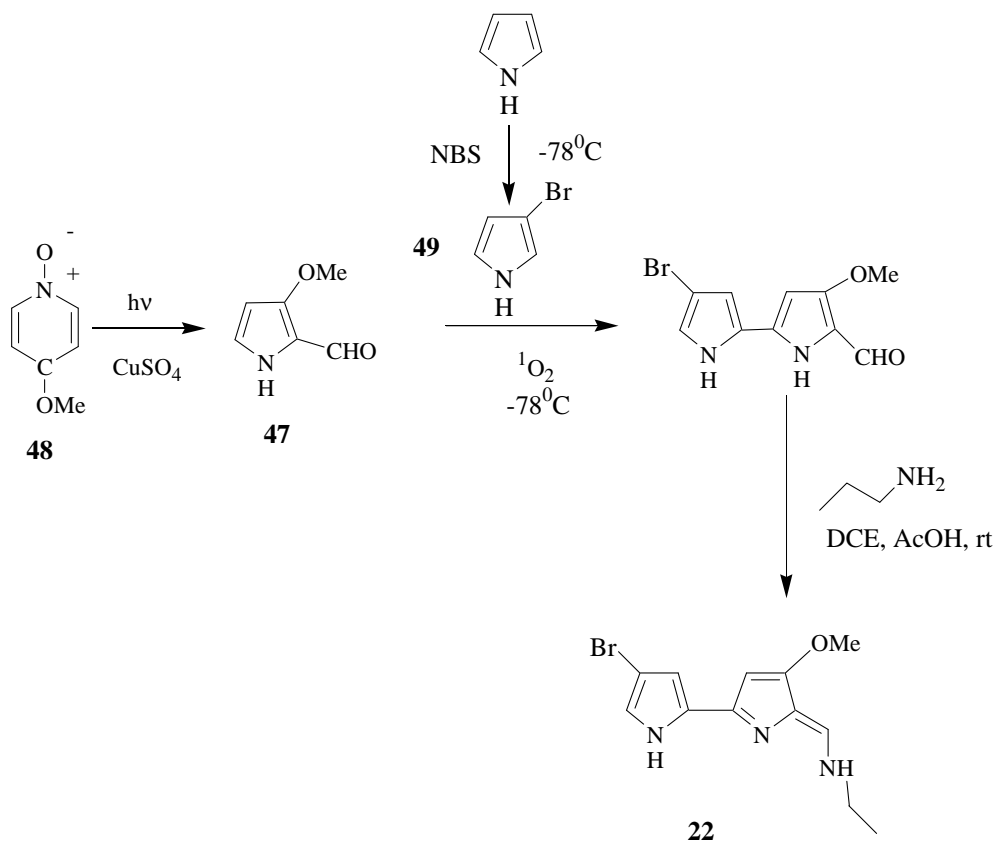
Scheme 3.10 Proposed pathway for the synthesis of tambjamine L (**22**).

3.5 Synthesis of 3-methoxy-2-formyl pyrrole (47)
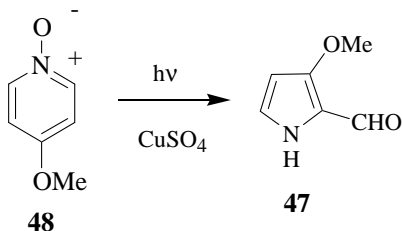
The synthesis of 3-methoxy-2-formyl pyrrole was carried out as per the published procedure of Bellamy *et al.* by irradiating an aqueous solution (400 mL) of **48** (2 g, 15.8 mmole) and copper sulfate (40 g, 15.8 mmole) in a classical immersion well-photoreactor at room temperature (see Figure 3.1).

Figure 3.1 The immersion well-photoreactor used to synthesise 3-methoxy-2-formyl pyrrole (**47**).

The decrease in the amount of starting material (**48**) present in the reaction mixture was followed using UV-spectroscopy (see Figure 3.2). Shortly after beginning the irradiation, the blue copper sulfate solution changed to a green colour from the formation of the green copper-pyrridine-N-oxide complex.[77] After irradiation (4-9 hr), the aqueous solution was saturated with sodium chloride and partitioned with chloroform. Compound **47** was obtained in a crude yield of 40%, the major product of the reaction was a black intractable gum soluble in neither water nor chloroform. The ^{1}H NMR (DMSO-D$_6$) of this black gum was complex and suggested that the gum was polymeric in nature. 3-Methoxy-2-formylpyrrole was successfully purified by sublimation (100°C, 2.5 mmHg) to yield a white crystalline product (m.pt 109°C, Lit 120°C[77]). The ^{1}H NMR showed a

non-exchangeable resonance (δ 9.51) indicative of an aldehyde proton and an exchangeable NH resonance (δ 10.3).
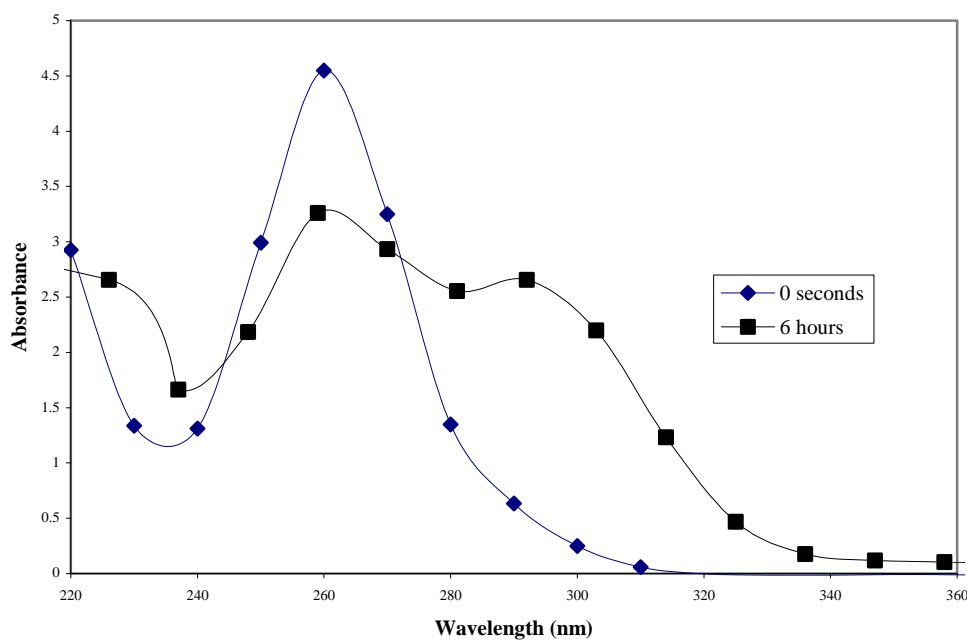
Figure 3.2 The UV spectrum of the photoirradiation reaction showing the decrease in the λ_{max} of **48** (260 nm) and the increase in the λ_{max} of **47** (298 nm).

Bellamy *et al.* proposed a mechanism for the ring contraction of **48** to give **47** (Scheme 3.11). In this mechanism, the intermediate (A) can either isomerise to an acrylonitrile or undergo a ring contraction to form the pyrroline (B). The copper salt is thought to interact with the intermediate (A) through a reversible electron transfer, thus driving the ring contraction.[77]
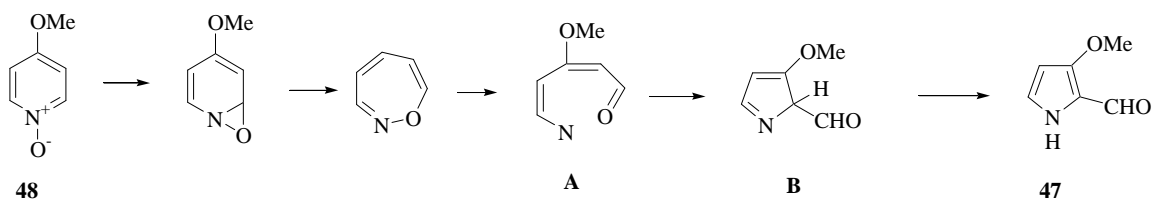
Scheme 3.11 Proposed mechanism of ring contraction during photoirradiation of **48**.[77]

Despite the relatively low yields of **47** obtained from this light induced ring contraction procedure, the ready availability of **48**, the ease of work-up and purification made the procedure a very attractive starting point for the synthesis of tambjamines.

3.6 Bipyrrole coupling using singlet oxygen oxidation

3.6.1 Attempted synthesis of 11 from 47
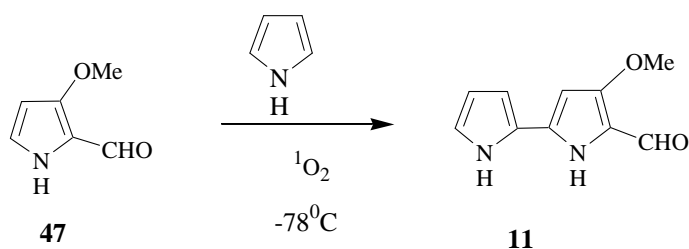
3.6.1.1 Methylene blue as a singlet oxygen producer

The bipyrrole coupling was then attempted following a similar procedure to that reported by Wasserman *et al* (Scheme 3.6).[72] The reaction was performed by stirring (10 min) a solution of **47** (20 mg, 160 μmole) and methylene blue (1 mg) in dichloromethane (20 mL) at room temperature to allow the methylene blue to dissolve. The solution was subsequently cooled (–78°C) and purged with oxygen (10 min). Irradiation (30 min) of the cold solution was carried out using a 350 W Tungsten light with a red filter to optimise the wavelength of light for methylene blue to generate singlet oxygen while preventing photodegradation. Oxygen was continually bubbled through the solution from a balloon (Figure 3.3). Although Wasserman *et al.* reported that a decrease in the starting material was observed following irradiation,[72] no apparent decrease or change was observed on either silica or C-18 TLC plates.

Figure 3.3: Apparatus used in the photooxidative bipyrrole coupling reaction.

Following irradiation, cold (-78°C) pyrrole (45 µL, 400 µmole) in dichloromethane (2 mL) was added and the solution was allowed to warm up to room temperature and stirred (1 hr). The methylene blue was removed by filtration through celite and the filtrate concentrated under reduced pressure. Chromatography of the concentrated filtrate (C_{18} Sep-Pak eluted with water, 25%, 50%, 75% aqueous methanol and methanol) yielded five fractions. ^{1}H NMR analysis of these chromatographic fractions revealed that the pyrrole products were confined to the 25% aqueous methanol fraction, which contained predominantly unchanged **47**. There was no spectroscopic evidence (NMR and UV) that suggested any oxidation of **47** to 3-methoxy-2-pyrrole carboxylic acid had occurred. The presence of the unchanged starting material was confirmed by UV-spectroscopy which showed a peak at 298 nm indicative of the **47**. Additional absorbances (λ_{max} 350 nm and 450 nm) were of interest as they are similar to that of tripyrrole **1** (λ_{max} 450 nm). ESIMS

(Electrospray ionisation mass spectrometry) in the positive ion mode conclusively showed that the **47** was the major product of the reaction from the peak observed at *m/z* 126.0.

The addition of a small amount of pyridine has been reported to enhance photooxidation reactions.[78] The addition of 3 drops of pyridine to the reaction mixture had no influence on our reaction, nor did the removal of the red filter. The singlet oxygen production of methylene blue under the experimental conditions was determined using the method described in Chapter 4 and was found to be similar to those reported in literature.[79]

3.6.1.2 Zinc phthalocyanine as a singlet oxygen producer

Following the apparent lack of observed reactivity of **47** at -78°C, the procedure was modified to use a solution of zinc phtalocyanine in DMSO-D_6 with irradiation at room temperature to produce singlet oxygen. The singlet oxygen production of zinc phtalocyanine has been well studied at Rhodes University. Deuterated solvents have been reported to increase the triplet lifetime of photo-excited compounds, as described in Chapter 4, and so it was hoped that this solvent would improve the success of the reaction. Furthermore, the use of DMSO-D_6 also allowed an easy method to follow the reaction using NMR without out any prior chromatographic work-up, which was suspected as being a possible source of decomposition of the bipyrrole if it had formed in the reaction.

The reaction was performed by dissolving **47** and zinc phthalocyanine in DMSO-D_6, purging the solution with oxygen for 10 minutes and then irradiating using a 350 W tungsten lamp with a red filter. Following irradiation (20 min), pyrrole was added and the solution was stirred (1 hr) at room temperature. The ^{1}H NMR spectrum showed resonances consistent with **47** and zinc phthalocyanine with no other major products suggesting that **47** had not reacted under the modified reaction conditions.

The unusual stability of **47** could possibly be explained by the 3-methoxy functionality and the pyrrole NH taking part in a vinylogous ester or amide reaction with the aldehyde

carbonyl.[80] The stability of vinylogous esters and amides is well established.[81,82] Figure 3.4 shows possible vinylogous esters (**49**) and amide (**50**) canonical structures of **47**.
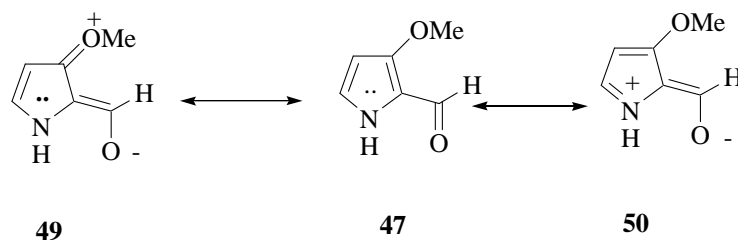
Figure 3.4: Possible vinylogous ester (**49**) and amide (**50**) canonical structures of **47**.

Given the stability of **47** in the singlet oxidation reduction and our reluctance to convert the aldehyde to the ester, to avoid the McFayden-Stevens reduction, alternative modifications to **47** were investigated to counter the stability of the vinylogous systems thought to be hampering the coupling of **47** to pyrrole.

3.6.2 Modifications of 47 to improve reactivity

3.6.2.1 Attempted 2,2-bipyrrole coupling *via* singlet oxygen oxidation of the 2-propylimino-3-methoxypyrrole (51)

Given the unreactivity of the **47** to oxidation with singlet oxygen, the aldehyde functionality was first converted into the propyl imine (**51**) in an attempt to improve the reactivity of **47** by masking the aldehyde functionality. This conversion had the added advantage of providing the complete right hand hemisphere of tambjamine K (**21**).
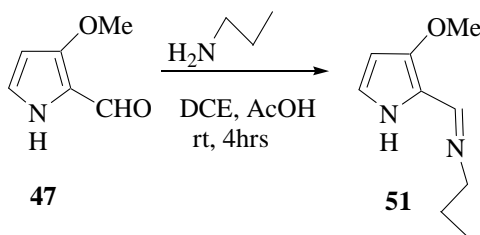
The synthesis of the **51** was a modification of the method reported by Davis *et al.*[83] Compound **47** (10 mg, 80 µmole) was added to anhydrous 1,2-dichloroethane (1-2 mL) under constant argon followed by the propylamine (66 µL, 800 µmole) and acetic acid

(46 µL, 800 µmole). The solution was then stirred (4 hr) at room temperature, and partitioned between aqueous sodium carbonate (10% w/v) and dichloromethane. The dichloromethane partition layer was then concentrated under vacuum, which removed most of the unreacted amine. Although Davis *et al.* reported a quantitative conversion of the bipyrrole aldehyde (**11**) to enamine,[66] the best conversion we obtained was 95% (established from ^{1}H NMR by comparing the integration of the aldehyde proton δ_H 9.51 with the enamine proton δ_H 8.04). The amount of acetic acid added was crucial to obtaining an acceptable conversion because of the competing reverse hydrolysis reaction. Optimum conversion was obtained when the quantity of acetic acid was added in slightly less than the 10 molar equivalence reported by Davis *et al.*[66] Attempts to purify the enamine using a C-18 Sep-Pak were unsuccessful as only **47** was obtained, suggesting that hydrolysis either occurs on contact with the column packing material or in the aqueous eluting solvents. Consequently, we decided that given the almost quantitative yield of **51** the reaction mixture was not purified further prior to the singlet oxygen reaction.

Wasserman's singlet oxygen coupling reaction was then attempted using similar reaction procedures to those described for the attempted photooxidation of **47**. In a typical reaction, **51** (20 mg, 120 µmole) was dried on a freeze drier and then dissolved in anhydrous dichloromethane (20 mL), methylene blue (1 mg) was then added and the solution was stirred (10 min) at room temperature. The solution was then cooled to –78°C and purged with oxygen (10 min) prior to irradiation (30 min) using a 350 W tungsten light with a red filter under a constant flow of oxygen. Cold pyrrole (20 µL, 600 µmole) in dichloromethane (3 mL) was added and the solution allowed to warm to room temperature, followed by stirring (1 hr). The methylene blue was removed by filtration through celite 535. The ^{1}H NMR of the reaction solution showed a plethora of peaks in the region of interest (5-8 ppm) while UV analysis showed absorbances at 296 nm (starting material) and 330 nm, suggestive of a possible bipyrrole product. Once again ESIMS was used to analyse the products of the reaction. A major peak at *m/z* 248.7 in the ESI (positive ion mode) mass spectrum and was attributed to the structure of **52**. Substitution of an alcohol group at the C-5 position such as that in **52** has been reported

by Wasserman and co-workers in similar photooxidation reactions when the peroxide intermediate (Scheme 3.6) is reduced to an alcohol.[70,71]
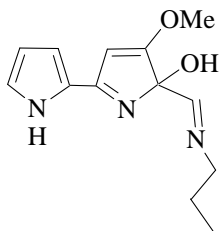
52

Disappointingly, attempts to isolate **52** using reversed phase HPLC were fruitless, with once again only **47** being isolated from the reaction mixture. It was concluded that although the results from ESIMS looked promising, the enamine **51** was too unstable to work with.

3.6.2.2 Lithium aluminium hydride reduction of 47

In an attempt to obtain a stable, reactive compound which could be used in the singlet oxygen oxidative coupling, the conversion of the aldehyde to the primary alcohol (**53**) was attempted.
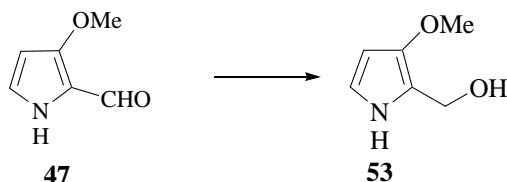
The reduction was first attempted by dissolving **47** (40 mg, 320 µmole) in anhydrous tetrahydrofuran (1 mL), following which lithium aluminium hydride (12 mg, 320 µmole) dissolved in anhydrous tetrahydrofuran (1 mL) was added dropwise *via* a canula at $0°C$. The reaction mixture was then warmed to room temperature and stirred (2 hr), before 5 drops of dilute hydrochloric acid were added. The reaction mixture was then partitioned between ethyl acetate and water and the ethyl acetate partition, washed three times with water to remove any unreacted acid. Both TLC and ^{1}H NMR indicated that no reduction had occurred and the major product was again **47**.

The procedure was then modified such that the reaction mixture was refluxed (1 hr) resulting in a dark red aqueous soluble, possibly polymeric product. None of the expected reduction product **53** formed in this reaction as evidenced by NMR analysis, disappearance of the aldehyde proton (δ_H 9.51) and appearance of a deshielded oxymethylene singlet would have indicated success of the reaction.

3.6.2.3 Preparation of the acetal derivative (54)

Again in the hope to improve the reactivity of the starting material in the photooxidation reaction, the protection of the aldehyde moiety as an acetal (**54**) was attempted.
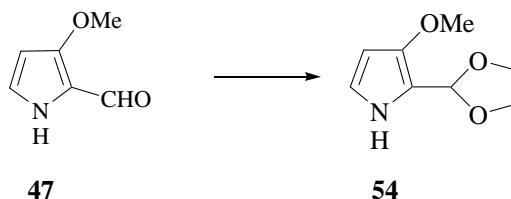
The protection was carried out using a standard procedure[84] by dissolving **47** (60 mg, 0.5 mmole), ethylene glycol (175 μL, 2.9 mmole) and *p*-toluene sulphonic acid (5 mg, 26 μmole) in anhydrous benzene (30 mL). The reaction solution was refluxed (24 hrs) with a Dean-Stark trap. The solution turned a dark red colour and a black solid precipitate formed suggesting that polymerisation had again occurred.

3.6.2.4 Attempted 2,2'-bipyrrole coupling *via* the singlet oxygen oxidation of the N-Boc protected derivative (55)

The unusually high stability of **47** was thought to be due to the vinylogous ester and amide resonance discussed earlier. It was thought that that use of the butyl ester derivative, **38**, as used by Wasserman, could have either prevented the delocalisation of electrons through the electron rich ester group or alternatively the bulky tertiary butyl group could alter the planar relationship between the pyrrole ring and the carbonyl substituent thus preventing resonance as the 2p orbitals were no longer aligned for optimal overlap. Given our reluctance to convert **47** to an ester, requiring the low yielding MacFayden-Stevens reduction back to the aldehyde at a later stage we proposed

an alternative approach that would remove electron density from the pyrrole ring and negate stable vinylogous amide/ester formation. N-Boc protection is a common procedure used to protect amines. It was hoped that the addition of the Boc group would both decrease the electron density in the pyrrole ring and provide a sterically bulky tertiary butyl group to force the aldehyde carbonyl group out of plane with the pyrrole ring. A modified procedure described by Davis for the N-Boc protection of pyrrole-2-carbaldehyde was followed.[83] Davis's procedure required mixing equimolar equivalents of di-*tert*-butyldicarbonate and pyrrole-2-carbaldehyde at room temperature. When the reaction was performed in our laboratory under these conditions, using pyrrole-3-methoxy-2-carbaldehyde, a yield of only 40% of the N-Boc protected pyrrole-3-methoxy-2-carbarldehyde was obtained in addition to some insoluble dark material suggestive of polymerisation. The increased polymerisation was attributed to the higher reactivity of **47** due to the methoxy substituent compared to pyrrole-2-carbaldehyde. In a successful attempt to reduce polymerisation, the procedure was modified to use a slight excess of di-*tert*-butyldicarbonate and lowering of the reaction temperature to 0°C as follows:
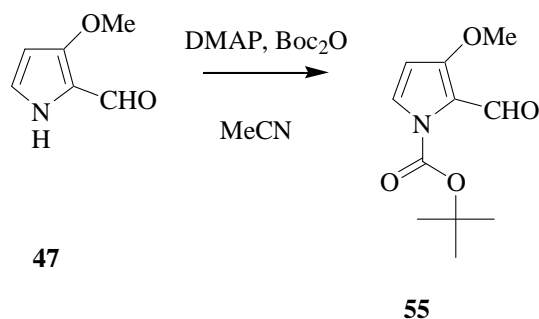
Compound **47** (140 mg, 1.12 mmole) was dissolved in acetonitrile (5 mL) and the solution cooled to 0°C, 4-dimethylaminopyridine (13 mg, 0.11 mmole) and di-*tert*-butyldicarbonate (366 mg, 1.68 mmole) were added and the solution was stirred (2 hr, 0°C) under argon. The reaction solution was concentrated and then purified using a silica flash column (100 x 10 mm), eluting with firstly using 100% hexane and secondly 100% dichloromethane. Compound **55** eluted in the 100% dichloromethane fraction and after evaporation *in vacuo* afforded white crystalline **55** (m.pt 74°C) in 97% yield.

The attempted singlet oxygen oxidation to give bipyrrole coupling was carried out in a similar way to that reported earlier in this chapter for the compound **47**. Compound **55** (20 mg, 93 μmole) was dissolved in dichloromethane (10 mL), cooled (-78°C) and purged with oxygen (10 min). The solution was irradiated using a tungsten lamp with a red filter (20 min, -78°C) under a constant steam of oxygen. Pyrrole (30 μL, 466 μmole) in cold dichloromethane (3 mL) was added under nitrogen and stirred (2 hr) allowing the temperature of the solution to rise to room temperature. Following concentration under reduced pressure, the ^{1}H NMR spectrum of the reaction showed a plethora of peaks in the 6-8 ppm region characteristic of pyrrole type compounds. High resolution FABMS was used to determined the presence of the required compound in the reaction mixture. A peak *m/z* 291.1345 was observed and supported a molecular formula of $C_{16}H_{18}N_2O_4$, suggesting that the reaction may have at last yielded the desired product (**56**).
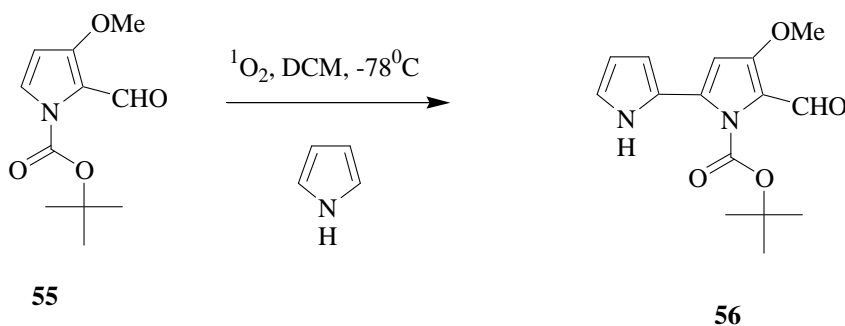
Purification of **56** proved to be problematic, various methods of purification were attempted; silica flash column (eluting with 100% hexane, 25%, 50%, 75% ethyl acetate/hexane and 100% ethyl acetate). Fractions eluted with 100% hexane and 50% ethyl acetate/ hexane from examination of their ^{1}H NMR spectra looked promising, however, again contained a variety of peaks in the 6-8 ppm region, the effect of the Boc protecting group on the proton shifts was not certain and hampered identification. The fraction eluting with 25% ethyl acetate/hexane contained pure **55**. HP-20 purification was then attempted using cyclic loading, similar to that described in Chapter 2, and eluting with 25%, 50%, 75% acetone/water and 100% acetone, the first two fractions from ^{1}H NMR contained mainly **55** whilst the 75% acetone/water and 100% acetone fraction had a variety of peaks in the 6-8 ppm region. Reversed phase HPLC was then attempted eluting with 80% methanol/water followed by a 100% methanol wash. Two

fractions were collected from HPLC, which from ^{1}H NMR spectrum appeared to contain the starting material **55** and **56** in a 1:0.6 ratio. At this point it was decided that the Boc protecting groups was making **55** and **56** inseparable and so methods of deprotection were investigated prior to separation.

Various methods of Boc-deprotection are reported in literature, the most common method cited is the use of trifluoroacetic acid, this method however is not always suitable for acid-labile molecules.[85-88] To develop a methodology for deprotection, initially **55** was used given the instability of **47** to acid. Compound **55** (10 mg, 0.05 mmole) was dissolved in dichloromethane (10 mL) and treated with trifluoroacetic acid (40 µL, 0.5 mmole) under argon. The reaction mixture was stirred at room temperature (1 hr) and then partitioned between aqueous potassium carbonate (10 mL) and dichloromethane. The organic partition was dried over magnesium sulphate and then concentrated. The ^{1}H NMR showed quantitative deprotection (loss of Boc protecting group methyl resonance δ_H 1.60) and no signs of polymerisation were observed.

In the synthesis of prodigiosin, D'Alessio and co-workers reported Boc-deprotection under basic conditions using potassium carbonate.[73,74] We were intrigued with the possibilities of this reaction as it might enable the synthesis of tambjamine L (**22**) in a one-pot synthesis from **55** as shown in Scheme 3.12.
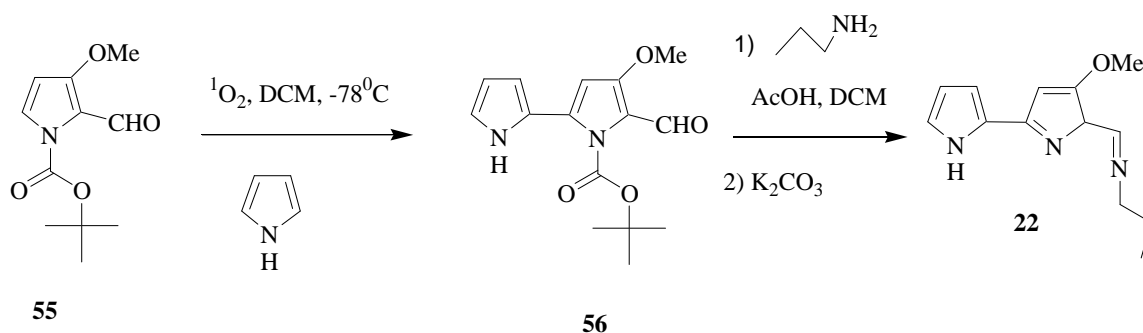
Scheme 3.12 Proposed deprotection and enamine synthesis.

This formation and deprotection was tested by dissolving **55** (10 mg, 44 µmole) in dichloromethane (6 mL) followed by the treatment with propylamine (60 µL, 0.80

mmole) and acetic acid (40μL, 0.75 mmole) under argon. The solution was stirred (4 hr) at room temperature, following which potassium carbonate (0.1 g) was added and the solution was stirred (12 hr) and then partitioned between water (6 mL) and dichloromethane (6 mL), the aqueous layer was washed three times with dichloromethane. The organic partition fraction was then dried over anhydrous magnesium sulphate and concentrated *in vacuo*. The ^{1}H NMR spectrum showed complete deprotection and quantitative conversion to the enamine, confirmed by the lack of an aldehyde proton resonance (δ_H 10.22) and the appearance of the enamine methine resonance (δ 8.04), two methylene resonances (δ_H 3.43 and δ_H 1.62) and a methyl resonance (δ_H 0.90).

The deprotection reaction was repeated in a similar manner on the inseparable reaction mixture from the singlet oxygen bipyrrole step (130 mg), described earlier. Care was taken to ensure that the amount of acetic acid added was slightly less than the 10 molar equivalents propylamine added. Following partioning between water (10 mL) and dichloromethane (10 mL), the organic partition was concentrated and then purified using reversed phase gradient HPLC using a gradient from 1:1 methanol/water to 100% methanol over 30 minutes. The first fraction collected (10.3 mg), from the ^{1}H NMR spectrum, appeared to contain a mixture of **47** (40%), **51** (50%) and **22** (10%). The presence of **51** was confirmed by both ESIMS (positive ion mode after the addition of a few drops of formic acid) and high resolution FABMS, however, from the mass analysis carried out there was unfortunately no indication of either **47** or **22**.

Attempts to purify the product were hampered by a red polymer which formed during concentration of the reaction mixture and was only soluble in 100% methanol making semi-preparatory HPLC difficult due to precipitation of the polymer in aqueous solvents necessary for reversed phase HPLC elution. The ^{1}H NMR spectrum of the red polymer did not shed any light on the nature of the polymeric material and strangely did not show any resonances in the 6 – 8 ppm region consistent with pyrrole type compounds.

Frustratingly neither **56** nor its enamine analogues could be isolated from the reaction mixture by HPLC. The continual formation of significant amounts of red polymeric material necessitated an analysis of the reaction conditions during the singlet oxygen induced pyrrole coupling with a view to reducing unwanted side reactions.

In addition to the observed possible polymerisation, some interesting colour changes were noted in the course of the reaction; during irradiation, the solution is a blue colour from the methylene blue, following reaction with pyrrole, the solution changes to a green colour similar to that of the tambjamine natural products. Finally, when the solution is concentrated it becomes a dark red oil suggesting that polymerisation has occurred. The polymerisation observed was thought to be due to either excess acid in the solution, free radicals following irradiation, excess singlet oxygen or exposure to sunlight. To investigate the cause(s) of polymerisation the singlet oxygen reaction was run as before however before concentrating under reduced pressure, where polymerisation was usually observed to occur, the reaction mixture was divided into four fractions and each fraction was separately treated with diazobicylooctane (50 mg) to remove any radicals, purged with argon to remove excess oxygen and neutralised with a 2% potassium carbonate solution. The fourth fraction was treated as a control and worked up in the normal way. Interestingly, on the addition of diazobicylooctane the green solution changed to a dark red colour immediately, all the other samples remained green when concentrated on a rotary evaporator followed by final concentration to dryness under a stream of nitrogen. Polymerisation, however, was observed in all the samples when they were kept in solution at room temperature for 10 minutes with the exception of the solution purged with argon which only polymerised after standing for several hours. These results suggested that exposure to sunlight may be contributing to polymerisation and the polymerisation is exacerbated in the presence of oxygen following irradiation.

The polymerisation of pyrrole when exposed to sunlight is easily observable as the clear solution rapidly turns a dark brown colour, for this reason, pyrrole was always freshly distilled before use. Given these observations the reaction procedure was modified, the flask containing the reaction mixture was covered in tin foil and purged with argon.

3.7 Synthesis of novel dipyrrole, methyl 4-aza-5-oxo-6,6-di-(2-pyrolyl)-2(*Z*)-hexenoate (57) from the photooxidation of 55

57
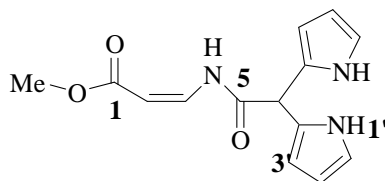
Using the modified procedure to reduce polymerisation, **55** (200 mg, 0.88 mmole) and methylene blue (1 mg) were dissolved in dichloromethane (10 mL) and stirred at room temperature to allow the methylene blue to dissolve, then cooled (-78°C) and purged with oxygen (10 min). The solution was then irradiated using a tungsten lamp with a red filter (30 min) under a constant stream of oxygen. Following irradiation, the flask containing the solution was immediately wrapped in tin foil to prevent exposure to light and freshly distilled pyrrole (420 μL, 6.3 mmole) in cold dichloromethane (3 mL) was added and the solution was stirred (2 hr). The reaction mixture was then concentrated *in vacuo* without heating. The green oil obtained was then purified using a silica flash column (30 x 7 mm) eluting with 70% ethyl acetate/ 30% hexane to remove any polymeric material. The eluent was concentrated under nitrogen without heating, in the dark and then further purified using normal phase HPLC (7:3 hexane: ethyl acetate) to yield three fractions. The first of these fractions showed a plethora of peaks in the ^{1}H NMR spectrum attributed to a mixture of three inseparable photooxidation products. ^{1}H and ^{13}C NMR analysis of the second fraction indicated that this fraction contained a single pure compound (**57**). Compound **57** was obtained in a 15% isolated yield. The third fraction was found to be un-reacted starting material.

3.7.1 Structure Elucidation of 57

The molecular formula of **57**, $C_{14}H_{15}N_3O_3$, was obtained from HRFABMS data (calcd. for $C_{14}H_{15}N_3O_3$ 273.1113, obs. 273.1118) implying nine degrees of unsaturation.

Analysis of the IR spectrum gave an indication of the functional groups present and showed N-H (3437 cm^{-1}), amide carbonyl (1633 cm^{-1}) and ester carbonyl (1718 cm^{-1}) absorbances. Only ten carbon and nine proton resonances were observed in the ^{13}C and ^{1}H NMR spectra respectively. The integration of the proton signals suggested two pyrrole substituents in **57**, with the three pyrrole protons (H-3' – H-5') (δ_H 6.14, 6.18 and 6.76) and exchangeable proton, NH-1' (δ_H 8.65) each integrating to two protons as shown in Figure 3.6.
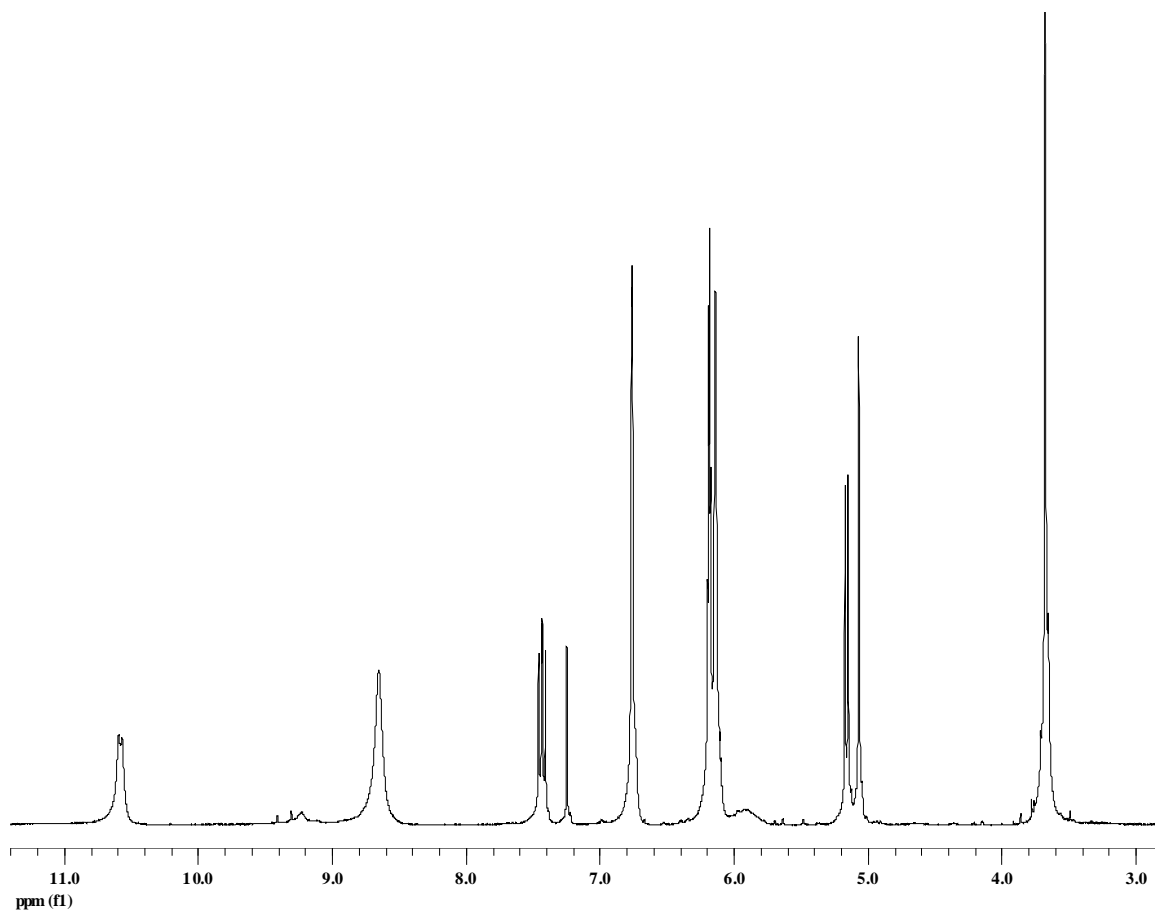
Figure 3.5: Expanded (δ 3-11 ppm) section of the ^{1}H NMR spectrum (400 MHz, CDCl$_3$) of **57**.
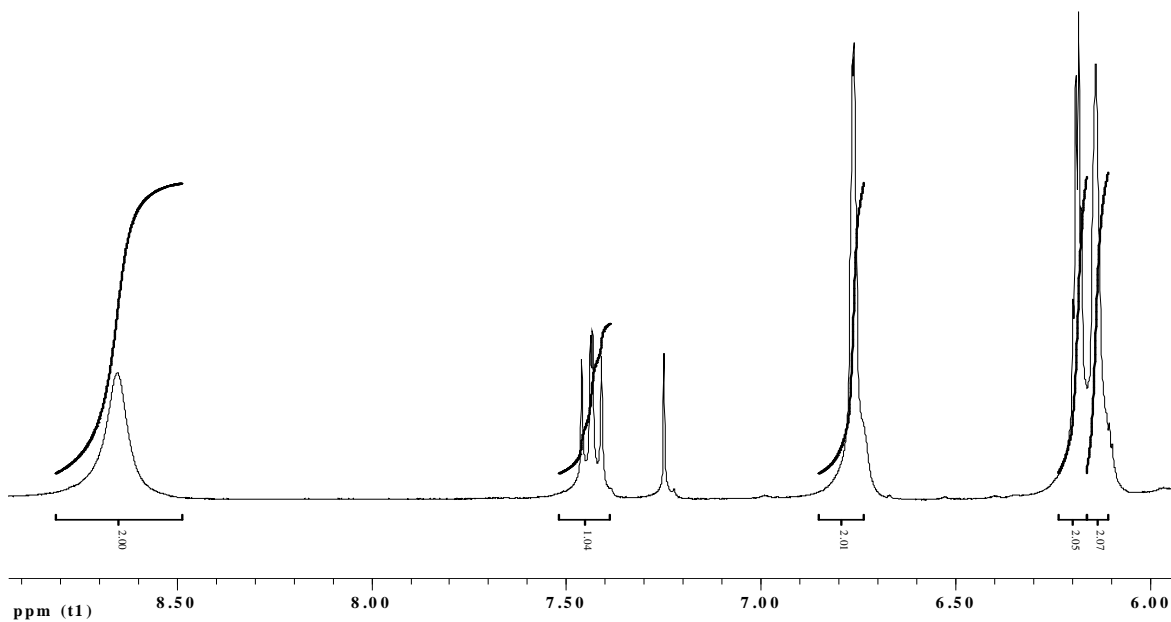
Figure 3.6: Expanded region (δ 6 – 9 ppm) of the ^{1}H NMR spectrum (400 MHz, CDCl$_3$) obtained for **57** showing integration of the pyrrole resonances.
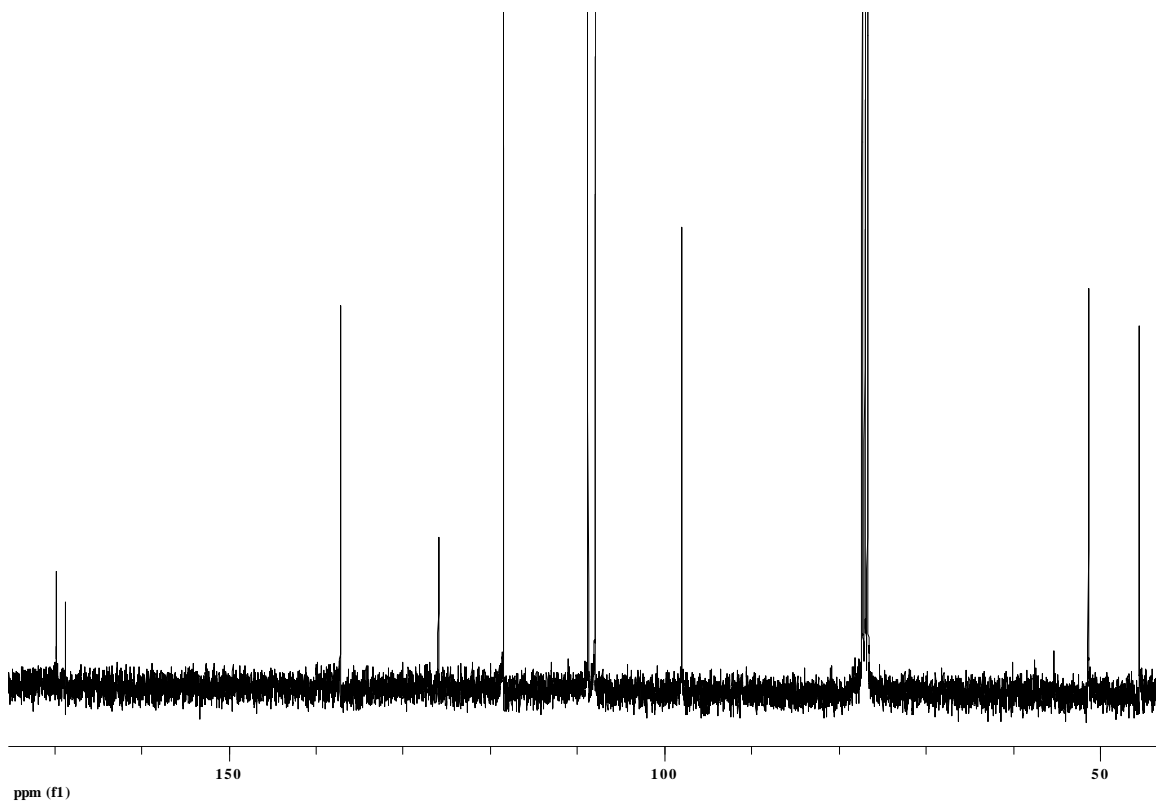
Figure 3.7: Expanded region (50 – 170 ppm) of the ^{13}C NMR spectrum (100 MHz, CDCl$_3$) of **57**.

Using HSQC to establish ^{13}C – ^{1}H connectivity, seven protonated carbon resonances were identified. Thus seven of the nine ^{1}H resonances, could be accounted for. The presence of two exchangeable proton resonances, was consistent with the N-H stretch observed in the IR spectrum. Three further non-protonated carbons were observed in the ^{13}C spectrum and these were assigned as carbonyls (δ_C 168.8, 169.7) and aromatic (δ_C 125.9) carbons (Table 3.1).

The COSY spectrum of **57** (Figure 3.9) revealed ^{3}J coupling between the two olefinic methines H-2 (δ_H 5.16) and H-3 (δ_H 7.43) and an exchangeable resonance H-4 (δ_H 10.58) and provided the partial structure A. The geometry of the double bonds was assigned as (Z) from the $J_{2,3}$ coupling constant (9 Hz). A small long range ^{4}J coupling was observed in the COSY spectrum from an exchangeable proton H-1'(δ_H 8.63) to the aromatic proton H-4'(δ_H 6.18). The H-4' proton was further coupled to two other aromatic protons H-5' (δ_H 6.76) and H-3' (δ_H 6.14). The exchangeable proton H-1' was also coupled to H-5'.

Partial structure A **Partial structure B**
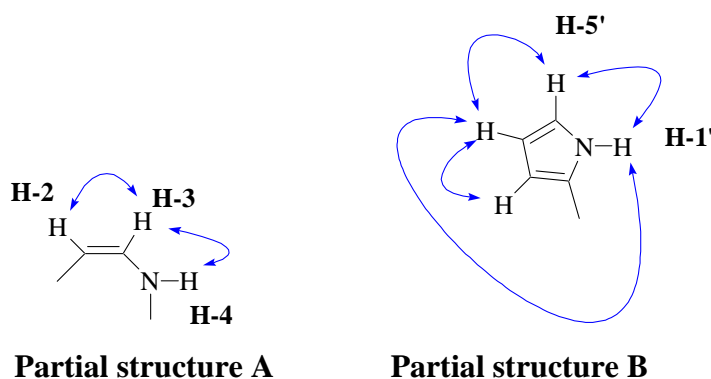
Figure 3.8: Important COSY correlations used to establish partial structures A and B.
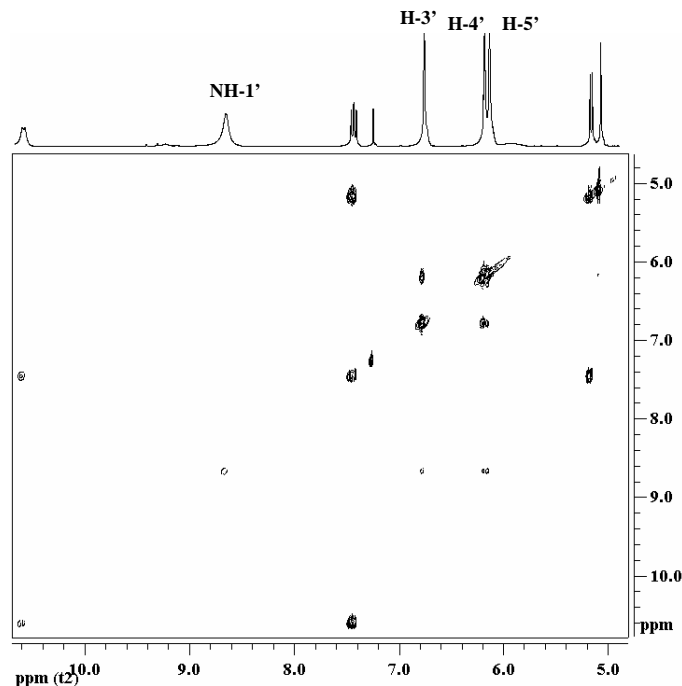
Figure 3.9: An expanded ($F_1 = F_2 = \delta$ 5-11 ppm) COSY spectrum of **57** (CDCl$_3$; 400 MHz) showing correlations used to establish partial structures A and B.

A three bond ^{1}H-^{13}C correlation in the HMBC spectrum, (Figure 3.11), was observed between the methoxy protons (δ_H 3.67, δ_C 51.3) and an ester carbonyl carbon C-1 (δ_C 168.8). Similarly an olefinic methine proton H-2 (δ_H 5.15, δ_C 98.0) showed correlations with this ester carbonyl carbon, an olefin carbon C-3 (δ_C 137.2) and an amide carbonyl carbon (δ_C 169.7). A further three bond correlation coupling was observed between the exchangeable proton H-4 (δ_H 10.58) and the amide carbonyl C-5 (δ_C 169.7). These observations allowed elaboration of substructure A to include both methyl ester and amide linkages as shown in substructure C (Figure 3.10).
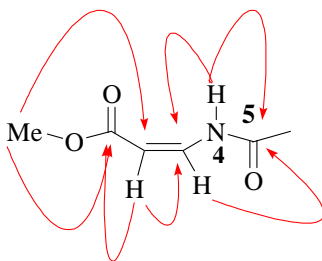
Substructure C

Figure 3.10: Important HMBC correlations used to construct substructure C.

Further correlations were observed in the HMBC spectrum between the three aromatic protons H-3' – H-5' and the aromatic quaternary carbon (δ_C 125.9) supported by the pyrrole substructure B. An HMBC correlation between H-6 (δ_H 5.07) and the pyrrole quaternary carbon, C-2' (δ_C 125.9, C-9) placed the two pyrrole rings at C-6 (δ_C 45.5). An additional HMBC correlation was observed from H-3' (δ_H 6.14) to the methine carbon C-6 implying a C-2' linkage of the two pyrrole rings to C-6. If the pyrrole was substituted in the C-3 position one would expect to see two HMBC correlations from pyrrole protons H-2' and H-4' to C-6. The C-2 linkage was unequivocally supported by the ^{1}H-^{13}C coupling constants obtained from the coupled gradient spectrum (Table 3.1). From literature values the ^{1}H-^{13}C coupling constant of the protons in the 2' and 5' positions is approximately 182 Hz whilst for protons in the 3 and 4 positions $J_{C,H}$ is approximately 170 Hz.[89] Methine protons H-3' (δ_H 6.14) and H-4' (δ_H 6.18) were found to have $J_{C,H}$ 170 Hz and 172 Hz respectively confirming that these protons were in the 3' and 4' position in the pyrrole ring whilst the methine proton H-5' (δ_H 6.761) was observed to have a $J_{C,H}$ of 185 Hz suggesting that this proton is at C-5'. Finally an HMBC correlation from H-6 to the amide carbonyl (δ_C 169.7) completed the structure elucidation of **57**.

The synthesis of product, **57**, generated some interesting mechanistic questions. Firstly, the Boc group was not present in **57**, which raised the question of whether or not the Boc group was lost during the reaction or in the chromatographic work-up. As the major product of the reaction isolated was unreacted **55** this suggests that the loss of the Boc protecting group was rather a function of the reaction than the work-up. The loss of the Boc group therefore raised the question of the importance of the Boc group in the reaction that yielded **57**. To test this hypothesis, the reaction was repeated using **47** treating the reaction mixture as previously described to reduce polymerisation by eliminating light. From normal phase thin layer chromatography of the final reaction mixture, there was no evidence of **57** or any other reaction products, suggesting that the Boc group had increased the reactivity of **47** and was required to produce **57**.

Similar ring opening as observed in **57** has been reported by Wasserman and co-workers in their singlet oxygen oxidation studies of 2-carboxy-3-methoxy-N-benzylpyrrole (**58**) shown in Scheme 3.13.[90] The ring opening observed was proposed to occur through intermediate **59** and a similar intermediate may be involved in our preparation of **57**.
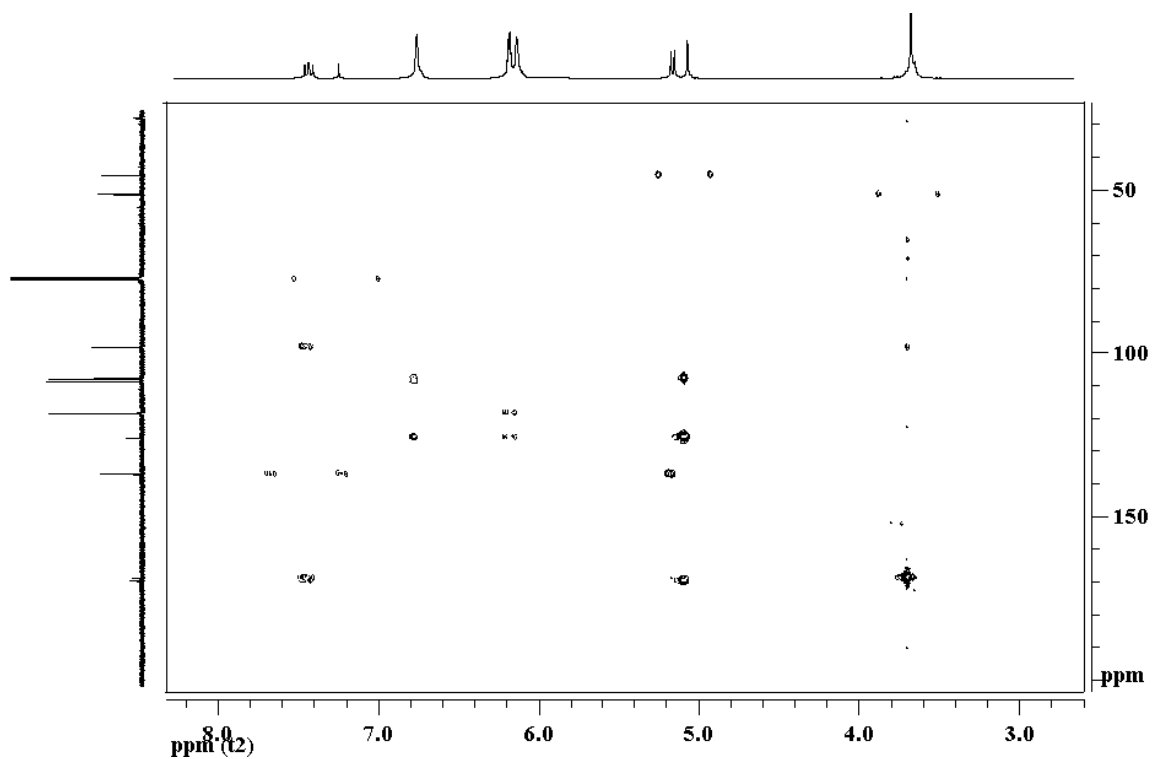
Figure 3.11: Expanded section (F_1 = 30 – 200 ppm, F_2 = 3 – 8 ppm) of the HMBC spectrum of **57**.

Position	δ_C ppm	δ_H ppm (int., mult., J/Hz)	HMBC correlation to	COSY coupling to	Coupled HSQC (J/ Hz)
1	168.8	-	-	-	
2	98.0	5.16 (1H, d, 8.8)	C-3	H-5	171
3	137.2	7.43 (1H, dd, 8.8, 11.1)	C-4, C-7	H-4, H-6	
4	-	10.58 (1H, d, 10.1)	-	H-5	
5	169.7	-	-	-	
6	45.5	5.07 (1H, s)	C-7, C-9, C-10	-	129
1'	-	8.65 (2H, s)	-	H-11, H-12	-
2'	125.9	-	-	-	
3'	107.9	6.14 (2H, t, 3.6)	C-9, C-12	-	170
4'	108.8	6.18 (2H, dd, 5.7, 2.8)	C-9, C-12	H-12, H-13	172
5'	118.4	6.76 (2H, dd, 3.9, 2.5)	C-9, C-11	H-11, H-13	185
Me	51.3	3.67 (3H, s)	C-3, C-4	-	148

Table 3.1: ^{1}H (400 MHz, CDCl$_3$), ^{13}C (100 MHz, CDCl$_3$), HMBC and COSY NMR data obtained for **57**.
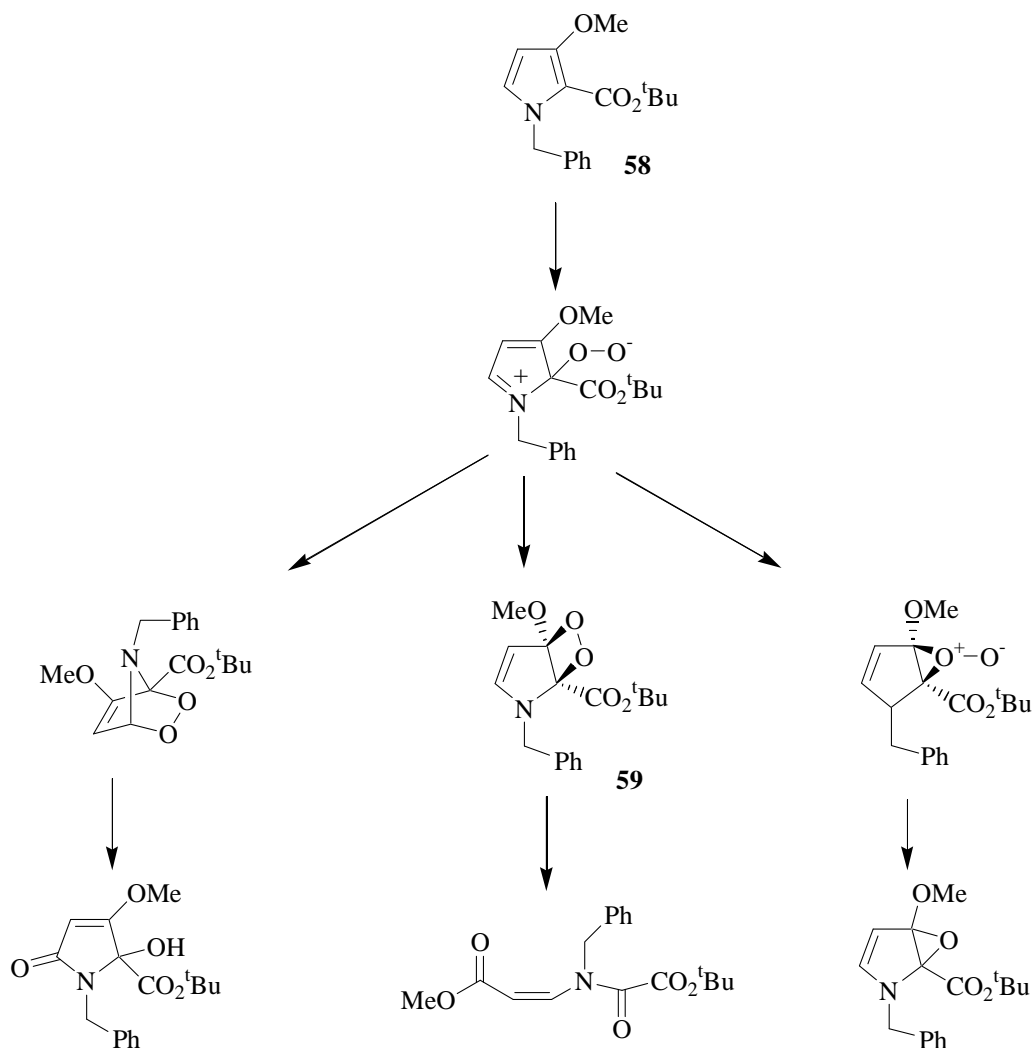
Scheme 3.13 Products from photooxidation reaction of **58**.

The C-6 di-pyrrole substitution in **57** is also of interest. Similar dipyrrole products have been reported from acid-catalysed condensation of aromatic aldehydes e.g. benzaldehyde. These dipyrrole precursors have been used in the synthesis of meso-substituted porphyrins and porphyrin analogues.[91-93] Interestingly, no acid was added to the reaction mixture, however given the catalytic amount of acid required to drive such reactions it is possible that a small amount of acid may have been generated during the irradiation which could drive the condensation on addition of pyrrole. Therefore a method of improving the low yield (15%) of **57** could be to add a small amount of trifluoracetic acid

following the addition of pyrrole to the reaction mixture. Conversely from our experience the addition of acid will probably enhance polymerisation and make **57** increasingly difficult to isolate.

3.8 Computer modelling

Following the success in increasing the reactivity of **47** using the Boc protecting group computer modelling was used to investigate possible reasons for this increased reactivity. As discussed earlier it was thought that the unreactivity of **47** could be due to the formation of the vinylogous ester (**49**) and amide (**50**) canonical structures.

49   **47**   **50**
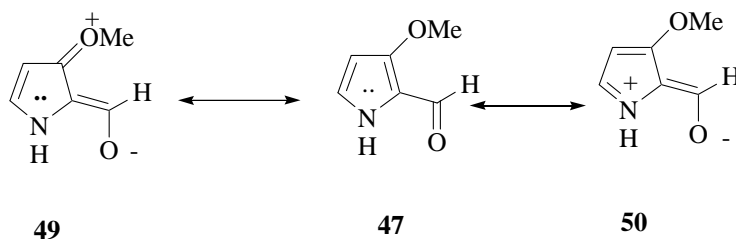
The addition of bulky substituents, such as the *tert*-butyl ester group in **38** used by Wasserman and co-workers in their synthesis of the bipyrrole (**11**) and the Boc protecting group necessary for the formation of **57**, could alter the planar relationship between the carbonyl substituent and pyrrole ring thus reducing the optimal overlap of the 2p orbitals necessary for resonance.

The first objective of the computer modelling was to investigate the effect of the bulky substituents in **38** and **55** on the planar relationship between the carbonyl sustituents and the pyrrole ring. The energy minimised structures of **38**, **47** and **55** were obtained using Dmol3 with the density functional theory using BLYP functional with DND as the basis set. Figure 3.13 and Figure 3.15 show the energy minimised diagrams of **47** and **55**, showing the carbonyl group out of plane in **55**.
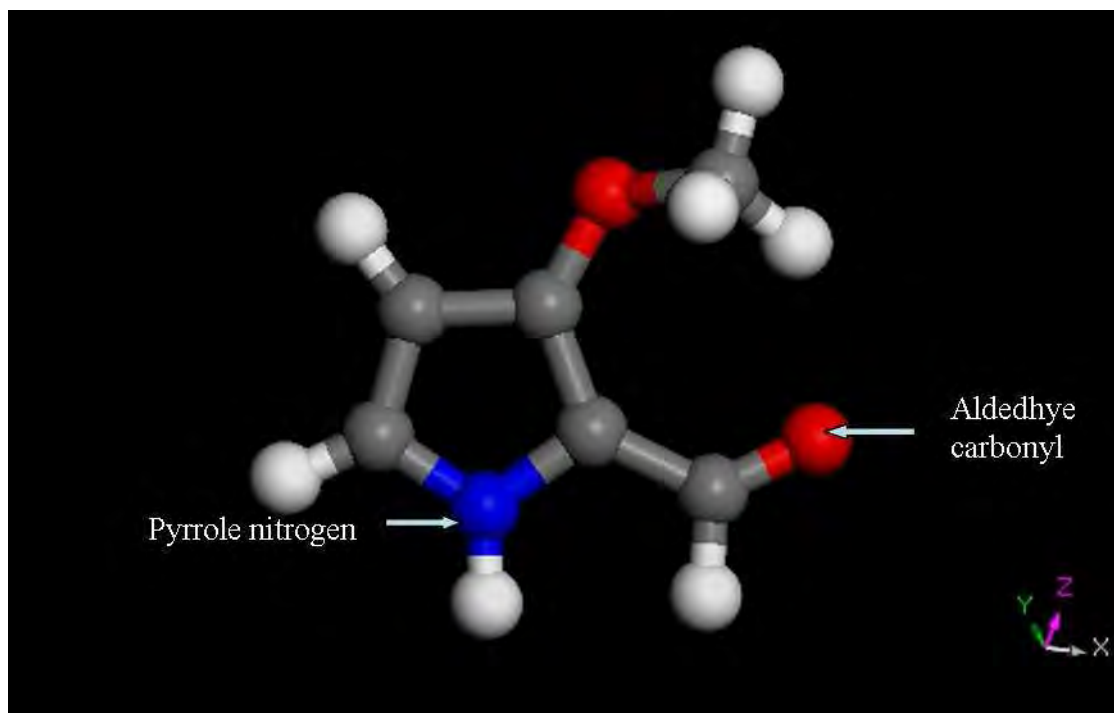
Figure 3.12 Energy minimised diagram of **47.**
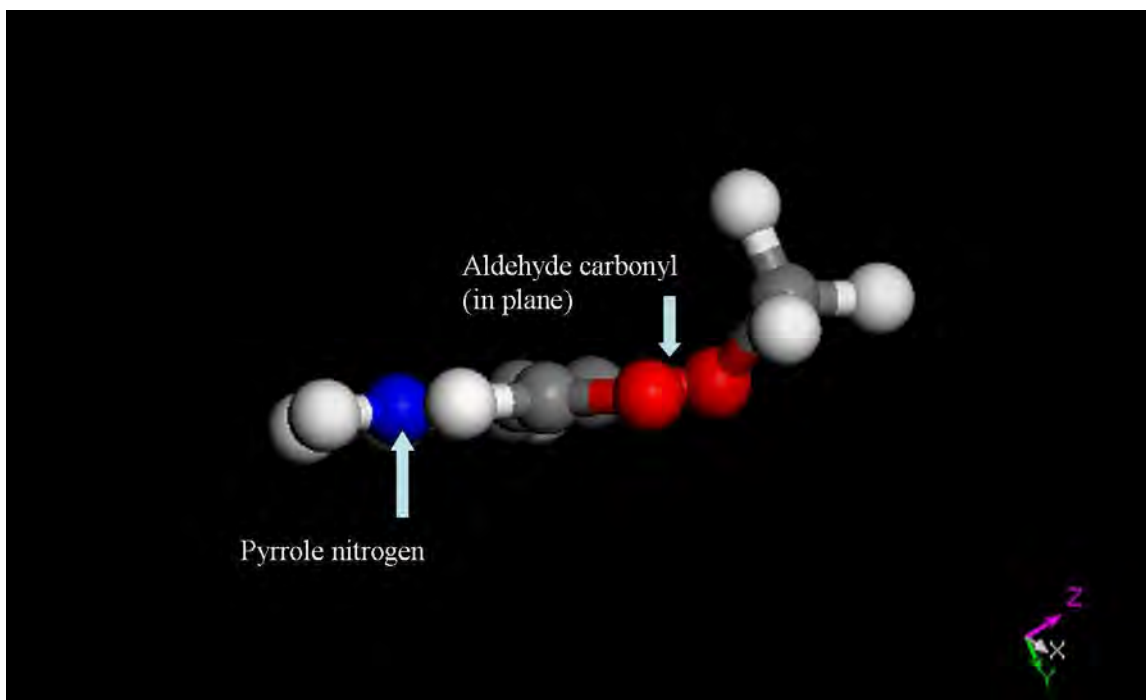
Figure 3.13 Energy minimised diagram of **47**, showing the aldehyde carbonyl functionality in plane with the pyrrole ring.
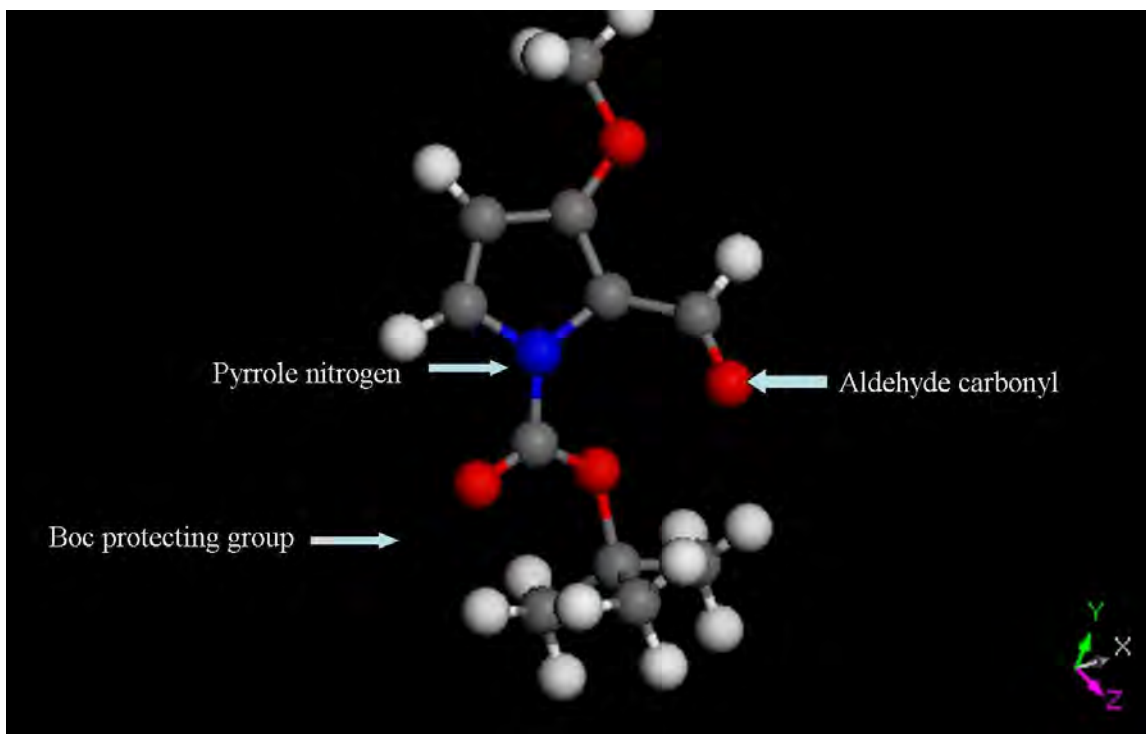
Figure 3.14 Energy minimised diagram of **55**.
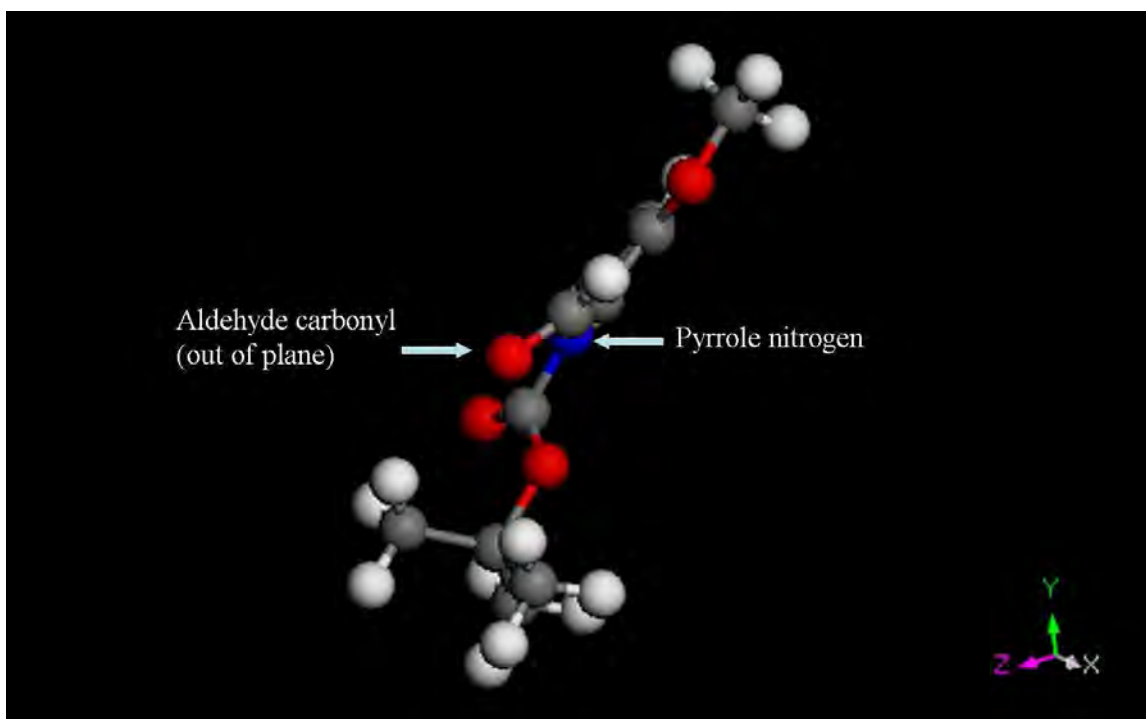
Figure 3.15 Energy minimised diagram of **55** showing the aldehyde carbonyl out of plane with the pyrrole ring.

The torsional angle between the carbonyl group and pyrrole ring in the energy minimised diagrams of **47**, **55** and **38** was measured to allow a quantitative comparison between the analogues, the results are shown below in Table 3.2.

Compound Number	Torsional angle between the aldehyde carbonyl and pyrrole ring
47	1.24°
38	-0.02°
55	2.68°

Table 3.2 Torsional angle between the carbonyl substituent and pyrrole ring.

The comparison of the torisonal angles provided some interesting results, as Table 3.2 shows, **38** was found to be the most planar, allowing maximal overlap of the 2p orbitals whilst in **55** even though the largest torsional angle was observed, one questions whether the angle of 2.68°, is significant enough to affect overlap of the p-orbitals and delocalisation of the π electrons. Surprisingly bulky substituents appeared to have very little effect on the planar relationship between the carbonyl and pyrrole ring.

An alternative explanation was that **47** could exist in a preferred tautomeric form (**59**) making it unreactive to singlet oxygen oxidation. To quantitatively compare the energies of the tautomers, the global minimum energy values of **47**, **38** and **55** were compared with their tautomeric forms **59**, **60** and **61** respectively (Table 3.3).
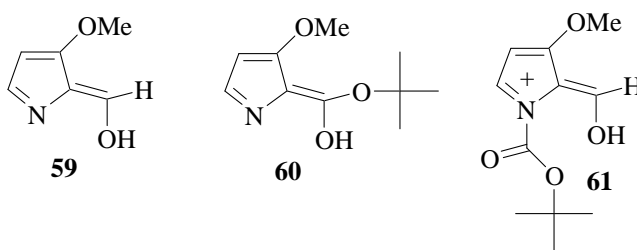
47	59
-438.0442 Hartrees	-438.0196 Hartrees
55	**61**
-783.5912 Hartrees	-783.8783 Hartrees
38	**60**
-670.5167 Hartrees	-670.4842 Hartrees

Table 3.3 Global energy minimum values calculated for **38**, **47** and **55** compared to tautomeric forms.

The global minimum energy values for **47** and **38** are lower than those of their tautomeric forms **59** and **60** respectively suggesting that they exist predominantly as **47** and **38** rather than their tautomeric forms. The difference between the two forms was calculated to be 0.0246 Hartrees for **47** and **59** and 0.0325 for **38** and **61** suggesting that the original form is more energetically favoured in **38** compared to that of **47**. The global energy minimum energy values for **55** and it tautomer suggest that the tautomeric form is energetically favoured, however due to the charge and atom difference the energy values cannot be directly compared.

Computer modelling found that bulky substituents have little effect on the planar relationship between the carbonyl group and the pyrrole ring and that when the global minimum energy values are compared there is no evidence of tautomerism occurring. Both of these observations are contrary to the proposed reasons for the unreactivity of **47** to singlet oxygen oxidation. This suggests that the unreactivity may be due to another factor which could not be readily be resolved by computer modelling.

3.9 Conclusion and further work

Initially 3-methoxy-2-formylpyrrole (**47**) appeared to be a very attractive starting point for the synthesis of the tambjamine and possibly prodigiosin natural products. The moderate yielding reaction gave **47** in a simple method, in good purity allowing us to

avoided the low yielding McFayden-Stevens reduction at a later stage in our synthesis. The work presented in this thesis conclusively shows that **47** is not suitable for the synthesis of the bipyrrole carboxyaldehyde intermediate **11**, required for tambjamine and prodigiosin natural product synthesis, using singlet oxygen oxidation. Attempts to improve the reactivity of **47** to singlet oxygen oxidation, revealed the instability of **47** to any form of acid treatment. Modification of **47** *via* N-Boc protection, appeared to yield the required precursor **56** however in such low yields that the product could not be isolated. However, N-Boc protected derivative (**55**) provided a route to the dipyrrole analogue **57**. The moderate biological activity of **57** is described in Chapter 4.

The synthesis of 4-methoxypyrrolic natural products by D'Alessio and co-workers' cross coupling methods (Scheme 3.7) have become increasingly popular.[56,73] Unfortunately, their pyrrolinone derived methodology cannot be directly applied to the synthesis of tambjamine natural products. Following the failure of singlet oxygen oxidation to give bipyrrole coupling another possible synthetic pathway using Stille coupling is proposed to give bipyrrole coupling (Scheme 3.14).
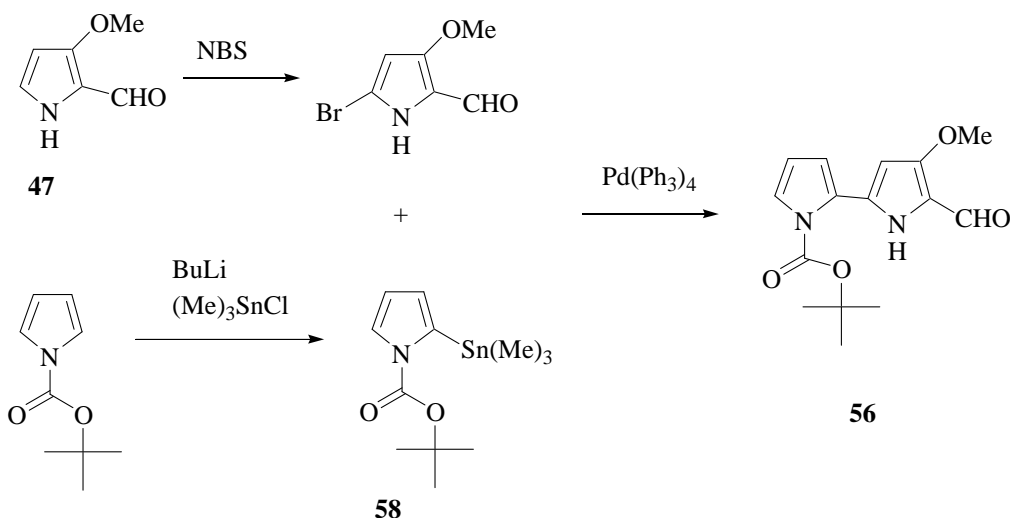
Scheme 3.14 Proposed bipyrrole synthesis using Stille coupling conditions.

D'Alessio and co-workers reported that Stille conditions were particularly poor for bipyrrole coupling.[73] However, in their synthetic pathway they utilised the triflate leaving group whereas our proposed method uses the bromine leaving group which could

improve the success of the coupling. The method proposed has the following advantages; firstly the synthesis of **58** has previously been reported in literature in high yields through a relatively simple procedure,[94] secondly the use of **47** as the starting material avoids the low yielding McFayden-Stevens reduction and thirdly the synthesis could be adapted to a combinatorial approach allowing the synthesis of a wide range of synthetic derivatives which could be useful for structure-activity studies.

Chapter Four

Bioactivity and physical properties of tambjamine E (**13**),

tetrapyrrole (**15**) and novel di-pyrrole (**57**)

4.1 Introduction

Cancer occurs when the genetic material of a cell is altered resulting in uncontrolled cell division leading to the formation of tumours. These tumours can be either benign or malignant. Currently treatment of cancer involves the removal of the tumour cells either through surgery, chemotherapy which utilises the different responses of normal and cancerous cells to cytotoxic drugs, or either radiotherapy or photodynamic therapy, which use ionizing radiation and cytotoxic oxygen species respectively to facilitate selective cell death.

The 4-methoxypyrrolic natural products, have been identified as defensive metabolites in the marine invertebrates producing them[4,24] and have become of interest due to their anticancer activity, against liver cancer and melanoma cell lines, and their immunosuppressive properties.[1,2] This chapter describes the bioactivity of **13**, **15** and **57** against oesophageal cancer and the physical properties of the natural products **13** and **15**. The physical properties were investigated firstly to explore further the mechanism of DNA cleavage first proposed by Manderville and co-workers,[1,46-49] and secondly to determine the potential of the 4-methoxypyrrolic natural products as photodynamic therapy agents.

4.2 Anticancer activity of the 4-methoxypyrrolic natural products

One of the most interesting properties of the 4-methoxypyrrolic natural products is their selective anticancer activity. As mentioned in Chapter 1, the 4-methoxypyrrolic natural products have been shown to facilitate cell death through apoptosis and show activity against melanoma and liver cancer cell lines. Two methods of action have been proposed for the anti-cancer activity; Manderville and co-workers proposed the DNA cleavage mechanism and were subsequently able to show that tambjamine E, prodigiosin and the tetrapyrrole natural products were all able to cause oxidative DNA cleavage in the presence of copper (II).[46,48,49] Ohkuma and Wasserman have shown an alternative method of action involving the prodigiosins ability to uncouple vacuolar ATPase.[39,44]

As part of an going collaboration with the Department of Medical Biochemistry at the University of Cape Town, aimed at developing pharmaceuticals for the treatment of oesophageal cancer,[95] the activity of **13**, **15** and **57** against oesophageal cancer cell

lines was investigated. Oesophageal cancer has an abnormally high incidence in Southern Africa amongst the black populations. The high incidence of this disease is associated with a range of environmental factors including cigarette smoking, woodsmoke, alcohol, the inadvertent consumption of carcinogenic mycotoxins produced by the *Fusarium* fungus that thrives on grain stored under damp conditions and a diet poor in fresh fruit and vegetables. The identification of novel agents with significant cytotoxic activity against oesophageal cancer cells would substantially enhance our ability to treat this debilitating disease in Africa. Given the strong anticancer activity of the 4-methoxypyrrolic natural products, provide reason to investigate the natural and synthetic products activity against oesophageal WHCO1 cancer cell lines. Preliminary screening data indicates that tambjamine A (**7**), tambjamine E (**13**) and the tetrapyrrole (**15**) are strongly active against oesophageal cancer, whilst dipyrrole (**57**) is moderately active. However, the highly pigmented nature of these compounds and their fluorescent properties interferes with the fluorescent dye based interpretation of the anticancer activity and this problem needs to be resolved before quantitative IC_{50} values can be calculated. The preliminary screening results are shown below in Figure 4.1 and 4.2.
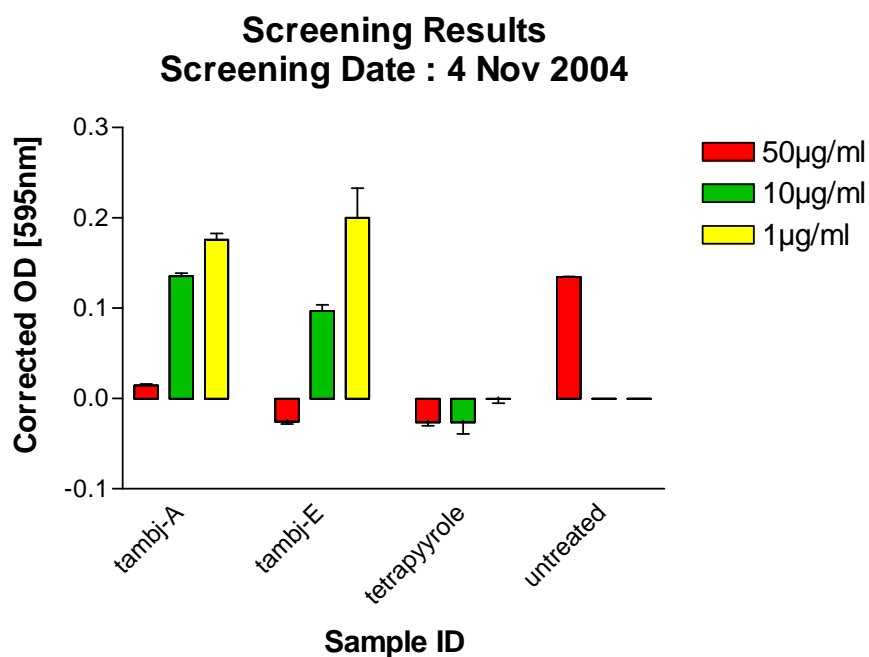
Figure 4.1: Preliminary screening results of the isolated natural products against oesophageal cancer WHC01 cancer cell lines.
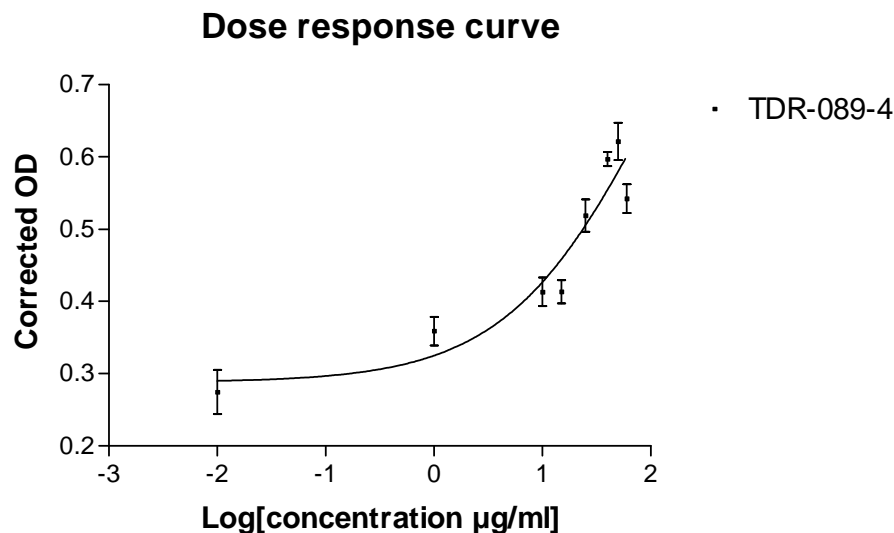
Figure 4.2: Dose response curve of novel dipyrrole (**57**) against oesophageal WHCO1 cancer cell lines.

4.2.1 Oxidative DNA cleavage proposed by Manderville and co-workers

Manderville and co-workers first proposed that oxidative DNA cleavage is the main mode of cytotoxic activity of the 4-methoxypyrrolic natural products. It was originally suggested that the planar bipyrrole structure[4,6,20,24,96] of the tambjamine natural products could enable them to intercalate with DNA, utilising the hydrogen bonding from the methoxy moiety and pyrrole nitrogens to facilitate this.[97] This hypothesis was confirmed as tambjamine E (**13**), prodigiosin (**1**) and tetrapyrrole (**15**) were shown to bind to calf thymus DNA by monitoring changes in the UV-vis absorption and fluorescence spectra. Based on the optical changes observed, it was concluded that 4-methoxypyrrolic natural products bind to DNA with a preference for adenine and thymine sites.[46-49]

As polypyrroles have been reported to be readily oxidised,[98] Borah *et al.* proposed that the tambjamine natural products could, in the presence of a redox-active metal, show nuclease activity.[46] Using gel electrophoresis, Manderville and co-workers investigated the DNA cleavage of supercoiled plasmid DNA, testing the effect of 4-methoxypyrrolic natural products alone and in the presence copper (II), iron (III), nickel (II) and zinc (II). Interestingly DNA cleavage was only observed in the presence of both the natural product and copper (II). DNA cleavage was not observed

when only the natural product or alternative redox metals were used.[46,48,49,99] The nuclease activity was thought to be a result of oxidative DNA cleavage. The reactive oxygen species responsible for the DNA cleavage was investigated using gel electrophoresis by treating the samples loaded onto the gel with argon and various oxygen radical scavengers. DNA cleavage was slightly reduced when an argon atmosphere was used and when treated with the singlet oxygen radical scavenger sodium azide. DNA cleavage was completely inhibited when samples were treated with catalase, an enzyme which breaks down hydrogen peroxide to oxygen and water. No inhibition of cleavage was observed when the samples were treated with *tert*-butyl alcohol, a hydroxyl radical or superoxide dismutase, a superoxide scavenger. Some inhibition was observed with the metal chelator EDTA. From the results obtained, it was concluded that hydrogen peroxide was the reactive oxygen species responsible for initiating DNA cleavage.[1,46-49]

In the early studies of DNA cleavage, Manderville originally used **13**, which was shown to cause single stand cleavage in the presence of copper (II). In their later work, it was shown that similar DNA cleavage was observed with **1** and **15**, however, **1** and **15** were found to cause the more lethal double strand DNA cleavage rather than the single strand cleavage.[47,49]

Melvin *et al.* used electrochemistry to investigate the mechanism of DNA cleavage further. After studying the electrochemical characterisation and bioactivity of **1** and its analogues, a structure activity relationship was proposed that showed the A-pyrrole ring to be of importance in determining the cytotoxicity of the prodigiosin derivatives. The addition of an electron withdrawing group to the A-pyrrole ring was shown to diminish cytotoxicity. On the basis of this information, two mechanisms for oxidative DNA cleavage were proposed, firstly endogenous oxidative DNA damage in a mechanism involving the reduction of copper (II) to copper (I) which in turn produces hydroxyl-like radicals capable of causing oxidative double-strand DNA cleavage.[47,100,101] The second proposed method involves base induced oxidation through the reduction of DNA bound copper (II), which could lead to single strand nicks.[48,76]

Electrochemical studies have been carried out on prodigiosin derivatives, which clearly showed differences in cytotoxicity of the derivatives. Prodigiosin analogues

with the lowest anodic oxidation were shown to be the most effective at promoting DNA cleavage. Interestingly polymerisation is not observed in prodigiosin (**1**) with repetitive scans where the scan only includes the first oxidation peak. This suggests that the first anodic oxidation peak is the oxidative process involved in DNA cleavage in the presence of Cu (II), reducing Cu (II) to Cu (I) forming a redox-active species which is capable of causing site-specific double strand-DNA cleavage.[5,99]

The electrochemistry of the closely related natural products tambjamine E (**13**) and the tetrapyrrole (**15**) has not been reported to date. Given that **13** and **15** cause different types of DNA cleavage, which could occur through two separate mechanisms, we sought to investigate these mechanisms further, through electrochemical studies of **13** and **15** in a hope to identify differences, which could result in the elucidation of the cytotoxic modes of action of **13** and **15**. To extend an understanding of the mechanism of action an attempt was made to gain a tetrapyrrole (**15**)-copper (II) complex using a procedure similar to that described by Park *et al.*[3]

4.2.2 Electrochemistry of tambjamine E (13) and tetrapyrrole (15)

Cyclic voltammeter is a very popular method to investigate redox systems and involves a linear change in potential with time. The resultant current is measured allowing the oxidative and reductive processes occurring to be investigated.[102] Cyclic voltametry was chosen as the method for investigating the oxidative processes of **13** and **15** using similar conditions to those reported by Melvin *et al.*[5]

The redox potentials of **13** and **15** were measured in acetonitrile using cyclic voltametry with a silver/silver chloride reference electrode. As Figure 4.3 shows, a single CV scan of tetrapyrrole showed three oxidation peaks ($E_{p/2}^1 = 0.51$ V, $E_{p/2}^2 = 0.88$ V, $E_{p/2}^3 = 1.2$ V) similar to that of **1** reported by Melvin *et al.*[5] The peak current (I_p^i) increased linearly with the square root of the scan rate at low scan rates. At scan rates higher than 400 V/s, however, this relationship was no longer observed indicating that polymerisation was occurring. Subsequent CV scans of tetrapyrrole were different from the first scan further indicating that polymerisation was occurring.[103]
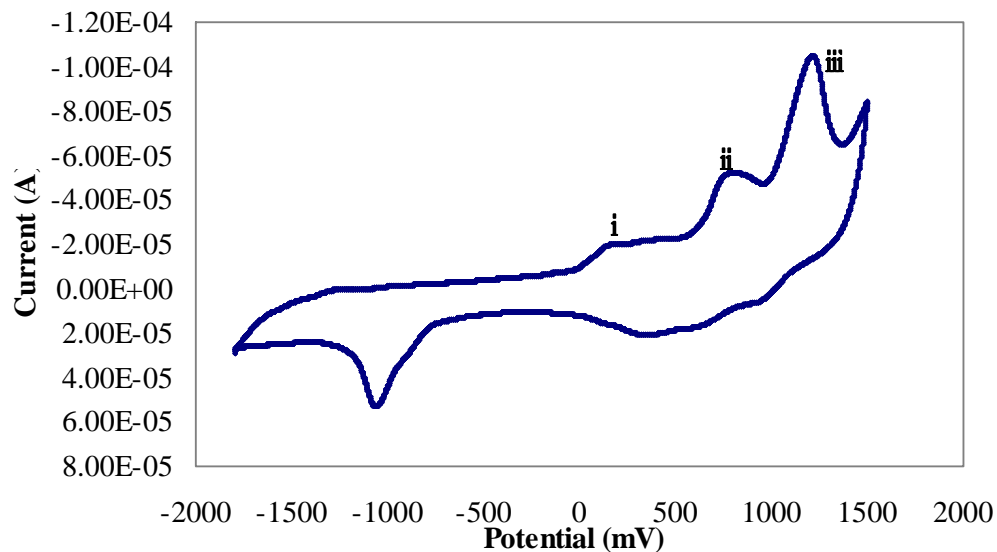
Figure 4.3: Cyclic Voltamogram of tetrapyrrole (**15** 6.0 mM) in acetonitrile (0.5 M TEAP) using a glassy carbon working electrode and a silver electrode coated with silver chloride reference, $\nu = 200$ V/s.

Similarly, three oxidation peaks were observed in the CV scans of tambjamine E ($E_{p/2}^1 = 0.14$ V, $E_{p/2}^2 = 0.79$ V, $E_{p/2}^3 = 1.2$ V) as shown in Figure 4.4. I_p^i increased linearly with the square root of the scan rate indicating that the process was diffusion controlled. Subsequent CV scans of **13** were different from the first scan indicating however that a similar polymerisation to **15** was occurring.[103]

Studies carried out by Melvin *et al.* showed that only analogues of prodigiosin with low anodic oxidation potentials in acetonitrile were capable of promoting DNA cleavage.[5] From our investigations, **15** was shown to have a lower first anodic oxidation potential of 0.14 V in comparison to **13,** which had a significantly higher potential of 0.5 V. The second and third anodic oxidation peaks occurred at similar potentials suggesting that these oxidative processes lead to polymerisation.
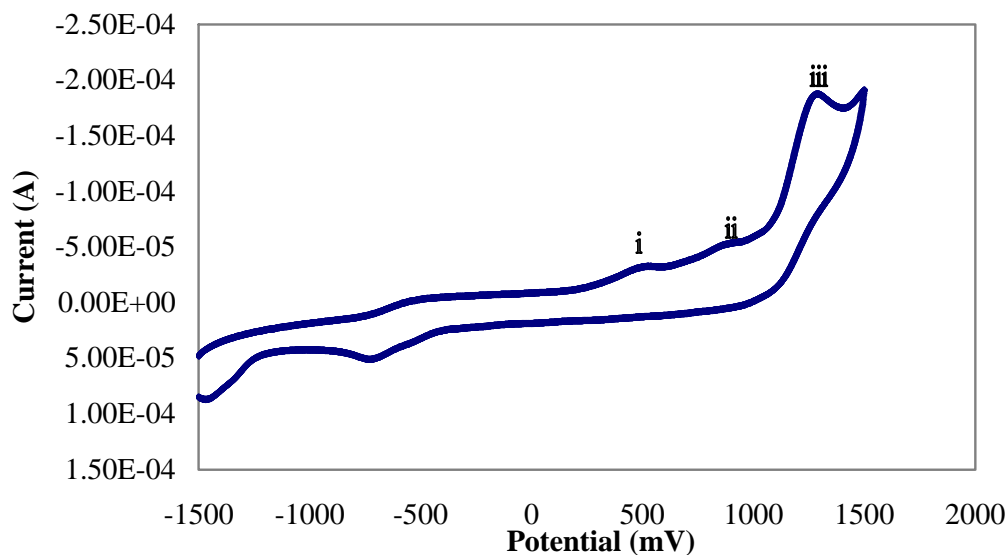
Figure 4.4: Cyclic voltamogram of tambjamine E (**13** 6.0mM) in acetonitrile (0.5 M TEAP) using a glassy carbon working electrode and a silver electrode coated with silver chloride reference, ν = 200 V/ s.

	Tambjamine E (13)	Tetrapyrrole (15)
i	508 mV	149 mV
ii	884 mV	794 mV
iii	1272 mV	1220 mV

Table 4.1: Oxidation peaks observed in the cyclic voltamograms of **13** and **15**.

In conclusion, our results suggest that **15** is capable of oxidising copper (II) more readily than **13**. The superior reducing potential of tetrapyrrole could allow it to cause the more lethal double strand DNA cleavage whilst tambjamine E, as a result of its lower reducing potential, causes single strand nicks.

To further this electrochemical study, the cyclic voltametry of tetrapyrrole and copper (II) was investigated. Given the insolubility of tetrapyrrole in aqueous systems and the poor solubility of copper (II) in organic solvents such as acetonitrile and dimethyl formamide, no conclusive data was obtained.

4.3 Copper binding studies

The crystal structures of prodigiosin/copper and prodigiosin/zinc complexes have been recently reported in literature.[3] Prodigiosin was found to complex with copper (II) in a 1:1 ratio compared to zinc (II), which complexed with a 1:2 ratio. Surprisingly, the C-pyrrole ring in the copper complex was found to have been oxidised and contained an OH group which was suggested to be derived from water in the solvent. Following the same procedure described by Park *et al.* the formation of a copper/tetrapyrrole complex was attempted to allow a crystal structure to be obtained.[3]

Tetrapyrrole (15 mg, 44.9 μmol) was dissolved in *tert*-butanol (5 mL) followed by the addition of potassium *tert*-butoxide (134 μmol) which yielded a dark blue solution. Copper (II) chloride (15 mg, 89 μmol) was then added in dimethyl sulfoxide (0.5 mL), following which the solution changed to a dark brown solution. After concentration under reduced pressure, a dark solid was obtained which was insoluble in all common organic solvents suggesting that polymerisation had occurred, similar to that reported by Manderville and co-workers with tambjamine E and copper (II).[48]

Given the lack of success, a weaker base than potassium *tert*-butoxide was sought which would hopefully reduce polymerisation. During the isolation of tambjamines, the natural products are often isolated as the acetate salt as a consequence of the ammonium acetate buffer used to prevent hydrolysis of the enamine motif. A literature method suggested using aqueous ammonia to convert the acetate salt into the natural product.[6] Using ammonia to adjust the pH of the solution, a modified procedure was attempted to obtain a single crystal of the tetrapyrrole/copper (II) complex.

Tetrapyrrole (10 mg, 25 μmol) was dissolved in a methanol solution (5 mL), the pH of the solution was adjusted to 10 using concentrated ammonia, to give a red solution with an absorbance at λ_{max} = 540 nm. Copper chloride (8.5 mg, 50 μmol) was then added and the solution changed to a dark green/brown colour, the UV spectrum indicated a dramatic decrease λ_{max} = 540 nm, indicating that complexation with copper had occurred. Following partitioning with ether, the organic extract was

concentrated and the resulting solid, dissolved in ethyl acetate. Polymerisation had again occurred, however, some of the solid redissolved in ethyl acetate. The ethyl acetate solution was filtered through cotton wool to remove undissolved polymeric material and although a pentane vapour diffusion method was attempted no crystals were obtained.

4.4 Photodynamic therapy

Both photodynamic therapy and radiotherapy utilise free radicals to cause damage and ultimately lead to cellular death of cancerous tumours. The method of free radical production differs in the two therapies. Radiotherapy involves the production of free radicals using radiation whilst photodynamic therapy utilises a photosensitiser to produce singlet oxygen and other reactive oxygen species.[104] Free radicals are molecules with an unpaired electron and are produced naturally through metabolic processes and as intermediates in the drug metabolism. If the free radical contains oxygen, they are termed reactive oxygen species (ROS) and are typically highly reactive and short-lived. Living organisms produce a range of antioxidants to prevent ROS from causing damage to macromolecules e.g. DNA. Some free radicals such as nitric oxide and superoxide, however, have been shown to be of importance in controlling blood pressure and in the bodies' defence against harmful bacteria. The cell damaging ability of free radicals has attracted interest in anti-cancer drug development.[104]

Photodynamic therapy involves the administration of a photosensitiser which accumulates preferentially in tumour cells. The photosensitiser upon irradiation with laser light produces highly toxic singlet oxygen ($^1O_2$) which damages various important macromolecules leading to cell death. The advantage of photodynamic therapy is that the photosensitiser is only toxic when activated by light. Using an optical fibre, only the required tumour is targeted thereby minimising the side-effects associated with traditional cancer therapies.

The following characteristics are desired in a photodynamic therapy agent:[105]

1) Strong absorption in the red light region to allow maximum penetration of irradiating light as red light is not absorbed by body tissue
2) Non-toxic in the absence of light

3) Excited triplet state with a life time sufficient to allow the production of singlet oxygen or other cytotoxic species

4) Selective retention in cancerous cells

5) Rapid removal from the body following treatment

Given the similarity in structure of the 4-methoxypyrrolic natural products to presently used photosensitisers e.g. haematoporphyrin derivative[106] or the sodium salt of the tetrasulfonated aluminium phthalocyanine which is currently at the end of the second stage of clinical trials,[107] it was thought that the 4-methoxypyrrollic natural products could be potential photodynamic therapy agents. To investigate this potential, the fluorescent quantum yields, singlet oxygen production and photodegradation of **13** and **15** were investigated.

4.4.1 Photochemistry

The term photosensitiser was first developed by Oscar Raab who showed that common dyes such as acridiens and xanthenes caused death in protozoa when exposed to light and oxygen, making the protozoa sensitised to normally harmless wavelengths of light.[108] Today, the term photosensitiser is used to describe a vast group of compounds, which when activated by light, generate oxygen species toxic to living cells. When a molecule absorbs light, there are various different relaxation pathways which it could undergo as shown in the Jablonski diagram in Figure 4.5.[104]
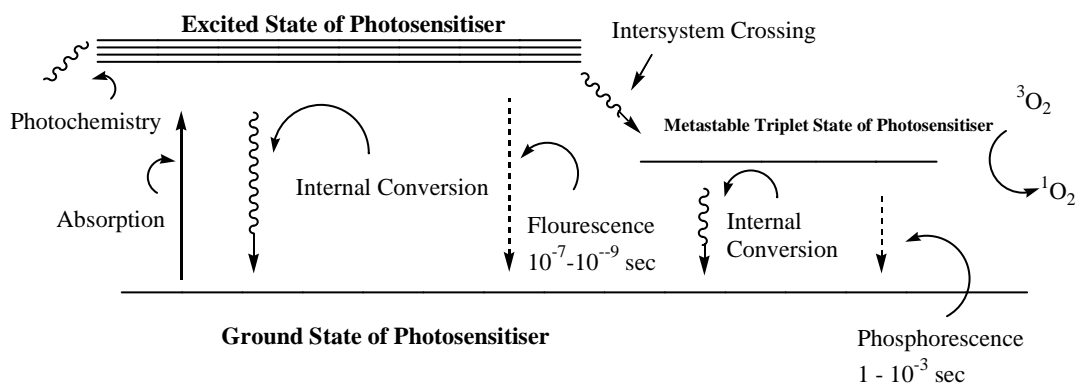
Figure 4.5: Jablonski diagram.

Depending on environment and molecular structure, one of the pathways shown in Figure 4.5 is followed after excitation. Internal conversion involves radiationless decay whilst fluorescence involves the emission of a photon typically at a higher wavelength than that at which absorption occurred. Intersystem crossing is another method of relaxation to the lower triplet state, this requires a spin inversion and is termed a forbidden transition, giving the triplet state longer lifetimes. This intersystem conversion is promoted by heavy atoms. The molecule in the triplet state can then either phosphoresce through radiative decay[109] or generate ROS in its relaxation from the triplet to ground state. In the generation of ROS there are two separate pathways that the activated photosensitiser can undergo. These two pathways differ in the reactive oxygen species produced, Type I leads to the production of radical forms of oxygen such as superoxide (O_2^-), hydrogen peroxide (H_2O_2) or hydroxyl radicals ($OH^\cdot$) whilst Type II produces the non-radical, highly toxic singlet oxygen ($^1O_2$).[108]

Figure 4.6 Formation of activated oxygen species from photosensitsers
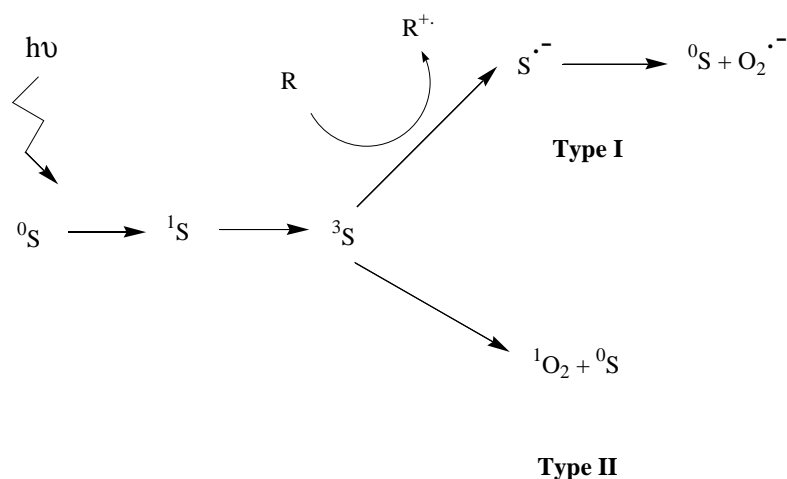
^0S – photosensitiser in ground state

^1S – photosensitiser in excited singlet state

^3S – photosensitiser in long-lived triplet state

R – reducing substrate

4.4.2 Photochemical techniques

In order to determine the potential of the 4-methoxypyrollic natural products as photodynamic therapy agents, the photobleaching, fluorescent quantum yields and singlet oxygen quantum yields of **13** and **15** were determined.

4.4.2.1 Photodegradation

Photodegradation was the first physical property of the 4-methoxypyrrolic natural investigated. Knowledge of the rate and mechanism of photodegradation is of importance when determining the photodynamic potential, as a PDT agent needs to be stable enough to produce singlet oxygen to give rise to the destruction of tumour cells, but also needs to breakdown in reasonable time in order to allow the body to remove the drug. During irradiation of the PDT agent, radicals such as singlet oxygen are produced that will lead to the destruction of the agent itself in addition to the cancerous cell. Photostabilities are expressed as photodegradation quantum yields (quantum $cm^{-2} s^{-1}$) which give an indication of how many molecules are degraded per quantum of light. The photodegradation quantum yields (Φ_D) is calculated using Equation 4.1:[104]

$$\Phi_D = \frac{(C_o - C_t) \ V}{I_{abs} \times t} \qquad \ldots\ldots..(4.1)$$

Where:

 V is the sample volume

t is irradiation time

C_o is the initial concentration of the natural product

C_t the final concentration of the natural product following irradiation

I_{abs} is the absorbed light determined using Equation 4.2:

$$I_{abs} = \frac{\alpha SI}{N_a} \qquad \ldots\ldots..(4.2)$$

Where:

α is the fraction of light absorbed

S is the irradiated cell area

I is the light intensity

N_a Avogardo's number

The mechanism of photobleaching was investigated by measuring the effect of saturating with oxygen and nitrogen, in the presence of the radical scavenger diazobicyclooctane (DABCO, 1×10^{-3} M) and in DMSO-D_6. Photodegradation studies were carried out by adjusting the concentration of the natural product to give an absorption of approximately 1 followed by irradiation using a tungsten lamp. A Wratten Special Filter 21+58 was used for **15** and water bath filter was used for **13** to optimise the wavelength for each natural product. The change in the UV-Vis absorption spectra was followed to monitor photodegradation. Figure 4.7 shows the rates of photodegradation of tetrapyrrole with the different treatments described.
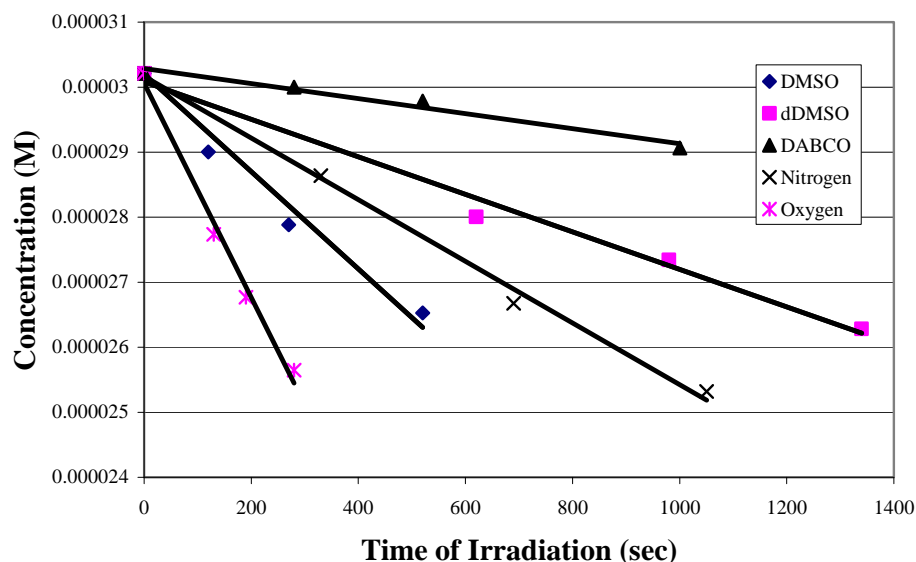
Figure 4.7: Effects of diazobicyclooctane, oxygen saturation, nitrogen saturation and deuterated dimethylsulfoxide on the photodegradation of tetrapyrrole natural product in dimethylsulfoxide.

As Table 4.2 and Figure 4.7 show the tetrapyrrole natural product degraded with a quantum yield of 1.04×10^{-4}. An increase in the rate of photodegradation was observed when the dimethylsulfoxide solution was saturated with oxygen. This result indicates the production of a reactive oxygen species which is involved in degradation, this species is not singlet oxygen however as no increase in the rate of photodegradation was observed with DMSO-D_6. Deuterated solvents are known to increase the lifetime of the triplet state.[104] Both nitrogen and DABCO reduced the

quantum yield from 1.04×10^{-4} to 8.93×10^{-5} and 1.57×10^{-5} respectively, suggesting that an oxygen radical species is involved in photobleaching.

Similar results were obtained for **13**, as with **15** the rate of photodegradation was increased when the solution was saturated with oxygen and slowed following purging with nitrogen gas and treatment with diazobicyclooctane. When dimethylsulfoxide-D_6 was used, a slight increase in the rate of photodegradation was observed however this is too small to be considered significant. From the photodegradation results, it can be concluded that **13** and **15** follow the same radical mechanism of degradation which could possibly be from the formation of an oxygen radical. Of particular interest is the higher photodegradation quantum yield of **13** (1.94×10^{-3}) compared to that of **15** (1.04×10^{-4}).

	Quantum Yields of Photobleaching of 13	Quantum Yields of Photobleaching of 15
DMSO	1.94×10^{-3}	1.04×10^{-4}
D^6-DMSO	2.94×10^{-3}	3.70×10^{-5}
DABCO	2.48×10^{-4}	1.57×10^{-5}
Nitrogen	2.90×10^{-3}	8.93×10^{-5}
Oxygen	5.11×10^{-3}	2.85×10^{-4}

Table 4.2: Photobleaching quantum yields of **13** and **15** when dimethylsulfoxide solution saturated with oxygen or nitrogen and in the presence of diazobicylooctane (2×10^{-3} M) and dimethylsulfoxide-D_6.

4.4.2.2 Fluorescence quantum yield determinations

As shown in Figure 4.3, following excitation one of the methods of relaxation is fluorescence, typically at a higher wavelength to that of absorption. Fluorescence is quantified using the fluorescence quantum yield, which is defined as the number of photons emitted relative to the number of photons absorbed. In order to standardise

the quantum yield values, the fluorescence is compared to a standard with a known quantum yield. To experimentally determine the fluorescence quantum yield the fluorescence at various concentrations is measured and calculated using the following equation:[104]

$$\Phi_F = \Phi_{F\,(standard)} \times \frac{grad_{(sample)} \times \eta^2_{(sample)}}{grad_{(standard)} \times \eta^2_{\,(standard)}} \qquad \qquad ....4.3$$

Where:

grad is the gradient when fluorescence is plotted against the respective absorbance

η is the refractive indices of the solvent used

In order to prevent fluorescence quenching, low concentrations were used with absorbance values less than 0.1.

Using dimethylsulfoxide as the solvent the fluorescence quantum yields of **13** and **15** were determined using chlorophyll and Rhodamine 6G as the respective standards. In dimethylsulfoxide **15** was found to have a maximum absorbance at 537 nm and **13**, a maximum absorbance at 350 nm. Excitation was carried out at these wavelengths. The fluorescence of tetrapyrrole was found to be very concentration dependant and aggregation was suspected to be occurring, thereby interfering with dilutions used in determinations. To standardise the experimental procedure following dilution, the solution was left to stand for 5 minutes.

The tetrapyrrole natural product (**15**) was found to exhibit a very high fluorescence quantum yield of 0.90 ± 0.01. It was expected that tambjamine E (**13**) would similarly show a high fluorescence quantum yield, however in dimethylsulfoxide at concentrations with absorbances ranging from 0.005 to 0.5, no fluorescence was detected. This result could be explained by solvent quenching given the low excitation wavelength used (350 nm). To ensure that solvent quenching was not taking place, the experiment was repeated using hexane as the solvent and again, very little fluorescence was observed. A similar result has been reported by Manderville and co-workers who state that tambjamine E, tetrapyrrole and bipyrrole aldehyde all exhibit weak emission spectra in water which increases slightly in methanol and chloroform.[49]

4.4.2.3 Singlet oxygen production quantum yield

Singlet oxygen production is quantified using the singlet oxygen production quantum yield, which describes the number of singlet oxygen species formed per photon of light absorbed. The method employed to determine the singlet oxygen quantum yield involved the use of 1,3-dipenylisobenofuran (DPBF) which absorbs with a maximum wavelength of 417 nm. DPBF is a quencher, which reacts with singlet oxygen and degrades the quencher, allowing easy measurement of singlet oxygen through monitoring the decrease in the absorption at 417 nm. Only the first 20% decrease is measured to ensure that first order kinetics data applies. Using the following equation, the singlet oxygen quantum yield can be determined:[104]

$$\frac{-[DPBF]}{dt} = K_q\,[DPBF][^1O_2] \qquad\qquad\qquad ....3.4$$

This equation can be rearranged as follows:

$$\Phi_\Delta{}^{sample} = \Phi_\Delta{}^{standard} \times \frac{(C_o - C_t)^{sample}}{(C_o - C_t)^{standard}} \times \frac{(\alpha t)^{standard}}{(\alpha t)^{sample}} \times \frac{[DPBF]^{standard}}{[DPBF]^{sample}}$$

Where:

$C_o - C_t$ is the change in DPBF concentration

α is the fraction of light absorbed ($\alpha = 1$, determined by S. Maree)[104]

t is the irradiation time

Determination of singlet oxygen production was carried out by irradiating a solution of tetrapyrrole and DPBF in dimethylsulfoxide using a Nd-YAG laser (532 nm), and measuring the decrease in the absorption of DPBF. Very little decrease in the absorption of DPBF was observed and photodegradation of the tetrapyrrole was observed evidenced by a decrease in absorption at 540 nm. This could be due to the high intensity of light, so the experiment was repeated using a tungsten lamp rather than laser light. Again, photodegradation of tetrapyrrole was observed and the singlet oxygen production quantum yield was determined to be less than 0.01. This result is not surprising given the high fluorescence quantum yield as fluorescence and the triplet states are in competition as explained earlier in Figure 4.3.

Singlet oxygen production by **13** was hampered by the similarity in absorption wavelengths of **13** and DPBF. When experiments were conducted using a water bath filter, a decrease in the absorption of DPBF was observed. The rate of decrease in the absorption of DPBF was found to be similar to that of the photodegradation of DPBF in the absence of **13**, suggesting that only photodegradation was occurring and not quenching of any singlet oxygen produced. The UV absorbance maxima of tambjamines, however, makes them unsuitable for use as a photodynamic therapy agent as compounds with a maximum absorbance greater than 600 nm are favoured for maximal absorbance of tissue penetrating red laser light.

4.5 Conclusion

While the 4-methoxypyrrolic natural products were shown to be poor singlet oxygen producers which may make them unsuitable for use as photosensitisers, their high fluorescence could however allow them to be used as a diagnostic dyes. Manderville and co-workers found that DNA cleavage carried out by the 4-methoxypyrrolic natural products with copper (II) was completely inhibited when the enzyme catalase was added, this could suggests that DNA cleavage could occur through a mechanism involving hydrogen peroxide as the reactive oxygen species. This work could be extended to investigate the production of hydrogen peroxide by 4-methoxypyrrolic natural products and compare the effect of copper on fluorescence and hydrogen peroxide production. Heavy metal atoms have been reported to promote intersystem crossing, thus when the 4-methxoypyrrolic natural products are complexed with copper (II), the triplet state could be promoted and rather than fluorescing, the excited molecules could relax through the mechanism described previously leading to the production of hydrogen peroxide as a cytotoxic species. The absorption spectrum of tetrapyrrole is very close to the required 600 nm for PDT, with slight synthetic modification, this absorption could be shifted to longer wavelengths.

Chapter Five

Experimental

5.1 General experimental procedures

5.1.1 Analytical

The ^{1}H (400 MHz), ^{13}C (100 MHz) and 2D NMR spectra were recorded on a Bruker AVANCE 400 NMR spectrometer. Chemical shifts are reported in ppm and are referenced to residual undeuterated solvent resonances. Infrared data were obtained on a Perkin-Elmer Spectrum 2000 FT-IR spectrometer with compounds as films (neat) on NaCl disks. Low resolution mass spectra were recorded on a Hewlett-Packard 5988A spectrometer using electrospray ionisation in the positive ion mode. High resolution fast atomic bombardment mass spectra (FABMS) were obtained by Professor L. Fourie of the Mass Spectrometry Unit at the University of Potchefstroom, South Africa. Melting points were obtained using a Gallenkamp melting point apparatus. Cyclic voltametry scans were performed using a BAS CV-50W Cyclic Voltametery Analyser. UV spectra were measured using a Varian Cary 500 UV/Vis spectrometer, and fluorescence data obtained using a Varian Cary Eclipse Fluorescence Spectrophotometer.

5.1.2 Chromatography

General laboratory solvents were distilled from glass before use. Analytical normal phase thin layer chromatography was carried out on 25 DC-Plastikfolien Kiesegel 60 F_{254} plates and reverse phase thin layer chromatography was carried out using DC-Ferigplatten RP18 F_{254} plates. TLC plates were viewed using a UV lamp (254 nm and 365 nm). Solid phase extraction was performed using at Waters C18 Sep-pak (2 g or 10 g) and Diaion HP-20®. Reversed phase semi-preparative HPLC separations were performed at a flow rate of 4 mL/min on a Phenomenex Luna 10µ C18 column, gradient elutions were performed on an Agilent HP1100 LC-MSD (consisting of a quaternary pump, a degasser, a DAD detector, an 1100 MSD and a ChemStation for data acquisition and processing) and isocratic elutions being performed using a Spectra Physics Isochrom LC Pump and a Waters R401 Differential Refractometer. Normal phase semi-preparative HPLC separations were carried out using a Whatman Magnum 9 Partsil 10 column using a Water 410 Differential Refractometer.

5.1.3 Synthesis

Anhydrous reactions were carried out using oven-dried apparatus (150°C) under an argon atmosphere. Solvents requiring drying were prepared by standard procedures,[110] prior to use. THF was distilled from sodium metal/benzophenone ketyl, CH_2Cl_2 was distilled from CaH_2 and pyrrole was distilled from glass. MeCN and CH_2Cl_2 were stored over 4 Å molecular sieves. All reactions were magnetically stirred. Potassium *tert*-butoxide, propyl amine, 4-methoxypyrridine-N-oxide were purchased from Sigma-Aldrich S.A. (Pty) Ltd.

5.1.4 Molecular modelling

Molecular modelling was performed on a Silicon Graphics computer employing Dmol 3 with the density functional theory using GGA functional with the Double Numeric d-function (DND) basis set. A molecular dynamics routine was used to explore conformational space and establish global energy minima of the compounds modelled. Atomic charges were calculated using a Muliken analysis.

5.1.5 Electrochemistry

Tetraethylammonium perchlorate (TEAP) electrolyte was prepared by mixing equal volumes of hot solutions of 1.0 M sodium perchlorate and 1.0 M tetraethylammonium chloride. The solution was then cooled in an ice bath and the resulting precipitate filtered, washed with cold ethanol and then recrystallised from hot redistilled ethanol. MeCN solvents used in electrochemistry were dried over CaH_2 and distilled before use. Nitrogen gas was bubbled through the solution prior to recording cyclic voltamograms, and the inert atmosphere was maintained throughout the cyclic voltametry scans. Prior to cyclic voltammetry scans, the working electrodes were polished using alumina pastes on a Buehler felt pad, followed by washing with deionised H_2O and rinsing with Me_2CO, MeOH and MeCN.

5.1.6 Photochemistry

Photodegradation and singlet oxygen studies were carried out using a general electric quartz lamp (300 W). A H_2O filter, to filter off ultraviolet and far infra-red radiation and an interference filter (Wratten Special Filter 21+58A), were placed before the

light source. The light intensity was measured using a power meter and was found to be 5×10^{16} photons/cm^2.[104] Singlet oxygen studies were carried out using the general electric quartz lamp using the setup explained above and Nd-Yag laser providing 400 mJ, 9 ns pulses of laser light at 10 Hz. All photochemical experiments were carried out in a spectrochemical cell of 1 cm pathlength using DMSO as a solvent without deoxygenating, or by bubbling of oxygen when stated. 1,3-diphenylisobenzofuran (DPBF) and 1,4-Diazabicyclo(2,2,2)octane (DABCO) were purchased from Aldrich.

5.2 Chapter two experimental

5.2.1 Animal material

Natural product isolation was carried out on 23 specimens of *Tambja capensis* specimens were collected from Simonstown in August 1999 (Tam99) and *Bugula dentata* (wet mass = 267 g, dry mass = 98 g) collected in Algoa Bay, 2003 (Bry03) using SCUBA. For details of samples used in the quantitative analysis of tambjamine and tetrapyrrole metabolites, see Table 2.2, page 25.

5.2.2 Extraction and isolation of 4-methoxypyrrolic alkaloids from *T.capensis*

Tam99 was steeped in Me$_2$CO at $-20°$C in the dark until February 2003. The Me$_2$CO extract was concentrated under reduced pressure to give an aqueous suspension that was partitioned between CH$_2$Cl$_2$. The organic extract was dried (MgSO$_4$) and concentrated to give a dark brown oil (427 mg) that was adsorbed onto C18 (2g) and applied dry to a Waters C-18 solid-phase extraction cartridge (10 g) equilibrated in 1:1 MeOH/H$_2$O solution containing 0.1 M NH$_4$OAc. The column was eluted under vacuum (flow-rate = 4 ml/min) using gradient elution (1:1, 3:2, 7:3, 4:1, 9:1 MeOH/H$_2$O, MeOH and 1:1 MeOH/CH$_2$Cl$_2$; all eluents buffered with 0.1 M NH$_4$OAc), using ^{1}H NMR spectroscopy to determine which fractions contained 4-methoxypyrrolic compounds. Of the 7 fractions collected, only the first fraction (276 mg; eluting with 1:1 MeOH/H$_2$O) was selected for further purification. Semi-preparative reversed phase gradient HPLC (isocratic elution with 1:1 MeOH/H$_2$O for 5 min, linear gradient of 1:1 MeOH/H$_2$O to MeOH over 30 minutes, isocratic elution with MeOH for 5 minutes; all eluents buffered with 0.1 M NH$_4$OAc; simultaneous DAD detection at 254, 405 and 590 nm) and isocratic reversed phase HPLC of

selected fractions (using either 6:4 MeOH/H_2O buffered with 0.1 M NH_4OAc or 7:3 MeOH/H_2O buffered with 0.1 M NH_4OAc) afforded (in order of elution) **7** (11 mg), **13** (10 mg) and **15** (3.3mg). Natural product **15** was converted from the OAc salt through treatment with NH_3 in MeOH.

7   **13**   **15**
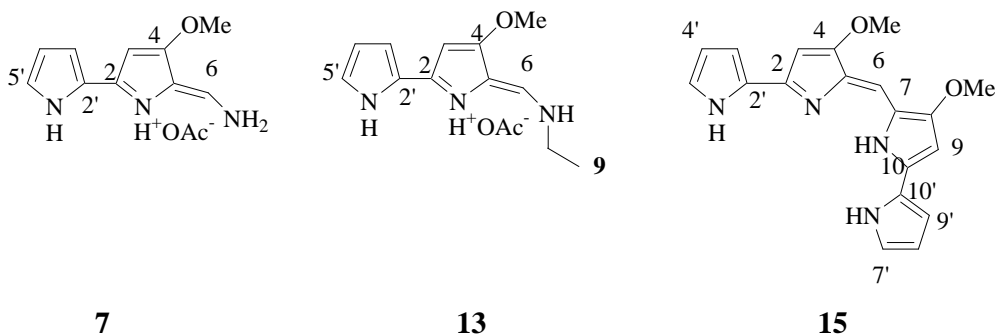
Tambjamine A (7): Green oil; IR ν_{max} 3635, 3480, 1675, 1605, 1535 cm^{-1}; UV (MeOH) nm (log ε) 397 (4.32); ^{1}H NMR (CDCl$_3$, 400 MHz) δ 12.06 (1H, s, H-7), 10.31 (1H, brs, H-1'), 7.41 (1H, brs, H-6), 7.08 (1H, dd, J = 3.7, 2.7 Hz, H-3'), 6.75 (1H, m, H-5'), 6.28 (1H, m, H-4'), 5.94 (1H, s, H-3), 3.93 (3H, s, OMe), 2.08 (3H, s, OAc); ^{13}C NMR (CDCl$_3$, 100 MHz) δ 178.9 (OAc), 165.2 (C-4), 144.8 (C-2), 138.6 (C-6), 124.7 (C-3'), 122.7 (C-2'), 114.1 (C-5'), 112.8 (C-5), 110.6 (C-4'), 91.6 (C-3), 58.3 (OMe), 24.4 (OAc); HRFABMS *m/z* 189.0902, calcd 189.0901.

Tambjamine E (13): Green solid, IR ν_{max} 3500, 2800, 1664, 1608, 1529, 1170, 977 cm^{-1}; UV (MeOH) nm (log ε) 405 (4.39); ^{1}H (CDCl$_3$, 400 MHz) δ 12.40 (1H, brs, H-1'), 7.33 (1H, brs, H-6), 7.03 (1H, dd, J = 2.3, 1.4 Hz, H-3'), 6.68 (1H, dd, J = 2.4, 1.2 Hz, H-5'), 6.24 (1H, dd, J = 3.6, 2.6 Hz, H-4'), 5.94 (1H, s, H-3), 3.89 (3H, s, OMe), 3.50 (2H, q, J = 7.6 Hz, H-8), 2.09 (3H, s, OAc), 1.34 (3H, t, J = 7.2 Hz, H-9); ^{13}C (CDCl$_3$, 100 MHz) δ 179.5 (OAc), 164.2 (C-4), 145.2 (C-2), 140.9 (C-6), 123.7 (C-3'), 123.0 (C-2'), 112.6 (C-5'), 111.2 (C-5), 110.1 (C-4'), 91.2 (C-3), 58.2 (OMe), 46.0 (C-8), 25.4 (C-9), 15.6 (OAc); HRFABMS *m/z* 217.1215, calcd 217.1215.

Tetrapyrrole (15): Blue solid, IR ν_{max} 1635, 1630, 1590, 1537, 1510, 1260, 1233, 960 cm^{-1}; UV (MeOH) nm (log ε) 591 (4.81), 555 (4.46), 325 (4.00), 280 (3.83); ^{1}H NMR (CDCl$_3$, 400 MHz) δ 11.98 (2H, brs, H-1', H-7'), 11.77 (1H, brs, H-11), 7.12

(1-H, brs, H-6), 7.11 (2-H, brm, H-5', H-7'), 6.79 (2H, ddd, J = 4.7, 2.4, 1.3 Hz, H-3', H-9'), 6.31 (2H, ddd, J = 4.6, 2.8, 0.7 Hz, H-4', H-8'), 6.07 (2H, d, J = 1.6 Hz, H-3, H-9), 3.95 (6H, OMe); ^{13}C NMR (CDCl$_3$, 100 MHz) δ 163.5 (C-4, C-8), 143.2 (C-2, C10), 124.8 (C-5'), 123.3 (C-2', C-10'), 117.6 (C-5, C-9), 114.4 (C-3', C-9'), 111.4 (C-4', C-8'), 109.6 (C-6), 92.7 (C-3, C-9), 58.8 (OMe); HRFABMS *m/z* 334.1429, calcd 334.1582.

5.2.3 Extraction and isolation of 4-methoxypyrrolic alkaloids from *B. dentata*

Extraction and cyclic loading:

The bryozoan sample (1.5 kg) was cut into small cubes (~2 cm per side) and was extracted twice with MeOH (2 x 2 L) for 12 hr. The second extract (2 L, 14.8 g) was passed through an HP-20 column (500 mL, 45 x 5 cm) conditioned by washing with Me$_2$CO (1.5 L) and MeOH (1.5 L). The eluent, was collected and diluted with 0.1 M NH$_4$OAc buffer (2 L) then passed through the same column. Finally, the eluent was diluted further with 0.1 M NH$_4$OAc buffer (4 L) and was passed again through the same column.

Stripping and backloading:

The column was then eluted with 1.5 L fractions 20%, 40%, 60%, 80% Me$_2$CO/0.1M NH$_4$OAc and 100% Me$_2$CO. Each fraction from the stripping stage was then loaded onto a second HP-20 column (100 mL, 15 x 4 cm) pre-equilibrated with Me$_2$CO (300 mL) and then stripped using MeOH (200 mL) and Me$_2$CO (200 mL) which were combined to give one fraction.

A similar procedure was carried out on the first extract (2 L, 44 g) however, given the large mass of the first extract, the extract was divided into three separate batches which were combined at the end of backloading. The second and first extracts were kept separate throughout the isolation procedure.   The ^{1}H spectra of the fractions showed peaks in the 6-8 ppm region, indicative of tambjamine natural products, in the 40%, 60% and 80% Me$_2$CO/ 0.1 M NH$_4$OAc buffer. From the masses of the samples obtained only the 60% and 80% Me$_2$CO/ 0.1 M NH$_4$OAc buffer fractions were chosen to be purified further using semi-preparative C-18 reversed phase HPLC (isocratic

elution with 1:1 MeOH/H_2O for 5 min, linear gradient of 1:1 MeOH/H_2O to MeOH over 30 minutes, isocratic elution with MeOH for 5 minutes; all eluents buffered with 0.1 M NH_4OAc; simultaneous DAD detection at 254, 405 and 590 nm) and isocratic reversed phase HPLC of selected fractions using 7:3 MeOH/H_2O buffered with 0.1 M NH_4OAc to give **15** (130 mg).

5.2.4 Analysis of tambjamine and tetrapyrrole content of collected samples

All of the samples analysed were steeped in redistilled acetone at –20°C in the dark until February 2003. The Me_2CO extracts were concentrated under reduced pressure to give an aqueous suspension that was partitioned with CH_2Cl_2. The organic extract was dried ($MgSO_4$) and concentrated. Using analytical reversed phase HPLC using a linear gradient of 1:1 MeOH/H_2O to MeOH over 30 minutes, followed by isocratic elution with MeOH for 5 minutes; all eluents buffered with 0.1 M NH_4OAc; simultaneous DAD detection at 254, 405 and 590 nm. Standard curves of tambjamine A (**7**), E (**13**), K (**21**), I (**22**) and tetrapyrrole (**15**) were established by measuring the absorbance at 405 nm and 590 nm with varying concentrations. Known concentrations of the sample extracts were then injected and the concentrations determined from their relative absorbances.

5.3 Chapter three experimental

5.3.1 Synthesis of 3-methoxy-2-formylpyrrole (47)

Compound **48** (2 g, 16 mmole) and $CuSO_4$ (39 g, 160 mmole) were dissolved in H_2O (500 mL) and irradiated in a classical well immersion photoreactor for (4-9 hr), then saturated with NaCl and partitioned with $CHCl_3$. The organic partition was concentrated under reduced pressure and purified through sublimation (100°C, 2.5 mmHg) to yield a white crystalline product (660 mg, 33% yield).
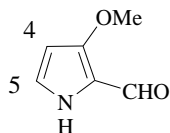
47

White crystalline solid; m.pt 109°C, Lit.[77] 120°C; IR ν_{max} 3138, 2918, 2850, 2360, 1625, 1513, 1344, 1074, 799, 749 cm^{-1}; UV (CHCl$_3$) nm (log ε) 284 (4.39); ^{1}H NMR (CDCl$_3$, 400 MHz) δ 10.30 (1H, brs, H-1), 9.51 (1H, s, H-7), 6.94 (1H, t, J = 2.8 Hz, H-5), 5.88 (1H, t, J = 2.4 Hz, H-4), 3.86 (3H, s, OMe); ^{13}C (CDCl$_3$, 100 MHz) δ 175.3 (CHO), 158.7 (C-3), 126.7 (C-5), 118.8 (C-2), 95.4 (C-4), 57.9 (OMe); ESIMS *m/z* [M+1]$^+$ 126.0; HRFABMS *m/z* 125.0476, calcd 125.0476.

5.3.2 Attempted synthesis of 3-methoxy-2,2'-bipyrrole carboxyaldehye (11)

Methylene blue singlet oxygen producer

Compound **47** (20 mg, 160 μmole) and methylene blue (1mg) was dissolved in dichloromethane, cooled (-78°C) and purged with oxygen gas (10 min). The solution was then irradiated using a 350 W tungsten lamp (30 min, -78°C) following which cold pyrrole (45 μL, 400 μmole) in CH$_2$Cl$_2$ (2 mL) was added and the solution was stirred (1 hr). The solution was then filtered through celite 535 and solvent removed under reduced pressure and purified using a C-18 Sep-pak eluted using 25%, 50%, 75% aqueous MeOH and 100% MeOH). The ^{1}H NMR spectrum showed that the major product of the reaction was unreacted **47**, which eluted in the 25% aqueous MeOH fraction.

ZnPc singlet oxygen producer

Compound **47** (20 mg, 160 μmole) and ZnPc (1 mg) was dissolved in DMSO-D$_6$ and purged with oxygen followed by irradiation using a 350 W tungsten lamp (30 min) under a constant stream of oxygen. Pyrrole (45 μL, 400 μmole) was added and the solution was stirred (1 hr). ^{1}H NMR spectrum showed the major components of the reaction mixture were **47**, pyrrole and ZnPc.

5.3.3 Synthesis of 2-propylimine-3-methoxypyrrole (51)

Compound **47** (10 mg, 80 μmole) was added to anhydrous 1,2 EtCl$_2$ (1.2 mL) followed by the addition of propylamine (66 μL, 800 μmole) and AcOH (40 μL, 695 μmole) under argon and the solution stirred (4 hr). The solution was then partitioned between aqueous Na$_2$CO$_3$ (3 mL, 10% w/v) and CH$_2$Cl$_2$ (3 mL) and aqueous layer

washed with CH_2Cl_2 (3 x 3 mL). The organic partition was then concentrated under reduced pressure to yield **51** (13.0 mg, 98%).

51
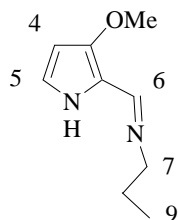
Red oil; IR ν_{max} 3589, 2088, 1634, 1556, 1520, 1428, 1346, 1281, 1073, 1005 cm^{-1}; UV (CHCl$_3$) nm (log ε) 329 (4.03), 301 (4.13); ^{1}H NMR (CDCl$_3$, 400 MHz) δ 8.04 (1H, s, H-7), 6.72 (1H, d, J = 2.8 Hz, H-5), 5.85 (1H, d, J = 2.8 Hz, H-4), 3.80 (3H, s, OMe), 3.43 (2H, t, J = 6.8 Hz, H-7), 1.62 (2H, sex, J = 7.2 Hz, H-8), 0.90 (3H, t, J = 7.2 Hz, H-9); ^{13}C NMR (CDCl$_3$, 100 MHz) δ 148.7 (C-3), 126.0 (C-5), 121.4 (C-6), 114.4 (C-2), 95.4 (C-4), 61.8 (C-7), 58.1 (C-8), 24.4 (OMe), 11.7 (C-9); ESIMS m/z [M+1]$^+$ 167.1; HRFABMS m/z 166.1106, calcd 166.1105.

5.3.4 Attempted synthesis of 21 from 51

Compound **51** (20 mg, 120 μmole) and methylene blue were dissolved in anhydrous CH_2Cl_2 (20 mL), the solution was stirred (10 min), cooled (-78°C) and purged with oxygen (10 min). The solution was then irradiated using a 350 W tungsten lamp with a red filter under a constant flow of oxygen following which cold pyrrole (20 μL, 600 μmole) in CH_2Cl_2 (3 mL) was added and solution was stirred (1 hr). The methylene blue was then removed by filtration through celite 535 and solution was concentrated under reduced pressure. No conclusions could be drawn from the ^{1}H NMR spectrum. The ESIMS (positive ion mode) showed a major peak at 248.7, this product could not be isolated, only unreacted **47** was isolated using gradient reversed phase HPLC.

5.3.5 Attempted reduction of 47 to the primary alcohol (53) using lithium aluminium hydride

Compound **47** (40 mg, 320 μmole) was dissolved in anhydrous THF followed by the addition of lithium aluminium hydride (12 mg, 320 μmole) in anhydrous THF (1 mL)

dropwise *via* a cannula at 0°C. The reaction mixture was then allowed to warm to room temperature and stirred (2 hr) followed by the addition of dilute HCl (5 drops) and partitioned between EtOAc and H_2O. The organic layer was washed with H_2O (3 x 3 mL). From TLC and ^1H NMR it was concluded that only unreacted **47** remained. When the solution was refluxed, a dark solution was obtained and the desired reduction product was not detected.

5.3.6 Attempted preparation of the acetal derivative 54

Compound **47** (60 mg, 480 µmole), ethylene glycol (175 µL, 2880 µmole) and *p*-TsOH (5 mg, 26 µmole) were dissolved in dry benzene (30 mL) and the solution was refluxed in a Dean-Stark trap (24 hr). A dark red solution was obtained with a black insoluble product suggesting that polymerisation had occurred.

5.3.7 N-Boc protection of 47

Compound **47** (140 mg, 1.12 mmole) was dissolved in anhydrous MeCN (5 mL) followed by the addition of Boc_2O (366 mg, 1.68 mmole) and DMAP (13 mg, 0.11 mmole) at 0°C, the solution was then stirred (2 hr) under argon. The mixture was evaporated to dryness *in vacuo* and the resulting residue was purified by flash chromatography on SiO_2 (40 x 15 mm) eluting with 100% hexane and 100% CH_2Cl_2. Compound **55** eluted with 100% CH_2Cl_2 and following evaporation afforded a white solid (244 mg, 97% yield).
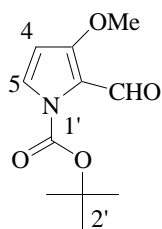
55

White solid; m.pt 74°C; IR ν_{max} 3445, 2981, 2939, 2103, 1746, 1651, 1557, 1448, 1257, 1149, 1090, 846, 753 cm^{-1}; UV (CHCl$_3$) nm (log ϵ) 298 (4.13), 275 (4.17); ^1H NMR (CDCl$_3$, 400 MHz) δ 10.22 (1H, s, CHO), 7.36 (1H, d, J = 3.2 Hz, H-5), 6.07 (1H, d, J = 3.6 Hz, H-4), 3.92 (3H, s, OMe), 1.60 (9H, s, H-3'); ^{13}C NMR (CDCl$_3$,

100 MHz) 180.9 (CHO), 158.9 (C-3), 148.7 (C-1'), 127.0 (C-5), 119.0 (C-2), 99.6 (C-4), 85.9 (C-2'), 58.9 (OMe), 28.3 (C-3'); HRFABMS *m/z* 225.1001, calcd 225.1001.

5.3.8 Attempted bipyrrole synthesis from N-Boc derivative (55)

Compound **55** (140 mg, 622 µmole) and methylene blue (1 mg) were dissolved in CH_2Cl_2 (20 mL), stirred (10 min), cooled (-78°C) and irradiated (30 min) followed by the addition of cold pyrrole (290 µL, 3262 µmole) in CH_2Cl_2 (2 mL) and stirred (1 hr) in the dark. Following concentration *in vacuo*, the residue loaded onto a SiO_2 flash column and eluted with 100% hexane, 25%, 50%, 75% EtOAc/hexane and 100% EtOAc. The ^{1}H NMR spectra of the fractions revealed that the fraction eluting with 25% EtOAc/hexane contained pure **55** whilst the other fractions contained unidentified material.

5.3.9 TFA Boc deprotection of 55

Compound **55** (10 mg, 44 µmole) was dissolved in CH_2Cl_2 (5 mL) and was treated with TFA (40 µL, 522 µmole) under argon. The solution was stirred at room temperature (1 hr) and then partitioned between aqueous K_2CO_3 (5 mL, 1% v/w) and CH_2Cl_2 (5 mL), the aqueous layer was washed with CH_2Cl_2 (3 x 5 mL) and organic partitions combined, dried over $MgSO_4$ and then concentrated under reduced pressure. The ^{1}H NMR data showed that quantitative deprotection had occurred.

5.3.10 K_2CO_3 Boc deprotection of 55

Compound **55** (10 mg, 44 µmole) was dissolved in CH_2Cl_2 (5 mL) and propyl amine (60 µL, 799 µmole) and AcOH (40 µL, 710 µmole) were added under argon and the solution was stirred at room temperature (4 hr). K_2CO_3 (0.1 g) was then added and the solution was stirred under argon (12 hr) followed by partitioning between H_2O and CH_2Cl_2. The aqueous layer was washed with CH_2Cl_2 (3 x 5 mL) and the organic layers were combined and then dried over $MgSO_4$ and then concentrated under reduced pressure. The ^{1}H NMR spectrum showed quantitative deprotection and conversion to the enamine (**51**).

5.3.11 Synthesis of methyl-4-aza-5-ox-6,6-di-(2-pyrroyl)-2(Z)-hexenoate (57)

Compound **55** (200 mg, 0.88 mmole) and methylene blue (1 mg) were dissolved in CH$_2$Cl$_2$ (10 mL) and the solution was stirred at room temperature (10 min), cooled (-78°C) and purged with oxygen (10 min). Irradiation (30 min) was then carried out (-78°C) under a constant flow of oxygen, followed by the addition of pyrrole (420 μL, 6.3 mmole) in cold CH$_2$Cl$_2$ (3 mL) and stirred (2 hr) in the dark. The solution was then concentrated without heating and the resulting residue was purified by flash column chromatography on SiO$_2$ (30 x 7 mm) eluting with 70% EtOAc/30% hexane and then purified further using normal phase HPLC using a 70% hexane/EtOAc eluting solvent to yield **57**. (16 mg, 15% yield).

57
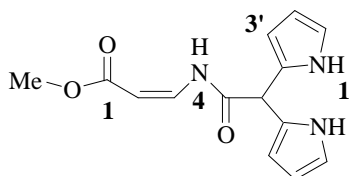
Red oil; IR ν_{max} 3437, 2960, 2067, 1718, 1633, 1464, 1382, 1273, 1205, 1122, 1073 cm^{-1}; UV (CHCl$_3$) nm (log ε) 271 (3.67); ^{1}H NMR (CDCl$_3$, 400 MHz) δ 10.58 (1H, d, J = 10.1 Hz, H-4), 8.65 (2H, s, H-1'), 7.43 (1H, dd, J = 8.8, 11.1 Hz, H-3), 6.76 (2H, dd, J = 3.9, 2.5 Hz, H-5'), 6.18 (2H, dd, J = 5.7, 2.8 Hz, H-4'), 6.14 (2H, t, J = 3.6 Hz, H-3'), 5.16 (1H, d, J = 8.8 Hz, H-2), 5.07 (1H, s, H-6), 3.67 (3H, s, OMe); ^{13}C NMR (CDCl$_3$, 100 MHz) 169.7 (C-5), 168.8 (C-1), 137.2 (C-3), 125.9 (C-2'), 118.4 (C-5'), 108.8 (C-4'), 107.9 (C-3'), 98.0 (C-2), 51.3 (OMe), 45.5 (C-6); HRFABMS *m/z* 273.1118, calcd 273.1113.

5.4 Chapter four experimental

5.4.1 Photochemical studies

The fluorescence quantum yield was determined by carrying out a series of dilutions in DMSO and plotting fluorescence against concentration. Fluorescence of **13** (406 nm) was determined after exciting at 350nm, compared to a chlorophyll a standard whilst fluorescence of **15** (590 nm) was measured after exciting at 537 nm against a Rhodamine 6G standard. For Rhodamine 6G standard the Φ_{fluor} is 0.95.[111]

Photodegradation experiments of **13** and **15** were performed whereby the solutions were deaerated with nitrogen, saturated with oxygen, addition of free radical scavenger DABCO ($2x10^{-3}$ M) and DMSO-D$_6$ in order to determine the mechanism for photobleaching.

The singlet oxygen quantum yields were determined relative to Rhodamine 6G standard (Φ_Δ in DMSO is 0.12) [111] using DPBF as a singlet oxygen scavenger (3 x 10^{-5} M).

5.4.2 Electrochemistry

Cyclic voltametry (CV) was carried out in MeCN using a three-electrode minicell consisting of a glassy carbon working electrode, Pt counter electrode and a Ag wire coated with AgCl reference electrode using TEAP as the supporting electrolyte.

5.4.3 Copper complex of 15 with Cu(II)

Potassium tert-butoxide as a base

15 (15 mg, 44.9 µmole) was dissolved in *tert*-butanol (5 mL) with 3 equivalents of potassium *tert*-butoxide to give a dark blue solution. CuCl$_2$.2H$_2$O (15 mg, 88 µmole) in DMSO (0.5 mL) was then added to afford a dark brown solution. Following removal of the solvents under reduced pressure, a dark insoluble residue was obtained which was thought to be a polymerisation product.

Ammonia as a base

15 (10 mg, 25 µmole) was added to MeOH (3 mL) which had been adjusted to a pH of 10 using NH$_3$, to give a red solution, followed by the addition of CuCl$_2$.2H$_2$O (8.5 mg, 50 µmole) to afford a dark green solution. The solution was then partitioned between H$_2$O (3 mL) and EtOAc (3 mL). The H$_2$O layer was washed with EtOAc (3 x 3 mL) and organic extracts combined and concentrated under reduced pressure. The solid was then dissolved in EtOAc (2 mL) and filtered to remove undissolved solid. Pentane was allowed to diffuse slowly into the EtOAc in the dark, only polymeric material was observed after the solution was left for two weeks.

References

1. Manderville, R. A.; *Curr. Med. Chem.: Anti-Cancer Agents.* **2001**, *1*, 195.

2. Fürstner A.; *Angew. Chem., Int. Ed.* **2003**, *42*, 3582.

3. Park, G.; Tomlinson, J. T.; Melvin, M. S.; Wright, M. W.; Day, C. S.; Manderville, R. A.; *Org. Lett.* **2003**, *5*, 113.

4. Carté, B.; Faulkner, D. J.; *J. Org. Chem.* **1983**, *48*, 2314.

5. Melvin, M. S.; Calcutt, M. W.; Noftle, R. E.; Manderville, R. A.; *Chem. Res. Toxicol.* **2002**, *2002*, 742.

6. Blackman, A. J.; Li, C.; *Aust. J. Chem.* **1994**, *47*, 1625.

7. Rapoport, H.; Holden, K. G.; *J. Am. Chem. Soc.* **1962**, *84*, 635.

8. Wasserman, H. H.; Rogers, G. C.; Keith, D. D.; *J. Am. Chem. Soc.* **1969**, *91*, 1263.

9. Gerber, N.; McInnes, A. G.; Smith, D. G.; Walter, J. A.; Wright, J. L. C.; Vining, L. C.; *Can. J. Chem.* **1978**, *56*, 1155.

10. Gerber, N.; *J. Antibiot.* **1971**, *24*, 636.

11. Gerber, N.; *J. Heterocycl. Chem.* **1973**, *10*, 925.

12. Gerber, N. N.; *Tetrahedron Lett.* **1971**, *11*, 809.

13. Gerber, N. N.; *Crit. Rev. Microbiol.* **1974**, *3*, 469.

14. Wasserman, H. H.; Keith, D. D.; Rogers, G. C.; *Tetrahedron.* **1976**, *32*, 1855.

15. Gerber, N. N.; McInnes, A. G.; Smith, D. G.; Walter, J. A.; Wright, J. L. C.; Vining, L. C.; *Can. J. Chem.* **1978**, *56*, 1155.

16. Williams, R. P.; Hearn, W. R. *Antibiotics;* Guttlieb, D and Shaw, P. D., Heidelberg; 1967; 410.

17. Gerber, N. N.; *Tetrahedron Lett.* **1970**, 809.

18. Gosliner, T. *Nudibranchs of Southern Africa;* Sea Challengers & Jeff Hamann: Tokyo, 1987; p. 100.

19. Osburn, R. C.; *Allan Hancok Pacific Exped.* **1950**, *14*, 1.

20. Lindquist, N.; Fenical, W.; *Experientia.* **1991**, *47*, 504.

21. Wasserman, H. H.; Friedland, D. J.; Morrison, D. A.; *Tetrahedron Lett.* **1968**, *6*, 641.

22. Kazlauskas, R.; Marwood, J. F.; Murphy, P. T.; Wells, R. J.; *Aust. J. Chem.* **1982**, *35*, 215.

23. Matsunaga.; Fusetani, N.; Hashimoto, K.; *Experientia.* **1986**, *42*, 84.

24. Paul, V. J.; Lindquist, N.; Fenical, W.; *Mar. Ec. Prog. Ser.* **1990**, *59*, 109.

25. Karuso, P.; Scheuer, P. J.; *Molecules.* **2002**, *7*, 1.

26. Haygood, M. G.; Schmidt, E. W.; Davidson, S. K.; Faulkner, D. J.; *J. Mol. Microbiol. Biotechnol.* **1999**, *1*, 33.

27. Boger, D. L.; Patel, M.; *Tetrahedron Lett.* **1987**, *28*, 2499.

28. Boger, D. L.; Patel, M.; *J. Org. Chem.* **1988**, *53*, 1405.

29. Castro, A. J.; *Nature.* **1967**, *213*, 903.

30. Boger, D. L.; Coleman, R. S.; Panek, J. S.; *J. Org. Chem.* **1985**, *50*, 5377.

31. Yamamoto, C.; Takemoto, H.; Kuno, H.; Yamamoto, D.; Tsubura, A.; Kamata, K.; Hirata, H.; Yamamoto, A.; Seki, T.; Inoue, K.; *Hepatology.* **1999**, *30*, 894.

32. Yamamoto, D.; Kiyozuka, Y.; Yamamoto, C.; Takemoto, H.; Hirata, H.; Tanaka, K.; Hioki, K.; Tsubura, A.; *J. Cancer. Res. Clin. Oncol.* **2000**, *126*, 191.

33. Diaz-Ruiz, C.; Montaner, B.; Perez-Tomas, R.; *Histol. Histopathol.* **2001**, *16*, 415.

34. Montaner, B.; Perez-Tomas, R.; *Life Sci.* **2001**, *68*, 2025.

35. Montaner, B.; Navarro, S.; Pique, M.; Vilaseca, M.; Martinell, M.; Giralt, E.; Gil, J.; Perez-Tomas, R.; *Br. J. Pharmacol.* **2000**, *131*, 585.

36. Boyd, R. R. *in Anticancer Drug Development Guide: Preclinical Screening, Clinical Trials and Approval;* Ed. Teicher, B., Humana Press Inc: Ottowa, 1987; 23.

37. Greenlee, R. T.; Murray, T.; Bolden, S.; Wingo, P. A.; *Cancer J. Clin.* **2000**, *50*, 7.

38. Stevens, T. H.; Forgac, M.; *Annu. Rev. Cell. Dev. Biol.* **1997**, *13*, 779.

39. Ohkuma, S.; *Seikagaku.* **1984,** *56*, 1499.

40. Mellman, I.; Fucks, R.; Helenuius, A.; *Annu. Rev. Biochem.* **1986**, *55*, 663.

41. Dean, R. T.; Jessup, W.; Roberts, C. R.; *Biochem J.* **1984**, *217*, 27.

42. Ohkuma, S. *in Lysosomes: Their role in Protein Breakdown;* Ed. Glaumann, H.; Ballard, F. J., Academic Press: New York, 1987; p. 115.

43. Sato, T.; Konno, H.; Tanaka, Y.; Kataoka, T.; Nagai, K.; Wasserman, H. H.; *J. Biol. Chem.* **1998**, *273*, 21455.

44. Ohkuma, S.; Sato, T.; Okamoto, M.; Matsuya, H.; Arai, K.; Katoaka, T.; Nagai, K.; Wasserman, H. H.; *Biochem J.* **1998**, *334*, 731.

45. Montaner, B.; Perez-Tomas, R.; *Toxicol. Lett.* **2002**, *129*, 93.

46. Borah, S.; Melvin, M. S.; Lindquist, N.; Manderville, R. A.; *J. Am. Chem. Soc.* **1998**, *120*, 4557.

47. Melvin, M. S.; Wooton, K E.; Rich, C. C.; Saluta, G. R.; Kucera, G. L.; Lindquist, N.; Manderville, R. A.; *J. Inorg. Biochem.* **2001**, *87*, 129.

48. Melvin, M. S.; Tomlinson, J. T.; Saluta, G. R.; Kucera, G. L.; Lindquist, N.; Manderville, R. A.; *J. Am. Chem. Soc.* **2000**, *122*, 6333.

49. Melvin, M. S.; Ferguson, D. C.; Lindquist, N.; Manderville, R. A.; *J. Org. Chem.* **1999**, *64*, 6861.

50. Stepkowski, S. M.; Nagy, Z. S.; Wang, M. E.; Behbod, R.; Erwin-Cohen, R.; Kahan, B. D.; Kirken, R. A.; *Transplant. Proc.* **2001**, *33*, 3272.

51. Stepkowski, S. M.; Erwin-Cohen, R.; Behbod, F.; Kahan, B. D.; Kirken, R. A.; *Blood.* **2002**, *99*, 680.

52. Zhou, B. N.; Hoch, J. M.; Johnson, R. K.; Mattern, M. P.; Eng, W. K.; Ma, J.; Hecht, S. M.; Newman, D. J.; Kingston, D. G.; *J. Nat. Prod.* **2000**, *63*, 1273.

53. Burris, H. A.; Hanauske, A. R.; Johnson, R. K.; Marshall, M. H.; Kuhn, J. G.; Hilsenbeck, S. G.; von Hoff, D. D.; *J. Natl. Cancer. Inst.* **1992**, *84*, 1816.

54. Sim, S. P.; Gatto, B.; Yu, C.; Liu, A. A.; Li, T. K.; Pilch, D. S.; LaVoi, E. J.; Liu, L. F.; *Biochemistry.* **1997**, *36*, 13285.

55. McGovren, J. P. *in Cancer Chemotherapy Handbook;* Ed. Orr, R. T.; von Hoff, D. D., Appleton & Lange: Norwalk, 1994; p. 15.

56. D'Alessio, R.; Bargiotti, A.; Carlini, O Colotta F.; Ferari, M.; Gnocchi, P.; Isetta, A.; Mongelli, N.; Motta, P.; Rossi, A.; Tibolla, M.; Vanotti E.; *J. Med. Chem.* **2000**, *43*, 2557.

57. Copley, R. C. B.; Davies-Coleman, M. T.; Edmonds, D. R.; Faulkner, D. J.; McPhail, K. L.; *J. Nat. Prod.* **2002**, *65*, 580.

58. McPhail, K. L.; Davies-Coleman, M. T.; Starmer, J.; *J. Nat. Prod.* **2001**, *64*, 1183.

59. McPhail, K. L.; Davies-Coleman, M. T.; Copley, R. C. B.; Eggleston.D.S.; *J. Nat. Prod.* **1999**, *62*, 1618.

60. McPhail, K. L.; Davies-Coleman, M. T.; Coetzee, P. S.; *J. Nat. Prod.* **1998**, *61*, 961.

61. McPhail, K. L.; Davies-Coleman, M. T.; *Tetrahedron.* **1997**, *53*, 4655.

62. Gray, C. A, **2002**, Unpublished data.

63. Australian Museum.; *Australian Museum Online*, http://faunanet.gov.au.

64. Diaion HP-20, Supelco, Bellefonte, USA

65. Lindquist, N.; Hay, M. E.; Fenical, W.; *Ecol. Monogr.* **1992**, *62*, 547.

66. Davis, R. A.; Carroll, A. R.; Quinn, R. J.; *Aust. J. Chem.* **2001**, *54*, 355.

67. Jones, R. G.; McLaughlin, K. C.; *J. Am. Chem. Soc.* **1949**, *71*, 2444.

68. Brown, D.; Griffiths, D.; Rider, M. E.; Smith, R. C.; *Chem. Soc. Perkin Trans.* **1986**, *1*, 455.

69. Wasserman, H. H.; Lombardo, L. J.; *Tetrahedron. Lett.* **1989**, *30*, 1725.

70. Wasserman, H. H.; Power, P.; Petersen, A. K.; *Tetrahedron. Lett.* **1996**, *37*, 6657.

71. Wasserman, H. H.; Xia, M.; Wang, J.; Petersen, A. K.; Jorgensen, M.; *Tetrahedron. Lett.* **1999**, *40*, 6145.

72. Wasserman, H. H.; Petersen, A. K.; Xia, M.; Wang, J.; *Tetrahedron. Lett.* **1999**, *40*, 7587.

73. D'Alessio, R.; Rossi, A.; *Synlett.* **1996**, 513.

74. Rizzo, V.; Morelli, A.; Pinciroli, V.; Sciangula, D.; D'Alessio, R.; *J. Pharm. Sci.* **1999**, *88*, 73.

75. Furstner, A.; Krause, H.; *J. Org. Chem*. **1999**, *64*, 8281.

76. Furstner A.; Grabowske, J.; Lehmann, C. W.; Kataoka, T.; Nagai, K.; *ChemBioChem*. **2001**, *2*, 60.

77. Bellamy, F.; Martz P.; Streith, J.; *Heterocycles*. **1975**, *3*, 395.

78. Wasserman, H. H.; DeSimone, R. W.; *J. Am. Chem. Soc.* **1993**, *115*, 8457.

79. DeRosa, M. C.; Crutchley, R. J.; *Coord. Chem. Rev.* **2002**, *233*, 351.

80. Wasserman, H. H. 2004, Personal Communication.

81. Clayden, J.; Greeves, N.; Warren, S.; Wothers, P. *Organic Chemistry;* Oxford University Press: Oxford, 2001; p. 586.

82. Sha, C.; Tseng, W.; Huang, K.; Liu, K.; Lin, H.; Chu, S.; *Chem. Commun*. **1997**, 239.

83. Davis, R. A. Chemical Investigation of Great Barrier Reef Ascidians- Natural product and synthetic studies. PhD Thesis, Griffith University, Brisbane, Australia, 2001; p. 102.

84. Klein, R. Camphor-derived chiral auxillaries in asymmetric synthesis. MSc Thesis, Rhodes University, South Africa, 2000; p. 35.

85. Grehn, L.; Ragnarsson, U.; *J. Org. Chem*. **1981**, *46*, 3492.

86. Apelquist, T.; Wensbo, D.; *Tetrahedron. Lett*. **1996**, *37*, 1471.

87. Watson, R. T.; Gore, V. K.; Chandupatla, K. R.; Dieter, R. K.; Snyder, J. P.; *J. Org. Chem*. **2004,** *69*, 6105.

88. Routier, S.; Sauge, L.; Ayerbe, N.; Gerad, C.; Merour, J.; *Tetrahedron. Lett.* **2002**, *43*, 589.

89. Bhattacharyya, A.; Subramanian, N. S.; *J. Mol. Struct.* **1995**, *339*, 245.

90. Wasserman, H. H.; Rotello, V. M.; Frechette, R.; DeSimone, R. W.; Yoo, J. U.; Baldino, C. M.; *Tetrahedron*. **1997**, *53*, 8731.

91. Nagarkatti, J. P.; Ashley, K. R.; *Synthesis*. **1974**, 186.

92. Mizutani, T.; Ema, T.; Tomita, T.; Kuroda, Y.; Ogoshi, H.; *J. Am. Chem. Soc*. **1994**, *116*, 4240.

93. Littler, B. J.; Miller, M. A.; Hung, C-H.; Wagner, R. W.; O'Shea, D. F.; Boyle, P. D.; Lindsey, J. S.; *J. Org. Chem*. **1999**, *64*, 1391.

94. Martina, S.; Enkelmann, V.; Wegner, G.; Schluter, A.; *Synthesis*. **1991**, 613.

95. Davies-Coleman, M. T.; Dzeha, T. M.; Gray, C. A.; Hess, S.; Pannell, L. K.; Hendricks, D. T..; Arendse, C. E.; *J. Nat. Prod*. **2003**, *66*, 712.

96. Kojiri, K.; Nakajima, S.; Suzuki, H.; Okura, H.; *J. Antibiot.* **1993**, *46*, 1799.

97. Dervan, P. B.; *Science*. **1986**, *232*, 464.

98. Livache, T.; Roget, A.; Dejean, E.; Barthet, C.; Bidan, C.; Theoule, R.; *Nucleic Acid Res.* **1994**, *22*, 2915.

99. Keck, M. V.; Manderville, R. A.; Hecht, S. M.; *J. Am. Chem. Soc.* **2001**, *123*, 8690.

100. Lang, Q.; Dedon, P. C.; *Chem. Res. Toxicol*. **2001**, *14*, 416.

101. Drouin, R.; Rodriguez, H.; Gao, S. W.; Gebreyes, Z.; O'Connor, T. R.; Holmquist, G. P.; Akman, S. A.; *Free. Rad. Biol*. **1996**, *21*, 261.

102. Christensen, P. A.; Hamnett, A. *Techniques and Mechanisms in Electrochemistry;* Blackie Accademic and Professional: London, 1994; p. 33.

103. Raymond, D. E.; Harrison, D. J.; *Electroanal. Chem*. **1993**, *355*, 115.

104. Maree, S. Effects and Substituents on the photosensitising and electrocatalytic properties of phthalocyanines. PhD Thesis, Rhodes University, Grahamstown, South Africa, 2001; p. 3.

105. Phillips, D.; *Sci. Prog.* **1993**, *77*, 295.

106. Pandey, R. K.; J.F.Majchrzycki, K. M.; Smith, K. M.; Dougherty, T. J.; *Proc SPIE*. **1989**, *164*, 1065.

107. Lukyanets, E. A.; *J. Porphyrins and Phthalocyanines*. **1999**, *3*, 424.

108. Daub, M. E.; Ehrenshaft, M.; *Annu. Rev. Phytophathol*. **2000,** *38*, 461.

109. Grossweiner, L. I.; *Singlet Oxygen: Generation of Properties*; www.photobiology.com.

110. Perin, D. D.; Armarego, W. L. F. *Purification of Laboratory Chemicals;* Pergamon Press: Oxford, 1998; p. 391.

111. Petsold, O. M.; Byteva, I. M.; Gurinovich, G. P.; *Opt. Spectrosc*. **1973**, *34*, 343.